Synthese und Charakterisierung von bioabbaubaren Polymeren auf der Basis von Polydepsipeptiden

Synthesis and characterization of biodegradable polymers based on polydepsipeptides

Von der Fakultät für Mathematik, Informatik und Naturwissenschaften
der Rheinisch-Westfälischen Technischen Hochschule Aachen
zur Erlangung des akademischen Grades eines Doktors der
Naturwissenschaften genehmigte Dissertation

vorgelegt von
Yakai Feng
aus Hebei (V.R. China)

Berichter: Universitätsprofessor Dr. Hartwig Höcker
Universitätsprofessor Dr. Hans-Joachim Gais

Tag der mündlichen Prüfung: 10.11. 2000

D82 (Diss. RWTH Aachen)

Diese Dissertation ist auf den Internetseiten der Hochschulbibliothek
online verfügbar

Die vorliegende Arbeit wurde unter Anleitung von Herren Prof. Dr. H. Höcker am Lehrstuhl für Textilchemie und Makromolekulare Chemie der RWTH-Aachen in der Zeit zwischen September 1997 und August 2000 angefertigt.

Mein besonderer Dank gilt Herrn Prof. Dr. H. Höcker für die interessante Themenstellung und die Betreuung der vorliegenden Arbeit.

Frau PD. Dr. D. Klee möchte ich für die vielen Anregungen und Hinweise sowie ihre stete Diskussions- und Hilfsbereitschaft danken.

Herrn Dr. H. Keul möchte ich für seine stete Diskussions- und Hilfsbereitschaft danken.

Den Mitarbeitern des Lehrstuhls für Textilchemie und Makromolekulare Chemie, des Kompetenzzentrums für Biowerkstoffe Aachen (bwA) und des Deutschen Wollforschungsinstituts möchte ich für ihre Hilfsbereitschaft und Unterstützung danken.

Dem Deutschen Akademischen Austauschdienst und das Garg-Stiftung bin ich die Gewährung eines Doktorandenstipendiums zu großem Dank verpflichtet.

The work presented was supervised by Professor Dr. H. Höcker of the Department of Textile Chemistry and Macromolecular Chemistry, RWTH Aachen, from September 1997 to August 2000.

First of all, I would like to thank my supervisor Prof. Dr. H. Höcker for the interesting theme and his supervision.

I would sincerely like to thank PD. Dr. D. Klee for her suggestions, help and assistance.
I would like thank Dr. H. Keul for his discussion and help.

I would also like to thank all co-workers at the Department of Textile Chemistry and Macromolecular Chemistry, at the Aachen Centre of Competence for Biomaterials (bwA) and at the German Wool Research Institute for their help and assistance.

Finally, I would like to acknowledge the financial support of the German Academic Exchange Service (DAAD) and of the Garg-foundation.

For my parents and my wife

Abbreviation List

Amino acids, amino acid derivatives, peptides, depsipeptides and polydepsipeptides are abbreviated according to IUPAC-IUB-Commission recommended abbreviation.

α_c	crystallinity
BSA	albumin bovine fraction V
Lipase CA	lipase from *C. Antarctica*
CL	ε-caprolactone
CR	lipase type VII from *Candida rugosa*
DLLA	D,L-lactide
DMAc	dimethyl acetamide
DMAP	4-N,N-dimehtylaminopyridine
DMF	N,N-dimehtyl formamide
DMSO	dimethyl sulfoxide
DSC	differential scanning calorimeter
EAM	enzyme-activated-monomer
EO	ethylene oxide unit
F	mole fraction in the feed
f	mole fraction in the polymer
GA	glycolic acid
GPC	gel permeation chromatography
ΔH	enthalpy
IR	Infrared spectroscopy
LA	lactide
LLA	L-lactide
M	monomer
$\overline{M_n}$	number average molecular weight
$\overline{M_w}$	weight average molecular weight
MALDI TOF MS	matrix-assisted laser desorption/ionization (MALDI) time-of-flight mass spectrometry
MD	morpholine-2,5-dione

MJ	lipase from *Mucor javanicus*
NMR	nuclear magnetic resonance
Novozym-435	immobilized lipase from *C. Antarctica*
PC	lipase from *Pseudomonas cepacia*
PDLLA	poly(D,L-lactic acid)
PEO	poly(ethylene oxide)
PGA	poly(glycolic acid)
PLLA	poly(L-lactic acid)
PMD	poly(morpholine-2,5-dione)
PPL	*Porcine pancreatic* lipase type II crude
PS	lipase type XIII from *Pseudomonas species*
Q	polydispersity index
T_c	crystallization temperature
T_g	glass transition temperature
T_m	melting temperature
T_p	polymerization temperature
t_p	polymerization time
TFAA	trifluoroacetic anhydride
TMS	tetramethylsilane
UV	ultraviolet

SUMMARY

The thesis deals with the synthesis and characterization of bioresorbable polymers based on polydepsipeptides. Four different types of polydepsipeptide-polyether block copolymers were synthesized via ring-opening polymerization of morpholine-2,5-dione derivatives. The dependence of the macroscopic properties of the block copolymers on their structure is discussed. A new method for the synthesis of polydepsipeptides, i.e. the enzyme-catalyzed ring-opening polymerization of morpholine-2,5-dione derivatives, is presented.

Synthesis and characterization of new block copolymers based on polydepsipeptides

ABA block copolymers with polydepsipeptides (A) and poly(ethylene oxide) ($\overline{M_n}$ = 6000, PEO, B) blocks were synthesized via ring-opening polymerization of 3(S)-*sec*-butyl-morpholine-2,5-dione or 3(S)-isobutyl-morpholine-2,5-dione in the presence of hydroxytelechelic poly(ethylene oxide) with stannous octoate as a catalyst. $\overline{M_n}$ of the resulting copolymers increases with increasing amount of morpholine-2,5-dione derivatives. No racemization of the isoleucine or leucine residue takes place during both homopolymerization and polymerization of morpholine-2,5-dione derivatives in the presence of PEO and $Sn(oct)_2$. The melting temperature of the poly(Glc-Leu) segments in poly(Glc-Leu)-PEO-poly(Glc-Leu) block copolymers increases with increasing length of the poly(Glc-Leu) blocks. The poly(Glc-Leu) block crystallizes first upon cooling from the melt. This leads to imperfect crystallization or no crystallization of the PEO block. The melting temperature of the PEO block is lower than that of the homopolymer, and the crystallinity of the PEO block decreases with increasing length of the polydepsipeptide blocks in both triblock copolymers. Static contact angle measurement with water clearly reveal that the hydrophilicity of the resulting copolymers increases greatly with increasing PEO content in the copolymers.

Four different types of polydepsipeptide-polyether block copolymers were synthesized via ring-opening polymerization of 3(S)-*sec*-butyl-morpholine-2,5-dione or 3(S)-isobutyl-morpholine-2,5-dione in the presence of poly(ethylene oxide) with one, two, three and four terminal OH-groups with stannous octoate as a catalyst, i.e., an AB block copolymer, an ABA block copolymer, an $(A)_2B$ star shaped block copolymer and an $(A)_2B(A)_2$ star shaped block copolymer, respectively, where A is a polydepsipeptide and B a PEO block. The molar ratio

of depsipeptide to PEO was varied to obtain copolymers with different weight fractions of polydepsipeptide blocks ranging from 47 to 97.5 wt%. The crystallinity of the PEO block decreases in the following order: AB > $(A)_2B$ > ABA > $(A)_2B(A)_2$. The static contact angle θ with water decreases with increasing PEO content in the block copolymers.

Polydepsipeptides with protected functional groups were obtained by ring-opening copolymerization of DLLA with morpholine-2,5-dione derivatives having protected functional substituents. The copolymerization was carried out in the bulk at 140 °C in the presence of $Sn(oct)_2$ as a catalyst. Polyester amides with pendant carboxylic acid groups were prepared by catalytic hydrogenation of the protected copolymers.

Copolymers with a PEO8000 center block and two arms of random lactide/depsipeptides copolymers were synthesized and characterized. Increasing proportion of PEO results in a decrease in molecular weight of the block copolymer and higher crystallinity in PEO block. The block copolymers having a high fraction of PEO (> 40%) are brittle. The block copolymers based on depsipeptides, DLLA and PEO have much higher elongation at break and lower Young¡ ¯s modulus than the corresponding block copolymers based on depsipeptides, LLA and PEO. The mechanical properties are mainly influenced by the crystallinity of copolymer blocks, when the block copolymers were prepared from the same depsipeptide and with the same molar ratio, but different lactide, i.e., DLLA or LLA.

Hydrolytic degradation of block copolymers based on polydepsipeptides

In vitro degradation experiments reveal that the block copolymers based on depsipeptides, DLLA and PEO lose their weight faster than the block copolymers based on depsipeptides, LLA and PEO. The weight loss rates depend on the weight fraction of PEO in the block copolymers and the starting molecular weight. The molecular weight decreases quickly, while the molecular weight distribution increases up to a polydispersity from 1.63 to 4.29 with increasing degradation time.

CaH_2 as a co-initiator for the ring-opening polymerization of Cyclo(Glc-Val)

Block copolymers with poly(Glc-Val) and PEO6000 blocks were synthesized via the ring-opening polymerization of 3(S)-isopropyl-morpholine-2,5-dione in the presence of PEO with CaH_2 as a co-initiator at 140 °C for 24 h or 96 h. $\overline{M_n}$ of the resulting copolymers increases with increasing 3(S)-isopropyl-morpholine-2,5-dione content in the feed and reaction time.

According to ^{1}H NMR analysis, racemization of valine residue takes place during the polymerization. About 40% of 3(S)-isopropyl-morpholine-2,5-dione is racemized in 96 h at 140 °C during polymerization, while about 12% is racemized in 24 h. The glass transition temperature of the poly(Glc-Val) segments in the triblock copolymers is about 74 °C. The melting temperature of the PEO block upon first heating is lower than that of the homopolymer, and disappears with increasing length of the poly(Glc-Val) blocks.

Enzyme-catalyzed ring-opening polymerization of morpholine-2,5-diones

The enzymatic ring-opening polymerization of 6-membered cyclic depsipeptides, 3(S)-isopropyl-morpholine-2,5-dione, 3(R)-isopropyl-morpholine-2,5-dione, 3(R,S)-isopropyl-morpholine-2,5-dione, (3S, 6R,S)-3-isopropyl-6-methyl-morpholine-2,5-dione, 3(S)-isobutyl-morpholine-2,5-dione, 3(S)-sec-butyl-morpholine-2,5-dione, 6(S)-methyl-morpholine-2,5-dione and 6(R,S)-methyl-morpholine-2,5-dione in the bulk, was investigated by using the lipase PPL as a catalyst. In the absence of the enzyme, the monomers were recovered, indicating that the present polymerization proceeds through enzymatic catalysis. During the polymerization of morpholine-2,5-diones racemization of both the amino acid and the S-lactic acid moiety takes place. Enzymatic polymerization produces polydepsipeptides with a carboxylic acid group at one end and a hydroxyl group at the other one.

Selected commercial lipases were screened as catalysts for the polymerization of 3(S)-isopropyl-morpholine-2,5-dione at 100 °C in bulk. Polymerizations catalyzed with lipases PPL, PS and CR result in conversions of about 50%, and in molecular weights ranging from 3500 to 17500. Lipase PPL was selected for further studies. The apparent rate of polymerization increases with PPL concentration. When the PPL concentration is 5 wt% and 10 wt% with respect to the monomer, a conversion of about 70% is reached after 5 d and 7 d, respectively, while for PPL concentrations of 1 wt% and 0.5 wt% the conversion is less than 15% even after 11 d. High concentrations of PPL (10 wt%) result in high $\overline{M_n}$ values (< 4 d); with decreasing concentration of PPL poly(Glc-Val) of lower molecular weight is obtained. The highest molecular weight poly(Glc-Val), $\overline{M_n}$ = 30000 resulted from a polymerization conducted at 130 °C. Increasing polymerization time (and conversion) leads for high PPL concentration (10 wt%) first to an increase in $\overline{M_n}$ and later to a decrease. The general trends observed by variation of the polymerization temperature are the following: (i) increasing monomer conversion and $\overline{M_n}$ with increasing reaction temperature from 100 to 130 °C,.(ii)

increasing reaction temperature leads to a bimodal molecular weight distribution. Water is an important factor that controls not only the conversion but also the molecular weight. With increasing water content, enhanced polymerization rates are achieved while the molecular weight of poly(Glc-Val) decreases.

Polymerizations of 6(S)-methyl-morpholine-2,5-dione catalyzed with 10 wt% lipases PPL, PC and CR result in conversions of about 75% in 3 d, and in molecular weights ranging from 8200 to 12100. MJ showed lower catalytic activity for the polymerization. The apparent rate of polymerization increases with increasing PPL concentration when the temperature is 100 °C. When the PPL concentration is 5 wt% and 10 wt% with respect to the monomer, a conversion of about 70% is reached after 6 d and 1 d, respectively, while for PPL concentration of 1 wt% the conversion is less than 20% even after 6 d. High concentrations of PPL (10 wt%) result in high $\overline{M_n}$ values (< 3 d); with lower concentration of PPL poly(Lac-Gly) of lower molecular weight is obtained. The reaction temperature (100 - 130 °C) affects monomer conversion and $\overline{M_n}$ slightly. The effect of water on the conversion and the molecular weight is similar to that in the ring-opening polymerization of 3(S)-isopropyl-morpholine-2,5-dione in the presence of PPL.

The lipase-catalyzed ring-opening polymerization of 3(S)-*sec*-butyl-morpholine-2,5-dione was also studied in detail.

Copolymerization of 3(S)-isopropyl-morpholine-2,5-dione and D,L-lactide was carried out in the presence of PPL as a catalyst at 100 °C for 168 h. Copolymers of various compositions were obtained. The enzymatic polymerization of DLLA and 3(S)-isopropyl-morpholine-2,5-dione produces copolymers with a carboxylic acid group at one end and a hydroxyl group at the other end.

ZUSAMMENFASSUNG

Diese Arbeit beschäftigt sich mit der Synthese und Charakterisierung von bioresorbierbaren Polymeren auf der Basis von Polydepsipeptiden. Vier verschiedene Polydepsipeptide-Polyether wurden durch ringöffnende Polymerisation von Morpholin-2,5-dion-Derivaten hergestellt. Die Abhängigkeit der makroskopischen Eigenschaften der Blockcopolymere von ihrer Struktur wird diskutiert. Eine neue Synthese von Polydepsipeptiden über eine enzymatisch katalysierte ringöffnende Polymerisation wird vorgestellt.

Synthese und Charakterisierung von neuen Blockcopolymeren auf der Basis von Polydepsipeptiden

Blockcopolymere des Typs ABA aus Polydespsipeptiden (A) und Poly(ethylenoxid) ($\overline{M_n}$ =6000, PEO) (B) wurden durch ringöffnende Polymerisation von 3(S)-*sec*-Butyl-morpholine-2,5-dion oder 3(S)-Isobutyl-morpholine-2,5-dion in Gegenwart von hydroxytelechelischem PEO und Zinnoctoat als Katalysator synthetisiert. $\overline{M_n}$ der erhaltenen Copolymere steigt mit steigendem Anteil an Morpholin-2,5-dion-Derivat. Es erfolgt keine Racemisierung des Leucins oder Isoleucins während der Homopolymerisation oder der Copolymerisation der Morpholin-2,5-dion-Derivate in Gegenwart von PEO und $Sn(oct)_2$. Der Schmelzpunkt der Poly(Glc-Ile)-Segmente in Poly(Glc-Ile)-PEO-Poly(Glc-Ile)-Blockcopolymeren steigt mit zunehmender Länge der Poly(Glc-Ile)-Blöcke. Das Poly(Glc-Ile) kristallisiert beim Abkühlen aus der Schmelze zuerst. Dies führt zu einer unvollständigen, oder keiner Kristallisation der PEO-Blöcke. Der Schmelzpunkt der PEO-Blöcke liegt niedriger als der des Homopolymers und die Kristallinität des PEO-Blocks nimmt mit steigender Länge des Polydepsipeptidblocks in beiden Triblockcopolymeren ab. Die Ergebnisse der statischen Kontaktwinkelmessung mit Wasser zeigen, daß die Hydrophilie der erhaltenen Copolymere mit steigendem PEO-Gehalt stark zunimmt.

Vier verschiedene Arten von Polydepsipeptid-PEO-Blockcopolymeren wurden durch ringöffnende Polymerisation von von 3(S)-*sec*-Butyl-morpholine-2,5-dion oder 3(S)-Isobutyl-morpholine-2,5-dion in der Gegenwart von PEO mit einer, zwei, drei oder vier terminalen OH-Gruppen und Zinnoctoat als Katalysator, nämlich ein AB Blockcopolymer, ein ABA Blockcopolymer, ein $(A)_2B$ Sterncopolymer und ein $(A)_2B(A)_2$ Sterncopolymer, hergestellt. Das molare Verhältnis von Depsipeptid zu PEO wurde verändert, um Copolymere mit verschiedenen Anteilen von Polydepsipeptidsequenzen, von 47 bis 97.5 Gew.% zu erhalten.

Die Kristallinität der PEO Phase in den Copolymeren sinkt in der folgenden Reihenfolge: AB > $(A)_2B$ > ABA > $(A)_2B(A)_2$. Der statische Kontaktwinkel mit Wasser sinkt mit steigendem PEO-Anteil in den Blockcopolymeren.

Polydepsipeptide mit geschützten funktionellen Gruppen wurden durch ringöffnende Copolymerisation von DLLA mit Morpholin-2,5-dion-Derivaten mit geschützten Substituenten erhalten. Die Copolymerisation wurde in Substanz bei 140 °C in Gegenwart von $Sn(oct)_2$ als Katalysator durchgeführt. Polyesteramide mit seitenständigen Carboxylgruppen wurden durch katalytische Hydrierung der geschützten Copolymere hergestellt.

Copolymere mit einem PEO8000-Zentralblock und zwei Ketten von Lactid/Depsipeptid-Copolymeren wurden synthetisiert und charakterisiert. Steigender PEO-Gehalt führt zu einem Absinken des Molgewichtes und zu größerer Kristallinität in den PEO-Blöcken. Blockcopolymere mit einem hohen Gehalt an PEO (> 40%) sind spröde. Die Blockcopolymere, die auf Depsipeptiden, DLLA und PEO basieren, haben eine wesentlich größere Bruchdehnung und niedrigere elastische Module als die entsprechenden Blockcopolymere, die auf Depsipeptiden, LLA und PEO basieren. Die mechanischen Eigenschaften werden hauptsächlich beeinflußt durch die Kristallinität der Copolymerblöcke, wenn die Blockcopolymere aus den gleichen Depsipeptiden bei dem gleichen molaren Verhältnis, aber aus verschiedenen Lactiden, DLLA bzw. LLA, hergestellt werden.

Hydrolytischer Abbau von Blockcopolymeren auf der Basis von Polydepsipeptiden

In vitro Abbauversuche zeigen, daß die Blockcopolymere auf Basis von Polydepsipeptiden, DLLA und PEO an Gewicht wesentlich schneller verlieren als die Blockcopolymere die auf Depsipeptiden, LLA und PEO basieren. Die Geschwindigkeit des Gewichtsverlustes ist vom Gewichtsanteil des PEO in den Blockcopolymeren und dem Anfangsmolekulargewicht abhängig. Das Molekulargewicht sinkt sehr schnell, während die breite Molgewichtsverteilung mit steigender Abbauzeit zunimmt von einen Polymolekularitätsindex von 1.63 bis zu 4.29.

CaH_2 als Co-Initiator für die ringöffnende Polymerisation von Cyclo(Glc-Val)

Blockcopolymere aus Poly(Glc-Val) und PEO6000 wurden durch ringöffnende Polymerisation von 3(S)-Isopropyl-morpholin-2,5-dion in Gegenwart von PEO mit Calciumhydrid als Co-Initiator bei 140 °C in 24 h oder 96 h gewonnen. $\overline{M_n}$ der

resultierenden Copolymere steigt mit steigendem 3(S)-Isopropyl-morpholin-2,5-dion-Gehalt und längerer Reaktionszeit. Der ^{1}H NMR Spektroskopie folgend findet eine Racemisierung des Valinrestes während der Polymerisation statt. Etwa 40% des 3(S)-Isopropyl-morpholin-2,5-dion racemisieren in 96 h bei 140 °C während der Polymerisation und etwa 12% in 24 h. Die Glassübergangstemperatur des Poly(Glc-Val)-Segmentes in den Triblockcopolymeren beträgt etwa 74 °C. Die Schmelztemperatur der PEO Blöcke während des ersten Erhitzens liegt niedriger als die des Homopolymers und verschwindet mit steigender Länge der Poly(Glc-Val)-Blöcke.

Enzymkatalysierte ringöffnende Polymerisation von Morpholin-2,5-dionen

Die enzymatische ringöffnende Polymerisation von den 6-gliedrigen cyclischen Depsipeptiden, 3(S)-Isopropyl-morpholin-2,5-dion, 3(R)-Isopropyl-morpholin-2,5-dion, 3(R,S)-Isopropyl-morpholin-2,5-dion, 3(S), 6(R,S)-3-Isopropyl-6-methylmorpholin-2,5-dion, 3(S)-Isobutyl-morpholin-2,5-dion, 3(S)-*sec*-Butyl-morpholin-2,5-dion, 6(S)-Methyl-morpholin-2,5-dion und 6(R,S)-Methyl-morpholin-2,5-dion wurde in Substanz mit Lipase PPL als Katalysator untersucht. In Abwesenheit des Enzyms wurde das Monomer zurückgewonnen; das deutet darauf hin, daß die Polymerisation unter Enzymkatalyse stattfindet. Während der Polymerisation der Morpholin-2,5-dione racemisieren beide Aminosäuren und der S-Lactidrest. Die enzymatische Polymerisation ergibt eine Caboxylgruppe an einem, eine Hydroxylgruppe am anderen Ende.

Die ringöffnende Substanzpolymerisation von 3(S)-Isopropyl-morpholin-2,5-dion wurde mit käuflichen Lipasen als Katalysatoren bei 100 °C untersucht. Polymerisationen, die durch Lipase PPL, PS oder CR katalysiert wurden, liefern einen Umsatz von 3(S)-Isopropyl-morpholin-2,5-dion von ungefähr 50%, und Molekulargewichte der Produkte im Bereich von 3500 bis 17500. Die lipase PPL wurde für weiteren Untersuchungen ausgewählt. Die scheinbare Polymerisationsgeschwindigkeit erhöht sich mit steigender PPL Konzentration. Beträgt die Konzentration von PPL 5 bzw. 10 Gew.% bezogen auf das Monomer, wird ein Umsatz von etwa 70% nach 5 bzw. 10 Tagen erreicht, während Konzentrationen von 1 oder 0,5 Gew.% eine Umsatzrate von weniger als 15 % auch nach 11 Tagen erzielen. Hohe Konzentrationen von PPL (10 Gew.%) ergeben hohe $\overline{M_n}$ Werte (< 4 d); mit sinkender Konzentration von PPL werden Poly(Glc-Val) mit geringerem Molgewicht erhalten. Das höchste Molekulargewicht von Poly(Glc-Val), $\overline{M_n}$ = 30000 resultiert aus einer Polymerisation bei 130 °C. Steigende Polymerisationszeiten (und Umsätze) führen bei hohen

PPL Konzentrationen (10 Gew.%) zunächst zu einer Erhöhung von $\overline{M_n}$, später zu einer Abnahme. Die allgemeinen Tendenzen, die bei einer Änderung der Polymerisationstemperatur beobachtet werden, sind die folgenden: (i) steigender Monomerumsatz und steigendes $\overline{M_n}$ mit steigender Reaktionstemperatur von 100 bis 130°C, (ii) steigende Reaktionstemperatur führt zu einer bimodalen Molekulargewichtsverteilung. Wasser ist ein wichtiger Faktor, nicht nur bei der Kontrolle des Umsatzes, sondern auch des Molekulargewichtes. Mit steigendem Wassergehalt werden höhere Polymerisationsgeschwindigkeiten erhalten, während das Molekulargewicht des Poly(Glc-Val) sinkt.

Die ringöffnende Substanzpolymerisation von 6(S)-Methyl-morpholin-2,5-dion liefert mit 10 Gew.% Lipase PPL, PC und CR einen Umsatz von 75% in drei Tagen und Molekulargewichte von 8200 bis 12100. MJ zeigt eine geringere katalytische Aktivität. Die scheinbare Polymerisationsgeschwindigkeit erhöht sich mit steigender PPL Konzentration bei einer Polymerisationstemperatur von 100 °C. Wenn die PPL Konzentration zwischen 5 und 10 Gew.%, bezogen auf das Monomer beträgt, wird ein Umsatz von etwa 70 % nach 6 bzw. 1 Tag erreicht, während eine PPL Konzentration von 1 Gew.% zu einen Umsatz von weniger als 20% nach 6 Tagen führt. Hohe Konzentrationen von PPL (10 Gew.%) ergaben große $\overline{M_n}$ Werte (< 3 d); mit geringeren Konzentrationen von PPL werden kleinere Molekulargewichte von Poly(Lac-Gly) erhalten. Die Reaktionstemperatur (100-130 °C) beeinflußt den Monomerumsatz und $\overline{M_n}$ nur wenig. Der Einfluß von Wasser auf den Umsatz und das Molekulargewicht ist ähnlich wie bei der ringöffnenden Polymerisation des 3(S)-Isopropyl-morpholin-2,5-dion in Gegenwart von PPL.

Die Lipase-katalysierte ringöffnende Polymerisation von 3(S)-*sec*-Butyl-morpholin-2,5-dion wurde ebenfalls detailliert untersucht.

Die Copolymerisation von 3(S)-Isopropyl-morpholin-2,5-dion und D,L-Lactid wurde in Gegenwart von PPL als Katalysator bei 100 °C in 168 h durchgeführt. Copolymere verschiedener Zusammensetzungen wurden erhalten. Die enzymatische Polymerisation von DLLA und 3(S)-Isopropyl-morpholin-2,5-dion ergibt Copolymere mit einer Carboxylgruppe an einem und einer Hydroxylgruppe am anderen Ende.

1. INTRODUCTION

1.1 BIODEGRADABLE POLYDEPSIPEPTIDES

Synthetic biodegradable polymeric materials are often used for biomedical applications such as surgical sutures, resorbable bone plates, artificial skin, and carrier systems for the controlled release of drugs. These materials have been thoroughly investigated and discussed in several review papers[1-4]. The requirements in the selection of any biomedical material, beside biodegradability and resorbability, are that it should have suitable mechanical properties and lack toxic degradation products.

Two important classes currently investigated for a wide variety of surgical and pharmaceutical applications are poly(α-hydroxy acid)s and poly(α-amino acid)s[5,6]. The synthesis of poly(α-hydroxy acid)s has been extensively studied and reported. The most important method for the synthesis of biodegradable polyesters is the ring-opening polymerization of the corresponding cyclic mono- or diesters. Poly(glycolic acid) (PGA), poly(L-lactic acid) (PLLA), poly(D,L-lactic acid) (PDLLA) are synthesized by ring-opening polymerization of the corresponding six-membered cyclic diesters, i.e., glycolide, L-lactide and D,L-lactide. PGA and PLLA are semicrystalline polymers, whereas PDLLA is amorphous. PGA has a glass transition temperature (T_g) close to body temperature (T_g = 36 °C), whereas PLLA and PDLLA have T_g values above body temperature (T_g = 57 - 60 °C and T_g = 50 - 54 °C, respectively)[7,8]. PLLA is one of the most widely used biodegradable polymers, with a variety of biomedical and pharmaceutical applications. PLLA has excellent mechanical properties and can be slowly broken down into nontoxic metabolites. However, its applications have been somewhat limited because of difficulties in controlling the hydrolysis rate[9], poor hydrophilicity[10], and high rigidity and crystallinity[11,12].

Since the properties of homopolymers are more or less fixed, copolymers are required to provide materials with a wide range of properties. In 1979, Gilding reported that copolymers of lactic acid and glycolic acid (GA) showed a range of properties, depending on their composition[13].

Polypeptides for biomedical uses are classified into two categories: natural and synthetic polypeptides. The former includes, for example, collagen, gelatin, and other water-soluble proteins. Since proteins are composed of amino acids, many researchers have tried to develop synthetic polypeptides derived from amino acids to serve as models for structural, biological,

and immunological studies. In addition, many different types of synthetic polypeptides have been investigated for biomedical applications[14]. Synthetic polypeptides have several potential advantages as biomaterials. Many types of synthetic polypeptides have been prepared for biomedical applications, such as sutures, artificial skin substrates, and drug delivery systems[15-17]. Side chains offer sites for the attachment of drugs, crosslinking agents, or pendant groups that can be used to modify the physico-chemical properties of the polymer. Because these polymers release naturally occurring amino acids as the primary products of polymer backbone cleavage, their degradation products may be expected to show a low level of systemic toxicity. In spite of their apparent potential as biomaterials, synthetic polypeptides have actually shown few practical applications. Most synthetic polypeptides are highly insoluble and non-processible materials. Owing to these difficulties, only a few synthetic polypeptides, usually derivatives of poly((S)-glutamic acid) are currently investigated as implant materials.

Copolymers of α-hydroxy acids and α-amino acids, which are called polydepsipeptides, are a valuable addition to the existing list of synthetic biodegradable polymers. Since these polymers contain both ester and amide groups, their biodegradation behavior is different from that of the homopolymers. Linear polydepsipeptides were initially produced by stepwise active ester-peptide coupling reactions[18-28]. Ring-opening polymerization of morpholine-2,5-dione derivatives (cyclic dimers of α-hydroxy- and α-amino acid) is the second and more attractive way to produce these poly(ester amide)s.

In 1985, Helder et al. for the first time synthesized a polydepsipeptide by ring-opening polymerization of morpholine-2,5-dione[29]. The polymerization was carried out in the bulk at 130°C for 28 to 48h using stannous octoate as a catalyst. Many researchers studied the ring-opening polymerization of different morpholine-2,5-dione derivatives[30-32].

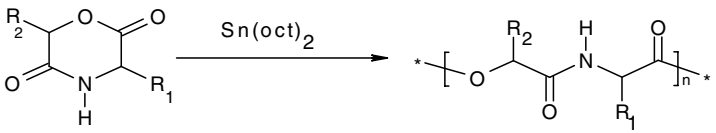

The first successful copolymerizations were performed with *p*-dioxanone and unsubstituted or alkyl-substituted morpholine-2,5-diones[33]. These copolymers showed *in vivo* accelerated resorption with excellent strength retention. Yonezawa synthesized copolymers of 6-isopropyl-morpholine-2,5-dione and 6-isopropyl-3-methyl-morpholine-2,5-dione and DLLA;

however, polymer yields and viscosities were rather low and the incorporation of depsipeptide units was extremely low[34].

Alternating poly(glycine-D,L-lactic acid) was obtained from 6-methyl-morpholine-2,5-dione by ring-opening polymerization[29], random copolymers were also synthesized by copolymerization with DLLA[35]. Some polydepsipeptides such as poly(glycolic acid-alanine-D,L-lactic acid) and poly(D,L-lactic acid-alanine) were obtained by ring-opening copolymerization of 3-methyl- and 3,6-dimethyl-morpholine-2,5-dione, respectively, with DLLA[36]. In 1989, Fung synthesized bioresorbable polydepsipeptides for medical implant devices from 3-alkyl-substituted-morpholine-2,5-dione[37]. Copolymerizations of ε-caprolactone (CL) with several morpholine-2,5-dione derivatives were investigated by In´t Veld and associates[30].

In order to improve the hydrophilicity of polydepsipeptides, one may introduce hydrophilic pendant functional groups into the polymer chain. Feijen et al. reported the copolymerization of CL and morpholine-2,5-dione with pendant hydrophilic functional groups[38-40]. However, they failed to achieve copolymers with a content of functional monomer exceeding 20%. The ε-amino groups in linear poly(L-lactic acid-co-S-lysine) with about 1% lysine content have been utilized to initiate the ring-opening polymerization of the amino acid N-carboxyanhydrides to yield graft copolymers[41]. However, the reaction process is very complicated. Ouchi et al. reported the synthesis of cyclo(Glc-Asp(OBzl))[28, 42] and its homopolymer. The molecular weight of the resulting polymer ranges from 1950 to 3280. Recently, Wang et al. synthesized the polymer with high molecular weight ($\overline{M}_n$ = 5800-13500) via homopolymerization using stannous octoate as a catalyst[43,44]. The IR spectrum of Wang¡ ¯s monomer is rather different from that of Ouchi¡ ¯s in the range of the N-H stretch band. This difference may indicate the existence of different association forms of the monomer on the basis of the hydrogen bond. The hydrogen bonding in the monomer has a large effect on its polymerization reactivity. Selection of a suitable recrystallization solvent system results in different types of monomer crystals in which either intramolecular or intermolecular hydrogen bonds are formed. This helps to achieve a higher reactivity in the ring-opening polymerization. Some examples of polydepsipeptides with or without functional groups are summarized in Tab.1.

The biodegradable L-lactic acid-depsipeptide copolymers having pendant reactive groups, poly[LLA-(Glc-Asp)] and poly[LLA-(Glc-Lys)], were obtained by ring-opening

polymerization of LLA with cyclodepsipeptides consisting of Glc and Asp or Lys[52]. The polymers showed enzymatic degradation and also fast degradation rates without the presence of enzymes, when compared with PLLA[52]. Recently, Ouchi et al. reported the preparation of biodegradable microspheres from poly[LLA-(Glc-Asp)] and poly[LLA-(Glc-Lys)] with low contents of depsipeptide units by the oil-in-water/solvent evaporation method[52]. The average diameters of the dried microspheres were estimated to be 390-450 nm by scanning electron microscopy. The amount of functionalized groups located on the surfaces increases with increasing content of depsipeptide units in the used copolymers. John synthesized biodegradable cross-linked microspheres from poly[CL-(Glc-Ser)][53]. Poly[CL-(Glc-Ser)] was prepared by copolymerization of CL and Cyclo[Glc-Ser(OBzl)]. After deprotection, the pendant OH groups of the serine residue were acrylated. Cross-linked beads of ca. 25-170 µm size were obtained by UV-suspension polymerization. The beads are opaque after swelling in water and transparent in DMSO and $CHCl_3$, and may be useful as biodegradable microspheres for drug delivery.

Tab. 1. Some examples of polydepsipeptides with or without functional groups

No.	Morpholine-2,5-dione	Co-monomer	Reaction temperature /time in °C/h	$\overline{M}_n$ 10^{-4}	Ref.
1	Cyclo(DLLA-Gly)		130/28-48	1.6-2.3 [a]	29
2	Cyclo(DLLA-Val)		125/48	2.5-3.5 [a]	45
3	Cyclo(DLLA-Ala)		134/48	0.9 [a]	45
4	Cyclo(LLA-Val)		142/48	2.95	46
5	Cyclo(LLA-Ala)		165/48	n.d.	45
6	Cyclo(Glc-Ala)		180/2	0.61 [b]	47
7	Cyclo(Glc-Asp(OBzl))		155/3-6	0.19-0.31	32
8	Cyclo(Glc-Glu(OBzl))		160/15-20	0.22	32
9	Cyclo(Glc-Lys(Z))		115/12-336	0.12-0.43	32
10	Cyclo(DLLA-Gly)	Glycolide	115-160/22-64	0.33-0.47 [c]	48
11	Cyclo(DLLA-Lys(Z))	CL, DLLA	130/48	0.54-2.0	39
12	Cyclo(DLLA-Cys(MBzl))	CL, DLLA	130/48	1.3-2.1	39
13	Cyclo(DLLA-Asp(OBzl))	CL, DLLA	130/48	1.1-3.1	39
14	Cyclo(LA-Lys(Z))	LLA	136/48	0.84-1.45	49
15	Cyclo(Glc-Ser(OBzl)	LLA	135/48	1.88	50
16	Cyclo(Glc-Cys(MBzl))	LLA	125/48	0.15-0.65	51
17	Cyclo(Glc-Asp(OBzl)), Cyclo(Glc-Lys(Z))	LLA	160/48	1.2-8.3	52
18	Cyclo(Glc-Ser(OBzl)	CL	130/48	2.1-3.73	53
19	Cyclo(Glc-Asp(OBzl))	CL	152/4.1	0.58-4.3	43,44

a) $\overline{M}_w$. b) intrinsic viscosity measured using an Ubbelhode viscometer and dichloroacetic acid as a solvent. c) intrinsic viscosity, hexafluroisopropanol as a solvent at 25 °C.

1.2 ENZYMATIC SYNTHESIS OF BIODEGRADABLE POLYMERS

Polymer industries rely heavily on inorganic catalysts for synthesis and processing, and some of these catalysts are prepared from toxic and/or precious metals[54]. Negative environmental impact has been a concern raised by use of many of these metals, and recently more emphasis is being given to green technology, including the use of nontoxic catalysts such as enzymes in materials processing. Enzymes are increasingly being used as catalysts in testing, evaluation, processing, and production in chemical, food, pharmaceutical, agricultural, and health care industries[55-58].

Enzymes are proteins with molecular recognition and biotransformation properties. To a large extent, the catalytic activity of an enzyme depends on its three dimensional structure and stability in a specific medium, its interaction and partition with substrates, monomers, ligands, and products, and properties of the medium such as ionic strength, pH, temperature, and polarity. Activities of these catalysts are generally studied under physiological conditions of pH, ionic strength, and temperature in aqueous media.

During the past decade, studies have shown that enzyme-catalyzed reactions also can be carried out in anhydrous organic solvents and solvents with differing amounts of water[59]. It turns out that water is not the ideal medium in some enzyme-catalyzed reactions for the following reasons: stereoselectivity and regioselectivity of reactions, new reactions with favorable specificity and thermodynamic equilibrium, improved solubility of hydrophobic monomers, oligomers, and polymers, control of molecular weight and dispersity of polymers, mild or ambient operating conditions such as pH, temperature, and pressure; improved stability of the enzyme, and control of microbial contamination in the medium. From a processing point of view, ease of separation and reuse of enzymes and separation of products from the reaction medium are additional advantages of non-aqueous enzyme-based reactions.

Recently, enzyme-catalyzed polymerization (enzymatic polymerization) has attracted much attention as a new method of polymer synthesis[60-61]. Specific enzymatic catalysis is expected to synthesize polymers with high selectivity or with novel structures. The term ¡ °enzymatic polymerization ” is always defined as a polymerization *in vitro* via a nonbiosynthetic pathway catalyzed by an isolated enzyme. Until now, there have been many papers on enzymatic syntheses of natural biopolymers as well as non-natural synthetic polymers.

Enzymatic polymerizations producing biodegradable polymers will be reviewed in the following Section.

Polysaccharides

The use of an enzyme for glycosylation in polysaccharide synthesis is one of the most promising methods for selective construction of a saccharide unit. The enzymes so far utilized can be classified into glycosidases, glycosyltransferases, and phosphorylases. Glycosidic bond formation with glycosidases can be achieved by using its reverse reaction of hydrolysis, employing a free sugar as glycosyl donor. The position of the equilibrium can be shifted by increasing substrate concentration, decreasing water, and removing the final product from the reaction mixture[62-64].

A glycosyl fluoride also acts effectively as a glycosyl donor[65]. Recently, the first *in vitro* synthesis of cellulose via a nonbiosynthetic pathway was achieved by an enzymatic polymerization of β-cellobiosyl fluoride as a substrate for cellulase[66]. The configuration of C_1 fluorine atom of the monomer was designed to form a reactive intermediate leading to a β(1⟶4) product of cellulose via a "double displacement mechanism" at the active site of the enzyme[67]. The reaction is proposed to proceed via an activated monomer mechanism (Scheme 1).

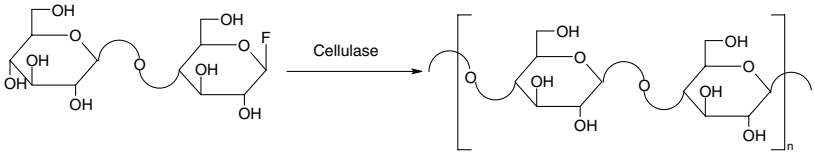

Scheme 1. Synthesis of cellulose via an activated monomer mechanism from cellobiosyl fluoride.

Novel cellobiosyl fluoride derivatives have been polymerized, giving rise to regioselectively methylated cellooligosaccharide derivatives[68]. The enzymatic polycondensation of a glycosyl fluoride monomer in aqueous organic solvents has been applied to amylase-catalyzed preparation of maltooligosaccharides[69].

Polypeptides

Fruton et al. reported the dipeptidyltransferase (cathepsin C)-catalyzed polymerization of dipeptide amides in an aqueous buffer solution[70]. From Gly-Tyr-NH_2 or Ala-Phe-NH_2, the

corresponding tetra- or hexa-peptide amide was formed in about 80% yield[71]. In the case of Gly-Tyr-NH_2, the hydrolysis of the amide linkage took place during the polymerization and formation of oligomers up to an octamer (22% yield) was observed.

Some proteases induce polymerization of esters of α-amino acids to water-insoluble products. Formation of di- or tripeptides was observed in the α-chymotrypsin-catalyzed reaction of isopropyl esters of S-methionine, S-threonine, S-phenylalanine, and S-tyrosine[72,73]. An S-leucine polypeptide, eight to nine units long, was synthesized by the papain-catalyzed polymerization of a leucine methyl ester[74]. Papain also catalyzed the polymerization of S-methionine, S-phenylalanine, and S-tyrosine esters to produce water-insoluble oligomers[75]. The polymerization of diethyl α,γ-S-glutamate was carried out in the presence of papain or α-chymotrypsin as a catalyst[76]. During the polymerization, a precipitate composed of five to nine glutamic acid residues was formed in 42% yield.

Wong et al. reported a mutant subtilisin from *Bacillus amyloliquefaciens*, which showed high activity and stability in N,N-dimethylformamide (DMF). The subtilisin-catalyzed polymerization of the S-methionine methyl ester was performed in an aqueous DMF solution to produce a degree of polymerization up to 50[77]. This is due to the improvement of the product solubility in high concentration of DMF. Another subtilisin variant, more stable in DMF, afforded polymethionine of larger molecular weight[78].

Polyesters

Enzymatic synthesis of polyesters has been attempted by different polymerization methods: polycondensation of hydroxycarboxylic acids, esters of hydroxycarboxylic acid, combinations of dicarboxylic acid/glycol and diesters of dicarboxylic acid/glycol, poly(addition-condensation) of cyclic acid anhydrides and glycols, and ring-opening polymerization of lactones. The possibility of preparing polyesters with high molecular weight by enzyme-catalyzed transesterification in organic solvent media was investigated[79,80]. Most of the transformations resulted in high regio- and/or stereoselectivity, while in case of chemical synthesis the esterifications have to be performed with optically active monomers to give optical selectivity.

Ajima et al. reported the polymerization of 10-hydroxydecanoic acid in benzene in the presence of poly(ethylene glycol)-modified lipase as a catalyst to give the corresponding

oligomer in 48 % yield[81]. Use of a large amount of lipase and the presence of a molecular sieve (3 Å) in the reaction system resulted in an increase of the molecular weight.

The transesterification of diphenyl carbonate with bisphenol A, as well as with a range of simple alcohols in water-saturated ether as a solvent, resulted in oligomers with molecular weight of up to 900. The enzymes used for the study were *porcine liver esterase* and the lipase from yeast *Candida cylindracea*. Among esterification reactions, lipase-catalyzed transesterification is often preferred to direct esterification because no water is formed in the reaction[79,80,82]. Enzymatic polytransesterification of aromatic diols was carried out in anhydrous organic solvent[83]. The protease from *Bacillus lichemiformis* catalyzes the polytransesterification of a diester of glutamic acid with aromatic diols such as 1,4-di(hydroxymethyl)-benzene. For the transesterification, monomer selection is an important factor since the yield and molecular weight can be altered by this factor. Large size monomers do not always result in high molecular weight polymers in the polyesterification reaction. For diols with 4 or 5 carbon atoms, polyesterification showed good yield and the polymers synthesized from this monomer exert a narrow molecular weight distribution.

Enzymatic polymerization has been extended to the ring-opening polymerization of nonsubstituted lactones with various ring sizes. The polymerization of CL was first and most extensively studied[84-87]. Various powdery lipases of different origin are commerically available and used as catalysts for the ring-opening polymerization of CL. The small size lactone β-propiolactone was polymerized in the presence of *Pseudomonas* family lipases, yielding a mixture of linear and cyclic oligomers[88]. Medium-size lactones (6- and 7-membered) as well as macrolides (12- and 16-membered) were polymerized to produce polyesters. The polymerization of the macrolides using lipase proceeded much faster than that of CL, due to the strong recognition of the macrolides by the lipase catalyst. From 11-undecanolide (12-membered), a polyester of molecular weight up to 2.2×10^4 was obtained by the reaction in bulk at 75 °C using *Candida cylindracea* lipase. The copolymerization of δ-valerolactone with CL using lipase in bulk afforded a copolymer of random structure with both units[89].

Facile control of polymer terminal structure is important because terminal-functionalized polymers, typically macromonomers and telechelics, are often used as prepolymers for the preparation of functional polymers. A single-step production of methacryl-type polyester macromonomers was developed in the ring-opening polymerization of lactones using the

respective initiator and terminating agent. Alcohol initiates the polymerization of lactones with lipase CA as a catalyst to introduce the terminal alcohol moiety[90]. Alkyl-glucopyranosides were also found to initiate the polymerization of CL in the presence of lipase CA to give the polymer bearing a terminal sugar moiety[91]. In the initiation step, the primary hydroxy group of the glucopyranoside is regioselectively acrylated.

Tremendous new opportunities are becoming available by the use of enzymatic synthesis of biomaterials. The opportunities include the ability to control molecular weight and polydispersity of biomaterials, and the synthesis of entirely new biomaterials. With advances in the isolation of biocatalysts, new techniques for engineering enzymes, the availability of an increasing range of novel reaction environments for enzymes, and better analytical tools to follow enzyme reactions, enzymatic polymerization is just beginning to impact traditional synthetic methods of polymers. The enzymatic synthesis for the formation or modification of biomaterials is compelling when these advances are coupled with environmental considerations.

1.3 AIM OF THE STUDY

Biodegradable polymers nowadays applied in temporary therapeutic aids generally consist of monomeric units which are also present in the human body, such as α-hydroxy acids and α-amino acids. In principle, these polymers degrade without formation of toxic products. With the development of therapeutics and pharmaceutics, novel biodegradable polymers with improved properties as compared to the existing biomaterials are expected. The aim of the study is to synthesize and characterize new biodegradable polyester amides and their block copolymers.

Block copolymers of polydepsipeptides and PEO

Different types of polydepsipeptide-polyether block copolymers will be synthesized via ring-opening polymerization of morpholine-2,5-diones in the presence of hydroxytelechelic poly(ethylene oxide) (PEO) with stannous octoate as a catalyst, i.e., an AB block copolymer, an ABA block copolymer, an $(A)_2B$ star shaped copolymer and an $(A)_2B(A)_2$ copolymer, where A is a polydepsipeptide and B a PEO block. The molar ratio of morpholine-2,5-dione to PEO will be varied to obtain copolymers with different weight fractions of polydepsipetide blocks.

Block copolymers with poly(Glc-Val) and PEO will be synthesized via ring-opening polymerization of 3(S)-isopropyl-morpholine-2,5-dione in the presence of PEO with calcium hydride (CaH_2) as a co-initiator. CaH_2 is selected because it is known as a PLA co-initiator and it is not supposed to lead to toxic impurities in the final product.

Block copolymers based on LLA or DLLA, amino acids and PEO

Block copolymers based on LA, amino acids and PEO will be synthesized via ring-opening polymerization of morpholine-2,5-diones and DLLA or LLA in the presence of PEO with stannous octoate as a catalyst. The properties of the block copolymers, especially the hydrophilicity and degradation behavior will be studied.

Enzyme-catalyzed polymerization of morpholine-2,5-diones

Stannous octoate is one of the most effective catalysts that produce both high yields and high molecular weight. However, stannous octoate, like many other catalysts, is more or less cytotoxic. Meanwhile, difficulties in removal of the catalyst from the resulting polymer have limited its utilization in many cases. To avoid these shortcomings enzymatic polymerization is a feasible method to obtain polyesters and polyesteramides. The ring-opening polymerization of morphoilne-2,5-diones will be carried out in the presence of enzymes, such as lipases. The thesis will explore important experimental variables and resulting effects on polymerization and polymer structure. The effects of enzymes, reaction temperature, time and water content on monomer conversion and product molecular weight will be investigated.

In this thesis the synthesis and characterization of new biodegradable polymers will be described. The new synthetic method to obtain polydepsipeptides via enzyme-catalyzed ring-opening polymerization of morpholine-2,5-diones will be discussed, too.

2. RESULTS AND DISCUSSION

2.1 $Sn(oct)_2$ catalyzed polymerization of cyclic depsipeptides

2.1.1 Synthesis and characterization of ABA triblock copolymers with poly(Glc-Ile) and PEO blocks

PEO is water soluble and shows favourable biocompatibility[92]. Considerable effort has been focused on the preparation of polyester-PEO di- and triblock copolymers using a monohydroxy or α,ω-dihydroxy poly(ethylene oxide) as an initiator for the polymerization of lactones[93-97]. Cohn and Younes synthesized block copolymers of polylactide-PEO by polytransesterification reactions of lactide in the presence of PEO using antimony trioxide as a catalyst[98]. Such amphiphilic di- and triblock copolymers exhibit different properties, i.e. permeability, degradability, which may lead to new application possibilities. Chen et al.[99] reported multiblock copolymers comprising of polylactide and PEO via ring-opening copolymerization of L-lactide and ethylene oxide by using isobutylaluminoxane or an Sn-Al bimetallic catalyst. The multiblock copolymers are useful for a wide range of biomedical applications including bioresorbable implant materials and tissue engineering.

Synthetic biodegradable polydepsipeptides are alternating copolymers of α-amino acids and α-hydroxy acids. They are known to be nontoxic and degradable *in vitro* and *in vivo*. They can be used as biomaterials for specific applications. The copolymerization of morpholine-2,5-diones (MD) with DLLA, GA or CL produces polyesteramides with a variety of properties[35,38].

In this part the synthesis and characterization of ABA block copolymers via polymerization of 3(S)-*sec*-butyl-morpholine-2,5-dione (Cyclo(Glc-Ile)) using hydroxy-telechelic PEO6000 as an initiator in the presence of stannous octoate are described.

Synthesis and characterization of poly(Glc-Ile)-b-PEO-b-poly(Glc-Ile) copolymers

Block copolymers poly(Glc-Ile)-*b*-PEO-*b*-poly(Glc-Ile) (PGI/EO) were synthesized by polymerization of Cyclo(Glc-Ile) in the presence of PEO6000 and $Sn(oct)_2$ as a catalyst at 140 °C for 9 h (Scheme 2). The copolymerizations with various mole fractions of Cyclo(Glc-Ile) in the feed, $F_{Cyclo(Glc\text{-}Ile)}$, ranging from 12 to 63% and the corresponding mole fractions of Cyclo(Glc-Ile) in the block copolymers, $f_{Cyclo(Glc\text{-}Ile)}$, are listed in Tab. 2 and 3. The composition of the triblock copolymers was determined by means of ^1H NMR spectroscopy

from the intensity ratio of the signals originating from the PEO block at δ =3.65 ppm (s; 4H, CH_2CH_2) and from the poly(Glc-Ile) block at δ = 0.92-0.99 ppm (m; 6H, $2CH_3$) according to the following equation (Fig. 1):

$$f_{Cyclo(Glc-Ile)} = \frac{I_{CH_3}/6}{I_{CH_3}/6 + I_{CH_2}/4},$$

where I_{CH_3} and I_{CH_2} are the intensity of the signals originating from the poly(Glc-Ile) block at δ = 0.92-0.99 ppm and from the PEO block at δ =3.65 ppm, respectively.

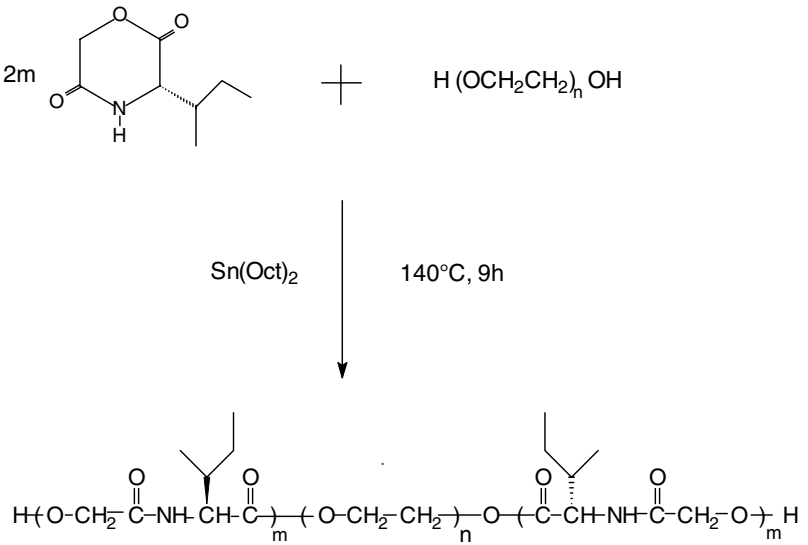

Scheme 2. Reaction scheme of the preparation of poly(Glc-Ile)-*b*-PEO-*b*-poly(Glc-Ile).

The data demonstrate that the triblock copolymers are obtained by ring-opening polymerization of Cyclo(Glc-Ile) with hydroxytelechelic PEO6000 in high yields (about 80%). $Sn(oct)_2$ as the catalyst forms an effective initiation system in conjunction with the α,ω-hydroxyl end groups of PEO. A reaction mechanism for the polymerization of lactide with hydroxytelechelic PEO was proposed and described in detail in several papers[97,100]. This mechanism can be extended to the polymerization of Cyclo(Glc-Ile), because the ring-opening of Cyclo(Glc-Ile) occurs exclusively at the ester group.

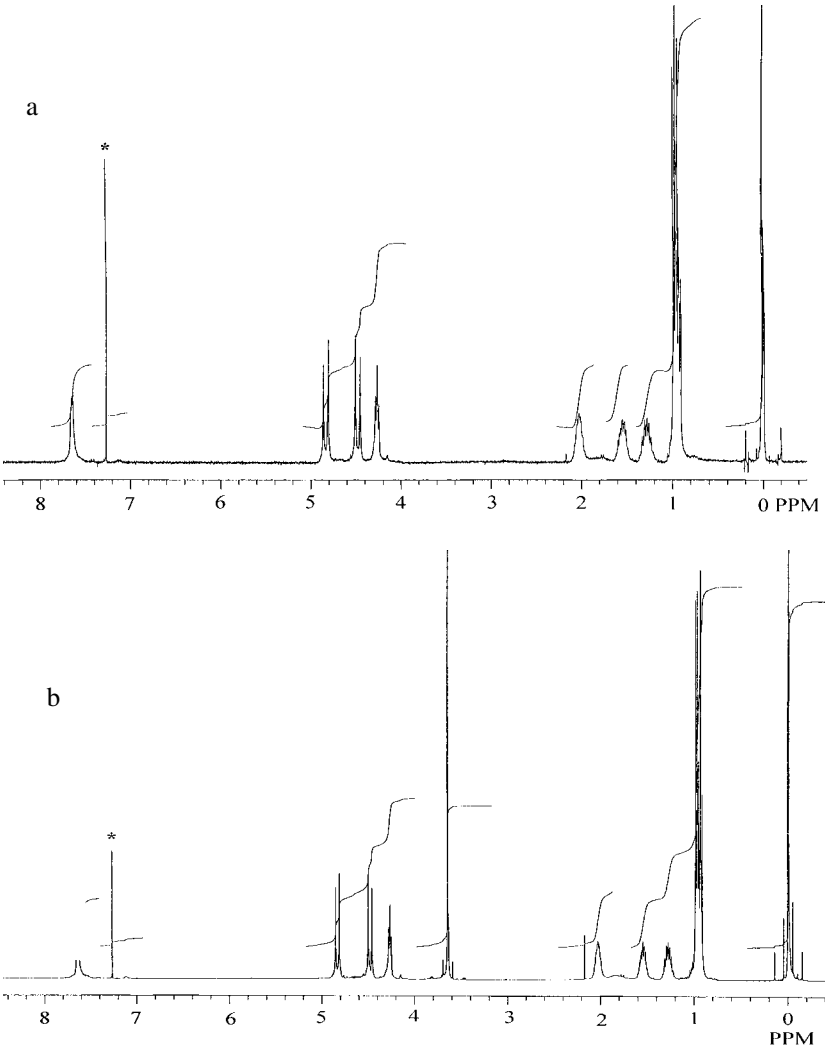

Fig. 1. a) ^{1}H-NMR spectrum of homopolymer of poly(Glc-Ile) in $CDCl_3$/TMS; b) ^{1}H-NMR spectrum of triblock copolymer PGI/EO1 in $CDCl_3$/TMS; * = $CDCl_3$ peaks.

Tab. 2. Copolymerization of Cyclo(Glc-Ile) with PEO in the presence of $Sn(oct)_2$ catalyst [a)]

No.	PEO in g	Cyclo(Glc-Ile) in g	$F_{Cyclo(Glc-Ile)}$ [b)] in %	M/OH [c)]	$W_{polymer}$ in g	Yield [d)] in %
Poly(Glc-Ile)	0	0.9863	100	-	0.83	84.2
PGI/EO1	0.1425	0.9476	63.1	116	0.89	81.6
PGI/EO2	0.2720	0.8206	43.7	52.8	0.86	78.7
PGI/EO3	0.4109	0.7066	30.6	30.1	0.90	80.6
PGI/EO4	0.5287	0.5390	20.8	17.9	0.89	83.3
PGI/EO5 [e)]	0.5287	0.5390	20.8	17.9	0	0
PGI/EO6	0.8103	0.4262	11.9	9.2	1.00	80.9

a) T_p = 140 °C, t_p= 9 h.
b) mole fraction of Cyclo(Glc-Ile) in the feed, $F_{Cyclo(Glc-Ile)}$ = [Cyclo(Glc-Ile)]/([Cyclo(Glc-Ile)] + [EO]) × 100%, EO is the repeat unit of PEO, ethylene oxide.
c) M/OH = [Cyclo(Glc-Ile)]/[OH].
d) calculated according to W/(Weight of PEO + Weight of Cyclo(Glc-Ile)) × 100%.
e) precipitation in methanol.

Tab. 3. Compositions and molecular weight of triblock copolymers

No.	$F_{Cyclo(Glc-Ile)}$ in %	$f_{Cyclo(Glc-Ile)}$ [a)] in %	$\overline{M}_{n,F}$ [b)] $\times 10^{-3}$	$\overline{M}_{n,f}$ [c)] $\times 10^{-3}$	$\overline{M}_n$ [d)] $\times 10^{-3}$	$\overline{M}_w$ [d)] $\times 10^{-3}$	$\overline{M}_w / \overline{M}_n$ [d)]
Poly(Glc-Ile)	100	100			25.9	54.0	2.09
PGI/EO1	63.1	56.8	45.9	36.7	30.9	50.6	1.64
PGI/EO2	43.7	35.4	24.1	18.8	17.6	29.8	1.69
PGI/EO3	30.6	22.5	16.3	12.8	15.9	24.1	1.52
PGI/EO4	20.8	16.2	12.1	10.5	15.6	23.3	1.50
PGI/EO6	11.9	4.6	7.6	7.13	14.3	18.8	1.32

a) mole fraction of Cyclo(Glc-Ile) in the copolymer, $f_{Cyclo(Glc-Ile)}$ = [Cyclo(Glc-Ile)]/([Cyclo(Glc-Ile)] + [EO]) × 100%, determined by ^{1}H NMR spectroscopy.
b) calculated by mole fraction of Cyclo(Glc-Ile) in the feed, $F_{Cyclo(Glc-Ile)}$.
c) molecular weight of triblock copolymers was estimated by ^{1}H NMR spectroscopy.
d) molecular weight of triblock copolymers was measured by GPC with DMAc as solvent.

The IR spectra of poly(Glc-Ile), PEO6000, and the triblock copolymer PGI/EO6 are shown in Fig. 2. The strong absorption band at 3390 cm^{-1} (Fig.2 (1) and (3)) is assigned to the stretching band of the N-H group in the poly(Glc-Ile) blocks. The band at 1752 cm^{-1} is due to the C=O stretching mode of the ester group, and the band at 1649 cm^{-1} to the bending vibration of the N-H bond and the stretching mode of the C-N bond of the CONH group. The amide II band appears at 1538 cm^{-1}. The characteristic absorption band of PEO at 1112 cm^{-1} (Fig. 2 (2)) overlaps with the absorption band of the C-O bond in poly(Glc-Ile) at 1142 cm^{-1} to show 1114 cm^{-1}. When the IR spectra of poly(Glc-Ile) and the block copolymers with

lower content of PEO (for example PGI/EO1, not shown in Fig.2) are compared, no significant differences are found.

Fig. 1(b) shows the ^{1}H NMR spectrum of the block copolymer PGI/EO1. The chemical shift at 3.65 ppm originates from the methylene protons in the PEO blocks, at 7.64 ppm from amide proton, at 0.92-0.99, 1.21-1.75, 1.96-2.04 and 4.24-4.28 ppm from the isoleucine residue in the poly(Glc-Ile) block and 4.86 ppm(AB-system, ^{AB}J = 15.6 Hz) from glycolate residue in the poly(Glc-Ile) block. In the ^{1}H NMR spectrum of the block copolymers there is no singlet at 4.65 ppm, which is evidence for the absence of racemization of the isoleucine residue during copolymerization of Cyclo(Glc-Ile) with PEO in the presence of $Sn(oct)_2$ [46].

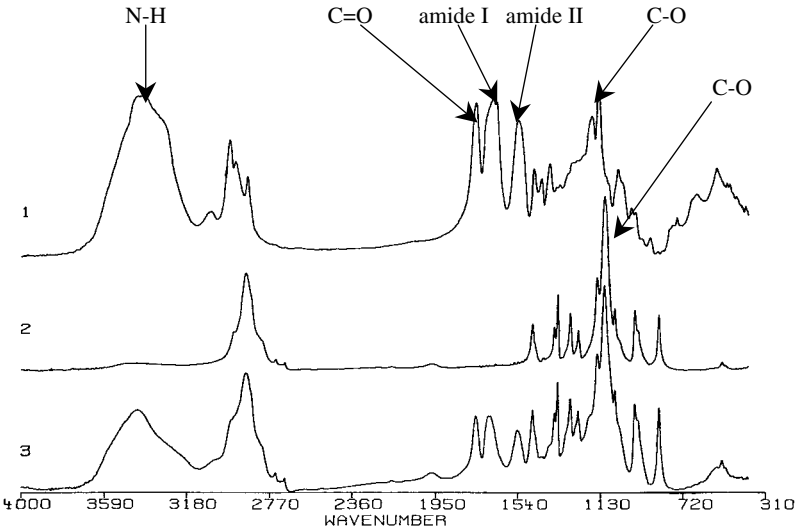

Fig. 2. IR of homopolymer of poly(Glc-Ile) (1), PEO6000(2), and copolymer PGI/EO6(3).

The data of copolymerization of Cyclo(Glc-Ile) with PEO are compiled in Tab. 2. It can be seen that when $f_{Cyclo(Glc-Ile)}$ is lower (No. PGI/EO5), no precipitate in methanol is collected after polymerization. This is due to the fact that the copolymers with short poly(Glc-Ile) segments are soluble in methanol and water. PGI/EO3 is only partly soluble in methanol and water, but PGI/EO2 and PGI/EO1 are insoluble. Fig. 3 shows the compositions of the copolymers as determined from ^{1}H NMR as a function of the mole fraction of Cyclo(Glc-Ile) in the feed. $f_{Cyclo(Glc-Ile)}$ increases with increasing $F_{Cyclo(Glc-Ile)}$, e.g., when $F_{Cyclo(Glc-Ile)}$ is 63.1%,

$f_{Cyclo(Glc-Ile)}$ is 56.8%, and hence nearly equal to the value of 57.4% calculated from the following equation:

$$f_{Cyclo(Glc-Ile)} = \frac{(W - W_{PEO})/M_{Cyclo(Glc-Ile)}}{(W - W_{PEO})/M_{Cyclo(Glc-Ile)} + W_{PEO}/M_{EO}},$$

where $M_{Cyclo(Glc-Ile)}$ and M_{EO} are the molecular weight of Cyclo(Glc-Ile) and the repeat unit of PEO, respectively.

It is found that all CH_2OH end-groups of PEO are esterified with Cyclo(Glc-Ile) units by analysis after reaction with trifluoroacetic anhydride[101]. The GPC measurements confirms that all PEO molecules have reacted with Cyclo(Glc-Ile), since there is no peak corresponding to PEO. Similar results were observed for the copolymerization of PEO with LA and GL by others[101, 102].

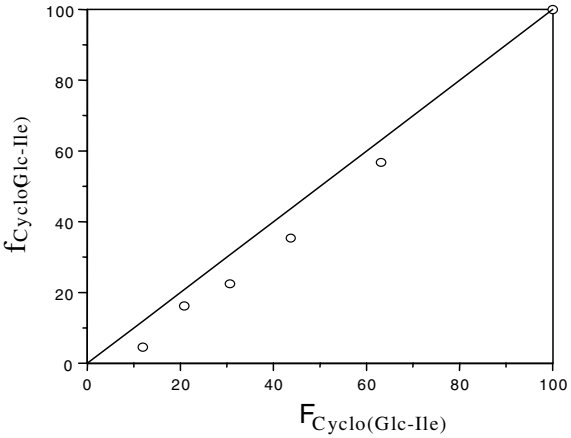

Fig. 3. Relation of $f_{Cylco(Glc-Ile)}$ with $F_{Cyclo(Glc-Ile)}$.

Thermal analysis of triblock copolymers

The melting and crystallization behaviour of the triblock copolymers with different composition was investigated by means of DSC. All samples were first heated above the melting temperature, then allowed to crystallize by cooling to —70 °C at a rate of 10 °C/min and finally heated at 10 °C/min from -70 to 150 °C.

PEO with molecular weight $\overline{M_n}$ =6000 exerts a peak on first melting (T_m = 60.6 °C) and crystallization (T_c = 36.3 °C). The endotherm of the second melting was found at 60.3 °C, although Wunderlich observed double peaks upon second heating[103].

The DSC curves of poly(Glc-Ile) with molecular weight $\overline{M_n}$ = 25900 show a single melting peak ($T_{m(1st\ heating)}$ = 97.2 °C, ΔH = 18.5 J/g) and glass transition ($T_{g(1st\ heating)}$ = 65.5 °C, $T_{g(cooling)}$ = 66.7 °C and $T_{g\ (2nd\ heating)}$ = 73.3 °C). The cooling curve and 2nd heating curve of poly(Glc-Ile) show a glass transition, and neither a crystallization exotherm at cooling nor a melting endotherm upon 2nd heating.

The DSC curves of the triblock copolymers obtained upon first heating are presented in Fig. 4. Curve 2 and 3 show one endotherm that corresponds to the melting of the PEO block. Curve 4 and 5 exert each one distinct endotherm and the indication of another endotherm that correspond to the melting of the constituent blocks. And curve 6 shows only one weak endotherm that belongs to the melting of poly(Glc-Ile) block in the copolymer. The crystallinity of the PEO block is calculated from the enthalpy of melting with respect to the PEO content. Crystallinity and melting temperature of the PEO block (Tab. 4) are considerably lower than those of the PEO homopolymer. The PEO block does not crystallize upon cooling after the first heating when the weight fraction of the poly(Glc-Ile) block in the triblock copolymer is more than 55 % (PGI/EO3).

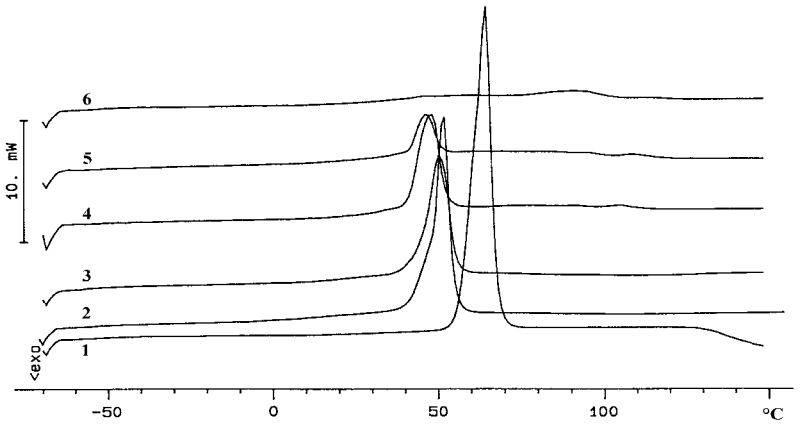

Fig. 4. DSC thermograms of copolymers of PGI/EO and PEO6000 upon first heating.

curve 1: PEO6000, curve 2: PGI/EO6, curve 3: PGI/EO4, curve 4: PGI/EO3, curve 5: PGI/EO2, curve 6: PGI/EO1.

Tab. 4. Crystallinity (α_c [a)]) and melting point of PEO block in PGI/EO triblock copolymers

No.	PEO[b)]	1st heating			Cooling		2nd heating		
	(wt%)	T_m(°C)	ΔH(J/g)	α_c(%)	T_c(°C)	ΔH(J/g)	T_m(°C)	ΔH(J/g)	α_c(%)
1	100	60.6	184.0	97.7	36.3	174.5	60.3	183.9	97.6
2	84.1	49.6	114.4	72.2	23.5	93.4	49.8	92.9	58.6
3	57.0	48.6	78.2	72.8	22.6	59.2	46.6	53.1	49.4
4	47.0	46.1	61.4	69.3	-	-	-	-	-
5	31.9	45.4	20.7	34.4	-	-	-	-	-
6	16.4	-	-	-	-	-	-	-	-

a) calculated from $\Delta H \times M_{EO} / (\Delta H_0 \times PEOwt\%) \times 100\%$, ΔH_0 (8.29 kJ/mol) is the enthalpy of 100% crystallinity of PEO.
b) weight percent of PEO block in triblock copolymers, estimated by ^{1}H NMR spectroscopy.

T_m of the PEO block in the copolymer is not observed when the weight fraction of PEO in the block copolymer is lower than 16% (PGI/EO1). This indicates that the PEO block in PGI/EO1 is an amorphous phase since the long poly(Glc-Ile) block hinders the crystallization of the PEO block.

Tab. 5 shows that the melting endotherm of poly(Glc-Ile) block increases with increasing poly(Glc-Ile) block content in the triblock copolymers. The melting temperature of the poly(Glc-Ile) block changes very little with increasing length of the poly(Glc-Ile) block, but it is smaller than that of the poly(Glc-Ile) homopolymer.

It is well known that PEO is a semicrystalline polymer, while polydepesipeptides are polymers of low crystallinity or amorphous polymers. The DSC data suggest that the crystallizability of the PEO blocks is effectively decreased by the attachment of poly(Glc-Ile) segments.

Tab. 5. Results of DSC of poly(Glc-Ile) block in PGI/EO triblock copolymers

No.	T_m(°C)	ΔH(J/g)
Poly(Glc-Ile)	97.2	18.5
PGI/EO1	90.7	12.8
PGI/EO2	90.3	1.5
PGI/EO3	89.8	0.9
PGI/EO4	-	-
PGI/EO6	-	-

Hydrophilicity of copolymers

The PGI/EO copolymers bearing hydrophilic PEO blocks synthesized here are expected to have better properties as a drug delivery matrix than poly(Glc-Ile). The hydrophilicity of triblock copolymers was determined by measuring the static contact angle of water. The results presented in Fig. 5 clearly show that the static contact angle θ decreases sharply with increasing PEO content in the triblock copolymers. For example, when the PEO content is 47 wt% the contact angle is 48° which is much smaller than that of poly(Glc-Ile) (θ = 82°). This reveals that the hydrophilicity of the block copolymers depends on the PEO content, in other words, PEO improve the hydrophilicity of the copolymers.

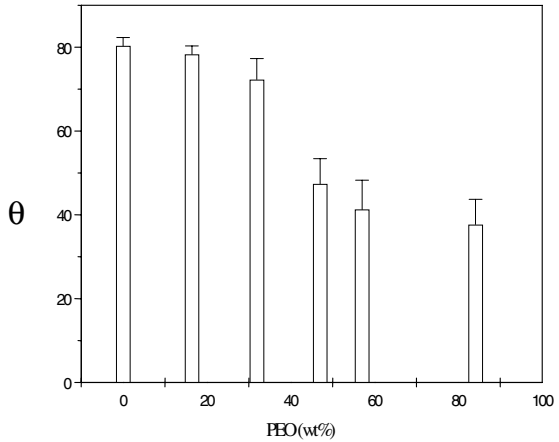

Fig. 5. Static contact angle (θ) of PGI/EO as a function of PEO (wt%).

2.1.2 Synthesis and characterization of ABA triblock copolymers with poly(Glc-Leu) and PEO blocks

Synthesis and characterization of poly(Glc-Leu)-b-PEO-b-poly(Glc-Leu)

Block copolymers poly(Glc-Leu)-*b*-PEO-*b*-poly(Glc-Leu) (PGL/EO) were synthesized by polymerization of Cyclo(Glc-Leu) in the presence of hydroxytelechelic PEO6000 and $Sn(oct)_2$ as a catalyst at 140 °C for 9 h. The copolymerizations with various fractions of Cyclo(Glc-Leu) in the feed, $F_{Cyclo(Glc-Leu)}$, ranging from 13.9 to 75.4 mol% and the corresponding mole fractions of Cyclo(Glc-Leu) in the block copolymers, $f_{Cyclo(Glc-Leu)}$, are listed in Tab. 6 and 7. The composition of the triblock copolymers was determined by means of ^{1}H NMR spectroscopy from the intensity ratio of the signals originating from the PEO block at $\delta = 3.51$ ppm (s; 4H, CH_2CH_2) and from the poly(Glc-Leu) block at $\delta = 0.83$-0.90 ppm (6H, $2CH_3$) according to the following equation:

$$f_{\text{Cyclo(Glc-Leu)}} = \frac{I_{CH_3}/6}{I_{CH_3}/6 + I_{CH_2}/4},$$

where I_{CH_3} and I_{CH_2} are the intensity of the signals originating from the poly(Glc-Leu) block at δ=0.83-0.90 ppm and from the PEO block at δ=3.51 ppm, respectively.

The data (Tab. 7) demonstrate that the triblock copolymers are obtained by ring-opening polymerization of Cyclo(Glc-Leu) with hydroxytelechelic PEO6000 as initiator in high yield (about 90%). $Sn(oct)_2$ as the catalyst forms an effective initiation system with the α,ω-hydroxyl end groups of PEO. A reaction mechanism for block copolymer formation of lactide with PEO was proposed and described in detail in several papers[97,100]. This mechanism can be extended to the block copolymerization of Cyclo(Glc-Leu) with PEO, because the ring-opening of Cyclo(Glc-Leu) occurs exclusively at the ester group (Scheme 3).

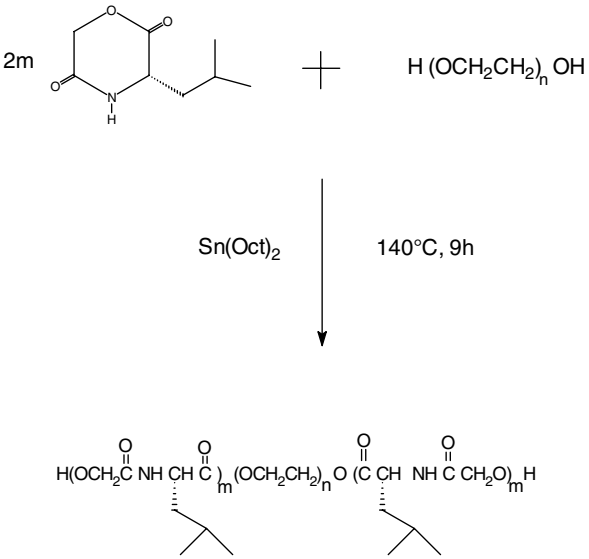

Scheme 3. Preparation of poly(Glc-Leu)-*b*-PEO-*b*-poly(Glc-Leu).

Tab. 6. Copolymerization of Cyclo(Glc-Leu) in the presence of PEO and $Sn(oct)_2$ catalyst[a)]

No.	PEO in g	Cyclo(Glc-Leu) in g	$F_{Cyclo(Glc-Leu)}$ [b)] in %	M/OH[c]	$W_{polymer}$ in g	Yield [d)] in %
Poly(Glc-Leu)	0	1.7312	100	-	1.55	89.5
PGL/EO1	0.7539	0.4747	13.9	11.0	1.04	84.6
PGL/EO2	0.5592	0.6268	22.4	19.6	1.06	89.4
PGL/EO3	0.5266	0.9790	32.3	32.6	1.32	87.7
PGL/EO4	0.3125	0.9555	44.0	53.6	1.17	92.3
PGL/EO5	0.1566	0.9840	63.0	110.1	1.04	91.2
PGL/EO6	0.0864	1.0321	75.4	209.3	1.06	94.8

a) [Cyclo(Glc-Leu)]/[$Sn(oct)_2$] = 125. b) mole fraction of Cyclo(Glc-Leu) in the feed. c) M/OH = [Cyclo(Glc-Leu)]/[OH]. d) calculated according to W/(Weight of PEO + Weight of Cyclo(Glc-Leu)) ×100%.

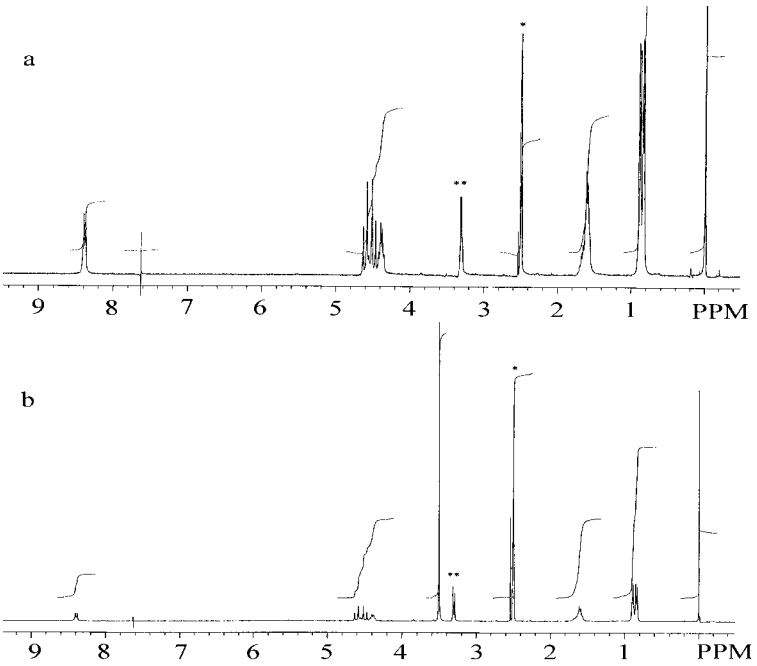

Fig. 6. a) ^{1}H NMR spectrum of homopolymer of poly(Glc-Leu) in DMSO-d_6/TMS; b) ^{1}H NMR spectrum of triblock copolymer PGL/EO3 in DMSO-d_6/TMS; *.= DMSO peaks; ** = H_2O peaks.

Tab. 7. Compositions and molecular weight of triblock copolymers

No.	$F_{Cyclo(Glc-Leu)}$ in %	$f_{Cyclo(Glc-Leu)}$ [a] in %	$\overline{M_n}$,F [b] $\times 10^{-3}$	$\overline{M_n}$,f [c] $\times 10^{-3}$	$\overline{M_n}$ [d] $\times 10^{-3}$	$\overline{M_n}$ [e] $\times 10^{-3}$	$\overline{M_w}$ [e] $\times 10^{-3}$	$\overline{M_w}$ / $\overline{M_n}$ [e]
Poly(Glc-Leu)	100	100				40.5	64.7	1.60
PGL/EO1	13.9	9.1	3.8	2.4	8.4	13.7	18.7	1.36
PGL/EO2	22.4	18.4	6.7	5.3	11.3	13.2	19.9	1.51
PGL/EO3	32.3	27.7	11.1	8.9	14.9	18.9	34.5	1.83
PGL/EO4	44.0	38.7	18.3	14.7	20.7	21.5	28.4	1.32
PGL/EO5	63.0	59.4	39.8	34.2	40.2	40.0	53.6	1.34
PGL/EO6	75.4	72.2	71.6	60.7	66.7	65.8	99.3	1.51

a) mole fraction of Cyclo(Glc-Leu) in the copolymer, determined by ^{1}H NMR spectroscopy.
b) calculated from mole fraction of Cyclo(Glc-Leu) in the feed.
c) estimated by ^{1}H-NMR spectroscopy.
d) molecular weight of triblock copolymers estimated from ^{1}H NMR spectrum.
e) molecular weight of triblock copolymers obtained from GPC with DMAc as solvent.

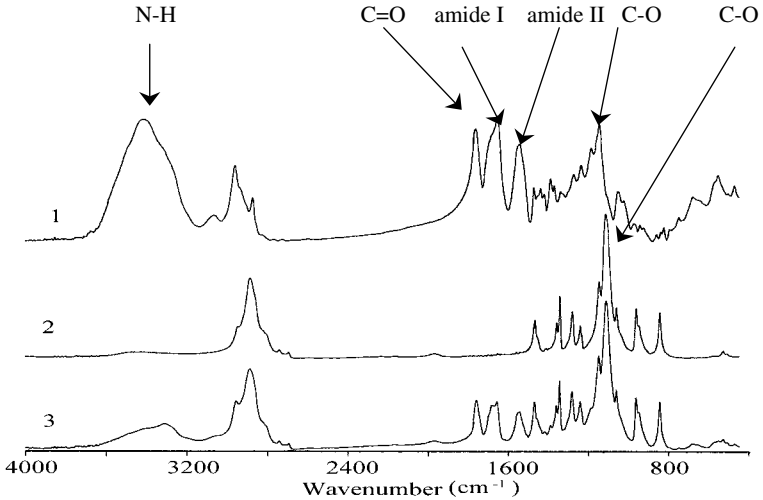

Fig. 7. IR of homopolymer of poly(Glc-Leu) (1), PEO6000 (2) and copolymer PGL/EO1 (3).

The IR spectra of poly(Glc-Leu), PEO6000, and the triblock copolymer PGL/EO1 are shown in Fig. 7. The strong absorption band at 3417 cm^{-1} (Fig. 7 (1) and (3)) is assigned to the stretching band of the N-H group in the poly(Glc-Leu) blocks. The band at 1757 cm^{-1} is due to the C=O stretching mode of the ester group, and the band at 1654 cm^{-1} to the bending vibration of the N-H bond and the stretching mode of the C-N bond of the CONH group. The amide II band appears at 1543 cm^{-1}. The characteristic absorption band of PEO at 1112 cm^{-1} (Fig. 7 (2)) is due to the C-O bond in the PEO block. When the IR spectra of poly(Glc-Leu) and the block copolymers with low content of PEO (for example PGL/EO6, not shown in Fig. 7) are compared, no significant differences are found, because the characteristic absorption band of the PEO block overlaps with the absorption band of the C-O bond in the poly(Glc-Leu) block.

Fig. 6(b) shows the ^{1}H NMR spectrum of the block copolymer PGL/EO3. The chemical shift at 3.51 ppm originates from the methylene protons in the PEO block, at 8.40 ppm from the amide proton, at 0.83-0.85, 0.88-0.90, 1.59-1.60 and 4.38-4.41 ppm from the leucine residue in the poly(Glc-Leu) block and at 4.47-4.64 ppm (AB-system, ^{AB}J = 14.6 Hz) from the glycolate residue in the poly(Glc-Leu) blocks. In the ^{1}H NMR spectrum of the block copolymers there is no singlet at 4.55 ppm, which is evidence for the absence of racemization of the leucine residue during copolymerization of Cyclo(Glc-Leu).

Fig. 8 shows the composition of the copolymers as determined from ^{1}H NMR as a function of the mole fraction of Cyclo(Glc-Leu) in the feed. $f_{Cyclo(Glc-Leu)}$ increases with increasing $F_{Cyclo(Glc-Leu)}$, e.g., when $F_{Cyclo(Glc-Leu)}$ is 63.0 mol% $f_{Cyclo(Glc-Leu)}$ is determined to be 59.4 mol%, and hence nearly equal to the value of 59.2 mol% which is calculated from the following equation:

$$f^*_{\text{Cyclo(Glc-Leu)}} = \frac{(W - W_{PEO})/M_{\text{Cyclo(Glc-Leu)}}}{(W - W_{PEO})/M_{\text{Cyclo(Glc-Leu)}} + W_{PEO}/M_{EO}},$$

where $M_{Cyclo(Glc-Leu)}$ and M_{EO} are the molecular weight of Cyclo(Glc-Leu) and of the repeat unit of PEO, respectively. W is the weight of the triblock copolymer, and W_{PEO} is the weight fraction of PEO in the feed.

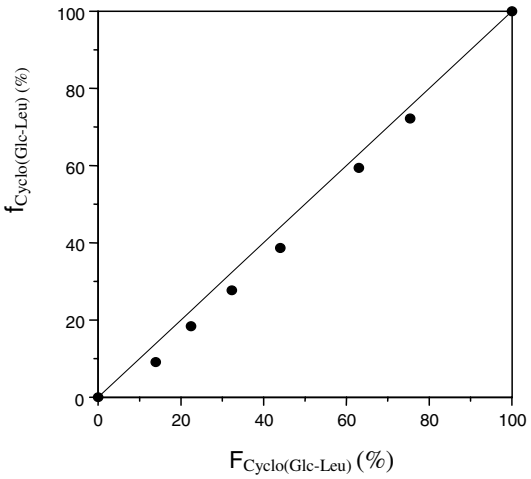

Fig. 8. Relation of $f_{Cyclo(Glc-Leu)}$ with $F_{Cyclo(Glc-Leu)}$.

The triblock copolymers were purified by dissolving them in DMSO and precipitating them from ether. Both reacted and unreacted PEO are soluble in DMSO and precipitate from ether. Thus, W-W_{PEO} is the weight fraction of the poly(Glc-Leu) block in the copolymers.

It is found that all CH_2OH end groups of PEO are esterified with Cyclo(Glc-Leu) units using the trifluoroacetic anhydride (TFAA) method[102]. TFAA causes rapid esterification of OH end-groups, and the neighboring CH_2 protons experience a downfield shift of about 0.6 $\pm$ 0.1 ppm. It was found that the chemical shift of CH_2OH end-groups of poly(Glc-Leu) changed from 3.85 ppm to 4.30 ppm when the triblock copolymers were reacted with TFAA. GPC of

the triblock copolymers shows a bimodal distribution at an elution volume below that of the starting PEO6000. The bimodal distribution has also been observed for copolymers of LA and GL with PEO by others[101]. Probably, phase separation occurs during the polymerization into a poly(Glc-Leu)/Cyclo(Glc-Leu) rich and a PEO rich phase, enhancing further chain growth of the longer poly(Glc-Leu) chains. The GPC result confirms that all PEO molecules have reacted with Cyclo(Glc-Leu), because there is no PEO6000 peak in GPC. Number average molecular weights determined by means of GPC and ^{1}H NMR spectroscopy are in good agreement. $\overline{M_n}$ of the triblock copolymers increases with increasing Cyclo(Glc-Leu) content in the feed (Tab. 7). The polydispersities of poly(Glc-Leu) and the triblock copolymers are in the range of 1.32 to 1.83.

Thermal analysis of triblock copolymers

The melting and crystallization behaviour of the triblock copolymers with different composition was investigated by means of DSC. All samples were first heated above the melting temperature, then cooled to -20 °C at a rate of 10 °C/min and finally heated at 10 °C/min from -20 to 220 °C.

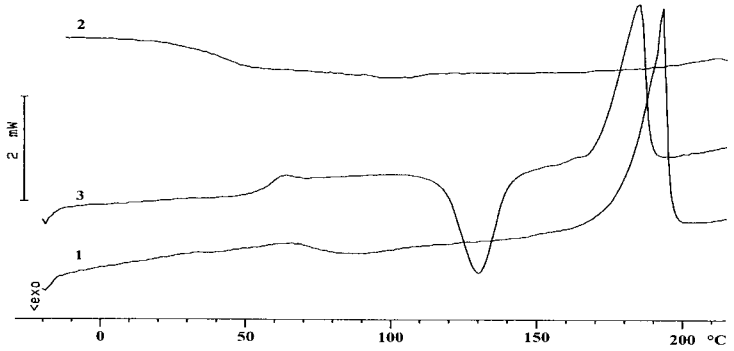

Fig. 9. DSC thermograms of poly(Glc-Leu).
curve 1: first heating, curve 2: cooling, curve 3: second heating.

The DSC curve of poly(Glc-Leu) with a molecular weight $\overline{M_n}$ = 40500 shows a single melting peak($T_{m(1st\ heating)}$ = 192.4 °C, ΔH = 52.2 J/g) and a glass transition temperature (T_g = 72 °C) upon first heating (Fig. 9). Upon cooling poly(Glc-Leu) does not crystallize, but upon the second heating it crystallizes at 130.1°C and the enthalpy of the exotherm is 35.4 J/g. The

second heating curve of poly(Glc-Leu) shows a glass transition at 56 °C and a melting endotherm (T_m = 184.6 °C, ΔH = 38.2 J/g).

The DSC curves of the triblock copolymers obtained upon first heating are presented in Fig 10. Curve 2 - 5 show two distinct endotherms that correspond to the melting of each constituent block. Curve 6 exerts only one endotherm that belongs to the melting of the poly(Glc-Leu) block in the copolymer. An endotherm due to the melting of the PEO block in the copolymer PGL/EO6 is not observed, because the mole fraction of poly(Glc-Leu) in this triblock copolymer is very high (72.2%). The crystallization of the poly(Glc-Leu) block hinders the crystallization of the PEO block. A similar result was observed for poly(trimethylene carbonate)-PEO-poly(trimethylene carbonate) with central PEO block by Wang et al[104] and PLLA-PEO-PLLA by Mohammadi-Rovshandeh[105].

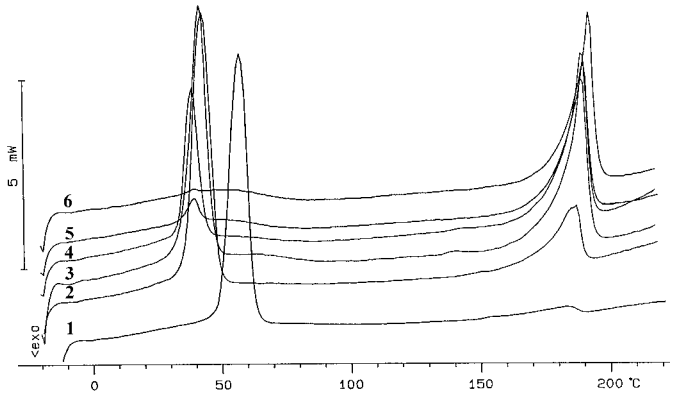

Fig. 10. DSC thermograms of triblock copolymers of PGL/EO upon first heating.

Tab. 8. Crystallinity and melting point of PEO block in PGL/EO triblock copolymers

No.	PEO[a] in	1st heating			Cooling		2nd heating		
	wt%	T_m/°C	ΔH/J/g	α_c/%	T_c/°C	ΔH/J/g	T_m/°C	ΔH/J/g	α_c/%
PEO	100	60.6	184.0	97.7	36.3	174.5	60.3	183.9	97.6
PGL/EO1	71.1	50.4	101.3	75.6	17.8	85.7	41.5	95.5	71.3
PGL/EO2	53.2	42.0	73.8	73.6	19.1[b]	29.7[b]	36.3	29.8	29.7
PGL/EO3	40.3	41.0	45.8	60.3	19.6	31.7	42.6	27.0	35.6
PGL/EO4	28.9	39.4	26.7	49.1	-	-	-	-	-
PGL/EO5	15.1	39.0	6.7	23.6	-	-	-	-	-
PGL/EO6	9.0	-	-	-	-	-	-	-	-

a) weight percent of PEO block in triblock copolymers, estimated by ^{1}H NMR spectroscopy.
b) crystallization at second heating.

The PEO block does not crystallize upon cooling after the first heating when the weight fraction of the PEO block in the triblock copolymer is less than 29% (PGL/EO4). T_g of the PEO component is not detected for copolymer compositions investigated in the present work. The crystallinity of the PEO block is calculated from the enthalpy of melting with respect to the PEO content. Crystallinity and melting temperature of the PEO block (Tab. 8) are considerably lower than those of the PEO homopolymer. The crystallinity decreases with decreasing PEO content in the triblock copolymers and with increasing length of the poly(Glc-Leu) block.

Tab. 9. Results of DSC of poly(Glc-Leu) block in PGL/EO triblock copolymers

No.	poly(Glc-Leu) [a]	1st heating		Cooling		2nd heating		
	in wt%	T_m/°C	ΔH/J/g	T_c/°C	ΔH/J/g	T_m/°C	ΔH/J/g	T_g/°C
poly(Glc-Leu)	100	192.0	52.2	130.1[b]	35.4[b]	184.6	38.2	56
PGL/EO1	28.9	179.8	4.5	-	-	-	-	-
PGL/EO2	46.8	186.7	22.2	-	-	-	-	-
PGL/EO3	59.7	187.1	36.2	75.3	12.2	163.7	17.6	85
PGL/EO4	71.1	188.4	39.7	63.2 85.9[b]	4.1 9.7[b]	163.7	20.5	
PGL/EO5	84.9	189.4	49.0	78.2	20.8	170.7	32.5	93.7
PGL/EO6	91.0	191.4	50.7	88.2	28.0	174.7	36.6	97.6

a) determined by ^{1}H NMR. b) at second heating.

Tab. 9 shows that the melting endotherm of the poly(Glc-Leu) block increases with increasing poly(Glc-Leu) block content in the triblock copolymers. The melting temperature of the poly(Glc-Leu) block is smaller than that of the poly(Glc-Leu) homopolymer. Flory showed that if T_{m0} represents the melting point of the perfect crystal, the melting point of polymers T_m having a number-average degree of polymerization P_n is reduced as follows:[106]

$$1/T_m = 1/T_{m0} + 2R/\Delta H_f P_n \quad ,$$

where R is the universal gas constant, and ΔH_f is the enthalpy of melting. Fig. 11 shows the relation of $1/T_m$ with $1/P_n$ of the poly(Glc-Leu) block. ΔH_f was determined to be 47.7 kJ/mol. T_m increases with increasing length of the poly(Glc-Leu) block.

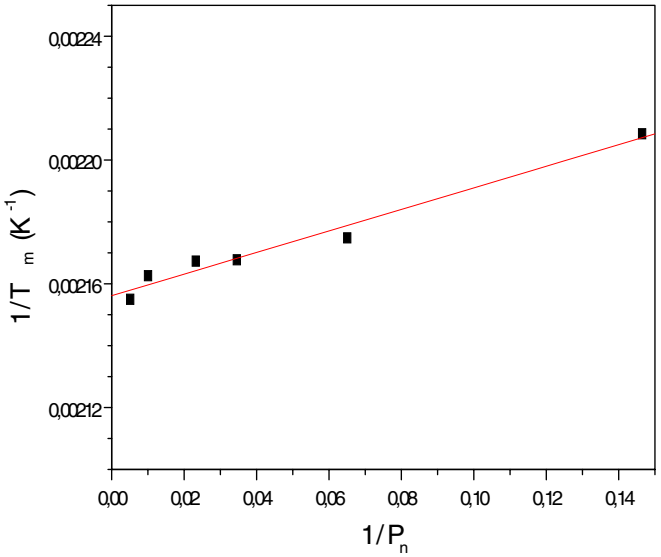

Fig. 11. Relation of $1/T_m$ and $1/P_n$.

T_g of the poly(Glc-Leu) block is dependent on the triblock copolymer composition. Tab. 9 shows that T_g of poly(Glc-Leu) homopolymer increases from 56 °C (T_g of poly(Glc-Leu)) to 93.7 °C (T_g of PGL/EO5), while the mole fraction of Cyclo(Glc-Leu) in the copolymers decreases from 100 to 59.4%.

The crystallization temperature of PEO and poly(Glc-Leu) blocks was found to be about 20 °C and about 80 °C, respectively. The crystallization temperature of the poly(Glc-Leu) block is much higher than that of the PEO block. This means that the poly(Glc-Leu) block crystallizes first from the melt. The crystallization of poly(Glc-Leu) leads to imperfect crystallization or no crystallization of the PEO blocks upon cooling. The DSC data suggest that the crystallizability of the PEO blocks is effectively decreased by the attachment of poly(Glc-Leu) segments.

Hydrophilicity of copolymers

Because the biodegradation rate of poly(morpholine-2,5-diones) (PMD) is very slow, the copolymerization of morpholine-2,5-diones with lactones or lactides such as CL and LA has been an effective approach to improve the degradation properties of PMD. Introducing

hydrophilic blocks into the main chain of the polymer is another attractive method to improve the degradation because the hydrophilic block accelerates the penetration of H_2O into the matrix. Poly(Glc-Leu) -*b*-PEO-*b*- poly(Glc-Leu), because of the hydrophilic PEO block, is expected to exert improved properties as a drug delivery system in comparison with poly(Glc-Leu). The hydrophilicity of triblock copolymers was determined by measuring the static contact angle of water. The results presented in Fig. 12 clearly show that the static contact angle θ decreases sharply with increasing PEO content in the triblock copolymers. For example, when the PEO content is 40.3 wt% the contact angle is 53° which is significantly smaller than that of poly(Glc-Leu) (θ=113°).

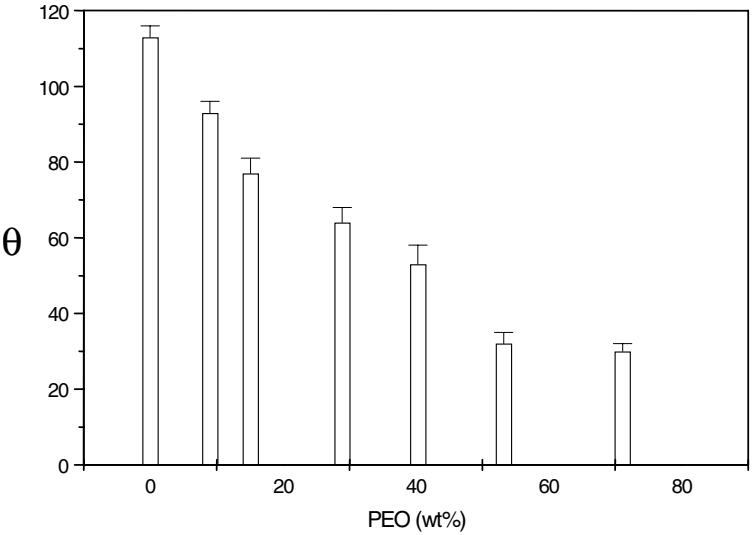

Fig. 12. Static contact angle(θ) as a function of PEO(wt%) content in poly(Glc-Leu)-*b*-PEO-*b*-poly(Glc-Leu) block copolymers.

2.1.3 Synthesis and characterization of block copolymers with PEO and poly(Glc-Ile) sequences

Recently, poly(ethylene oxide)-polyester block copolymers were prepared using monohydroxy or α,ω–dihydroxypoly(ethylene oxide) as the initiator for the polymerization of lactones[93-97]. Such amphiphilic block copolymers exhibit permeability, degradability and other properties which may lead to new applications. ABA type copolymers of lactide and PEO have been used as precursor polymers for the synthesis of biodegradable elastomers and thermosets[97,107,108].

However, the number of papers devoted to the synthesis and characterization of block copolymers of 3(S)-*sec*-butyl-morpholine-2,5-dione and PEO has been limited. We have designed and prepared four types of poly(Glc-Ile)-PEO block copolymers of different architecture with comparable total block length of poly(Glc-Ile) and PEO: (i) an AB diblock copolymer, (ii) an ABA triblock copolymer, (iii) an $(A)_2B$ star shaped block copolymer, and (iv) an $(A)_2B(A)_2$ star shaped block copolymer, where A is a poly(Glc-Ile) and B is a PEO block (Scheme 4).

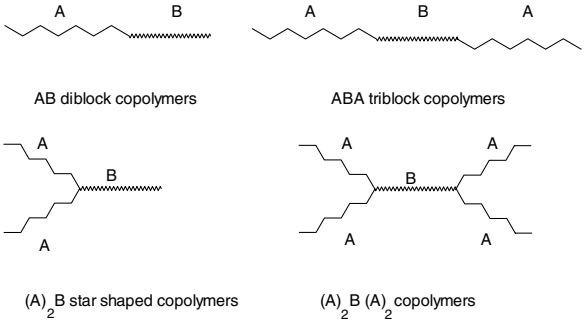

Scheme 4. Different types of poly(Glc-Ile)-PEO copolymers (A: poly(Glc-Ile), B: PEO).

Charaterization of PEO

Hydroxytelechelic PEO with a molecular weight of 1000 (PEO1000), 6000 (PEO6000), 8000 (PEO8000), 20000 (PEO20000) and monomethoxy-poly(ethylene oxide) with a molecular weight of 5000 (MPEO5000) were analyzed by MALDI-TOF MS and NMR. MALDI-TOF MS spectra of PEO6000 and $(HO)_2PEO(OH)_2$ are shown in Fig. 13. The mass difference between the peaks is 44 corresponding to one EO group. The major and center peak is labeled at 6268.9 m/z for PEO6000 and 6489.1 m/z for $(HO)_2PEO(OH)_2$. The peak 6268.9 m/z

corresponds to PEO with 141 repeat units plus K^+, i.e., $[HO(CH_2CH_2O)_{141}H + K^+]$. This indicates that PEO6000 has two hydroxyl end groups in each molecule. The peak at 6489.1 m/z corresponds to $[(HOCH_2CH_2)_2N(CH_2CH_2O)_{141}\text{-}CH_2CH_2N(CH_2CH_2OH)_2 + K^+]$. There is no peak assignable to $[HO(CH_2CH_2O)_{141}CH_2CH_2N\text{-} (CH_2CH_2OH)_2 + K^+]$.

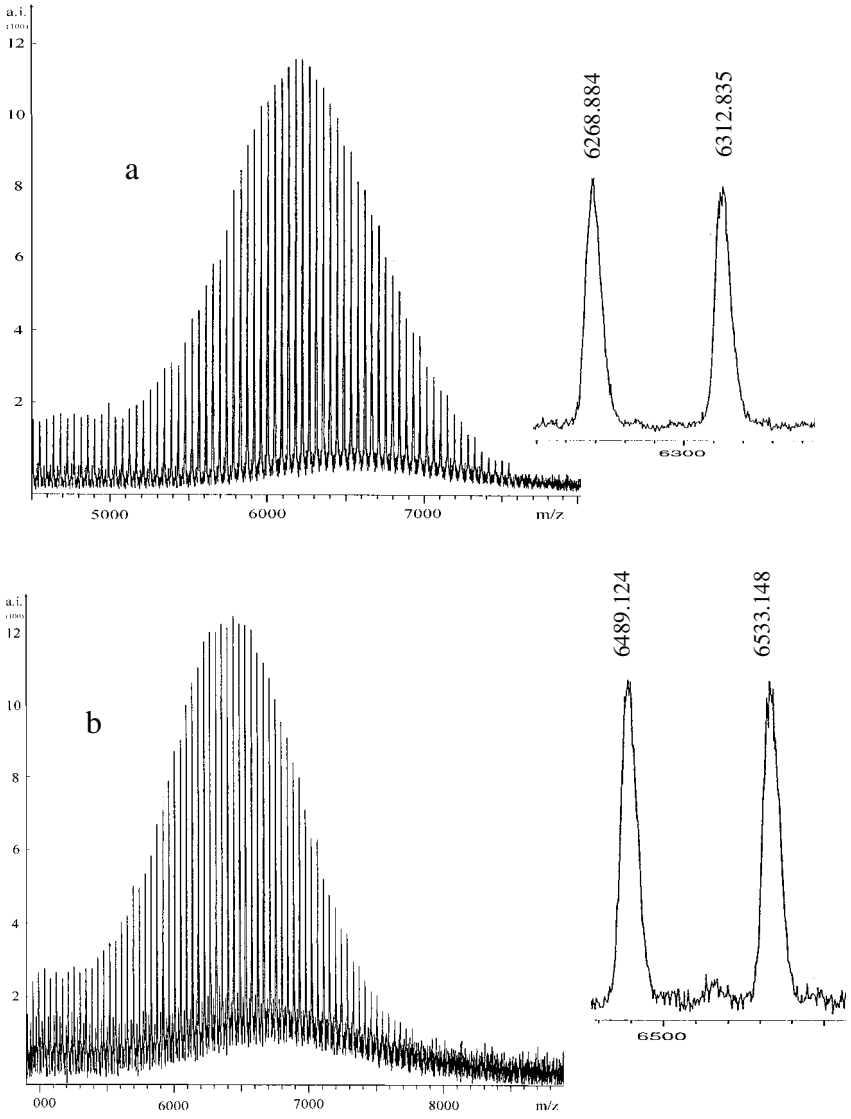

Fig. 13. MALDI TOF MS spectra of PEO6000(a) and $(HO)_2PEO(OH)_2$ (b) in methanol (CF_3COOK).

^{1}H NMR and ^{13}C NMR spectra of the various PEO were recorded from solutions in DMSO-d-6. A typical ^{1}H NMR spectrum of PEO6000 shows that signals in the range 3.4-3.8 ppm are characteristic of the main chain methylene units. The resonances in the range 4.5-4.6 ppm are assigned to hydroxyl end groups. The ^{13}C NMR spectrum of PEO shows resonances at 72.25, 69.70 and 60.13 ppm due to O<u>C</u>H$_2$CH$_2$OH, OCH$_2$<u>C</u>H$_2$O (except end groups) and OCH$_2$<u>C</u>H$_2$OH, respectively. In the ^{1}H NMR spectra of MPEO(OH)$_2$ and (HO)$_2$PEO(OH)$_2$ resonances at 4.5-4.6 ppm are absent and resonances appear at 4.2-4.3 ppm. This indicates that hydroxyl end groups in PEO were totally transformed to N(CH$_2$CH$_2$OH)$_2$ groups. In ^{13}C NMR spectra resonances at 72.25 and 60.13 ppm are absent while resonances at 69.00, 59.25, 57.01 and 53.98 ppm are assignable to O<u>C</u>H$_2$CH$_2$N(CH$_2$CH$_2$OH)$_2$, N(CH$_2$<u>C</u>H$_2$OH)$_2$, N(<u>C</u>H$_2$CH$_2$OH)$_2$ and OCH$_2$<u>C</u>H$_2$N(CH$_2$CH$_2$OH)$_2$, respectively. There is only one resonance at -74.639 ppm in ^{19}F NMR spectra of MPEO(OH)$_2$ and (HO)$_2$PEO(OH)$_2$ treated with trifluoroacetic anhydride (TFAA). In the contrast, the ^{19}F NMR spectra of PEO treated with TFAA show a resonance at -75.348 ppm. Thus, the results of ^{19}F NMR are in agreement with ^{1}H NMR and ^{13}C NMR results.

Tab. 10 shows the results of MALDI-TOF MS and NMR of PEO. They are in good agreement.

Tab. 10. Composition and molecular weight of PEO initiators

PEO	$\overline{M_n}$ a)	$\overline{M_n}$ b)	$\overline{M_n}$ c)	$\overline{M_w}$ c)	$\overline{M_w}$ / $\overline{M_n}$ c)	Structure
PEO1000	1000	1030	1012	1060	1.05	HO(CH$_2$CH$_2$O)$_n$H
MPEO5000	5000	5200	5200	5250	1.01	CH$_3$O(CH$_2$CH$_2$O)$_n$H
PEO6000	6000	6400	6270	6340	1.01	HO(CH$_2$CH$_2$O)$_n$H
MPEO(OH)$_2$	5100 d)	5300	5320	5350	1.01	CH$_3$(OCH$_2$CH$_2$)$_n$N(CH$_2$CH$_2$OH)$_2$
((HO)$_2$PEO(OH)$_2$	6200 d)	6440	6480	6520	1.01	(HOCH$_2$CH$_2$)$_2$N(CH$_2$CH$_2$O)$_n$CH$_2$CH$_2$-N(CH$_2$CH$_2$OH)$_2$

a) as declared by Fluka. b) from NMR. c) from MALDI-TOF MS. d) calculated from $\overline{M_n}$ of MPEO5000 / PEO6000 as obtained from Fluka.

Copolymerization

The block copolymers were synthesized via polymerization of Cyclo(Glc-Ile) in the presence of PEO with OH end groups as the initiator and Sn(oct)$_2$ as the catalyst at 140 °C for 9 h (Scheme 5). The results of the copolymerization are listed in Tab. 11.

The polymer obtained from precipitation in ether was purified by immersing in ethanol and deionized water to remove unreacted PEO. The chemical shift at 3.64 ppm originates from the methylene protons in the PEO block. The ratio of the intensity of the protons of poly(Glc-Ile) and PEO does not change before and after purification. This indicates that PEO is

chemically incorporated in the copolymer. GPC of the copolymers shows no changes before and after purification. Since an equimolar ratio of hydroxy groups of PEO as the initiator and $Sn(oct)_2$ as a catalyst was used it is assumed that all hydroxyl groups of PEO initiate the polymerization of Cyclo(Glc-Ile).

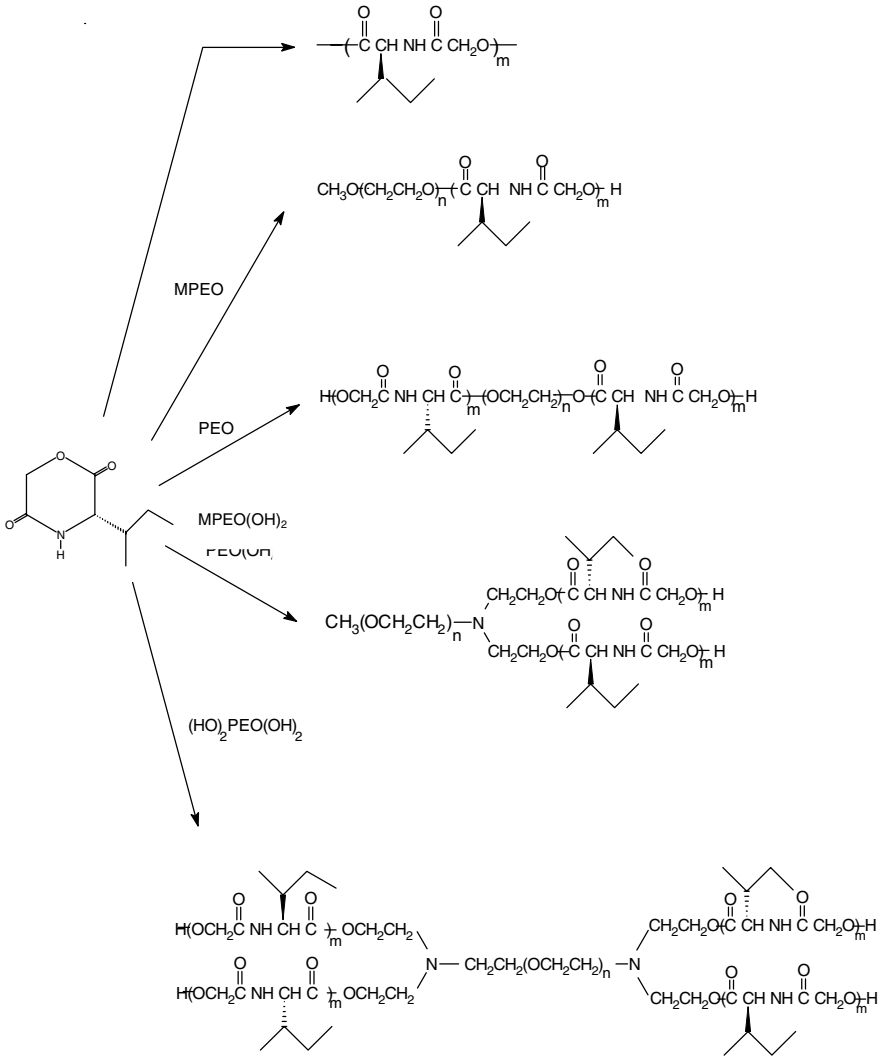

Scheme 5. Reaction scheme of the preparation of poly(Glc-Ile)-PEO copolymers.

Tab. 11. Copolymerization of Cyclo(Glc-Ile) with PEO

No.	Type of PEO	PEO in 10^{-5} mol	OH[a] in 10^{-5} mol	Cyclo(Glc-Ile) in 10^{-3} mol	Yield[b] in %	Copolymer[c]
1	-	-	-	5.76	84.2	Homopolymer
2	PEO1000	2.36	4.72	5.44	76.8	ABA
3	PEO20000	2.42	4.84	6.09	68.7	ABA
4	PEO20000	1.42	2.84	7.24	73.9	ABA
5	MPEO5000	4.20	4.20	5.19	84.5	AB
6	$MPEO(OH)_2$	2.90	5.80	6.74	78.5	$(A)_2B$
7	$MPEO(OH)_2$	1.82	3.64	8.22	75.3	$(A)_2B$
8	$(HO)_2PEO(OH)_2$	4.55	18.2	4.85	72.5	$(A)_2B(A)_2$
9	$(HO)_2PEO(OH)_2$	1.74	6.96	8.24	82.7	$(A)_2B(A)_2$
10	$(HO)_2PEO(OH)_2$	0.825	3.30	5.71	76.7	$(A)_2B(A)_2$

a) hydroxyl group in PEO. b) calculated by $W_{purified\ polymer}/(W_{PEO}+W_{Cyclo(Glc\text{-}Ile)})$.

c) A= poly(Glc-Ile); B=PEO.

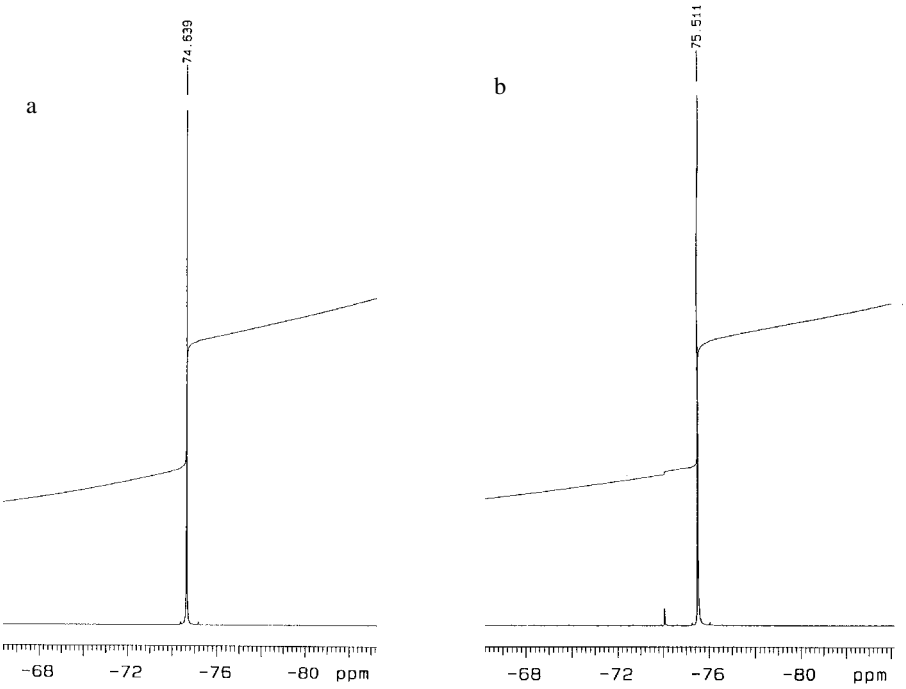

Fig. 14. a) ^{19}F NMR spectrum of $(HO)_2PEO(OH)_2$ treated with TFAA, b) ^{19}F NMR spectrum of $(A)_2B(A)_2$ block copolymer (No. 8 In Tab. 11) treated with TFAA, DMSO-d-6/TMS.

In the ^{1}H NMR spectrum of the block copolymers there is no singlet at a chemical shift of 4.65 ppm, which is evidence for the absence of racemization of the isoleucine residue during polymerization of Cyclo(Glc-Ile). In the ^{13}C NMR spectra there is no signal assignable to CH_2CH_2OH carbon atoms. This proves that PEO hydroxyl end groups were totally esterified. Furthermore, the hydroxyl end groups of the block copolymers were esterified with TFAA in $CHCl_3$ solution at room temperature for 3 h. The resulting block copolymers was precipitated in diethyl ether, dried and analyzed by ^{19}F NMR. The chemical shift of CH_2OCOCF_3 end-groups of poly(Glc-Ile) blocks appears at ©¥75.51 ppm (Fig. 14). Besides there is a small resonance peak at ©¥74.059 ppm, which may result from a very short block of poly(Glc-Ile). The absence of resonances at ©¥74.639 ppm indicates that all hydroxyl end groups of PEO initiated the ring-opening polymerization of Cyclo(Glc-Ile).

The data (Tab. 11 and Tab. 12) and results of NMR demonstrate that block copolymers are obtained by the ring-opening copolymerization of Cyclo(Glc-Ile) with monofunctional MPEO5000, bifunctional PEO6000, PEO20000 and $MPEO(OH)_2$, and tetrafunctional $(HO)_2PEO(OH)_2$ as macroinitiators in high yields (68.7-84.5%). The molecular weight determined from GPC is considerably different from that from NMR. The results from GPC are not reliable.

Tab. 12. Composition and molecular weight of poly(Glc-Ile)-PEO block copolymers

No.[a]	$\overline{M_n}$ [b] $\times 10^{-4}$	$\overline{M_n}$ [c] $\times 10^{-4}$	$\overline{M_n}$ of poly(Glc-Ile) block [c] $\times 10^{-4}$	poly(Glc-Ile) /PEO in wt% [c]	$\overline{M_n}$ [d] $\times 10^{-4}$	$\overline{M_w}$ [d] $\times 10^{-4}$	$\overline{M_w}$ / $\overline{M_n}$ [d]
1				100/0	2.59	5.40	2.08
2	4.06	4.00	3.90	97.5/2.5	1.02	1.30	1.27
3	6.33	4.97	2.97	59.8/40.2	2.18	4.68	2.15
4	10.7	8.30	6.30	75.9/24.1	3.05	7.55	2.48
5	2.63	2.00	1.50	75.0/25.0	2.63	6.20	2.36
6	4.50	3.51	3.01	85.8/14.2	2.39	4.00	1.67
7	8.26	6.53	6.03	92.3/7.7	2.60	4.90	1.88
8	2.43	1.82	1.22	67.0/33.0	1.85	3.40	1.84
9	8.75	7.57	6.97	92.1/7.9	2.90	5.48	1.89
10	12.5	13.94	13.34	95.7/4.3	3.54	7.82	2.21

a) block copolymers are the same as in Tab. 11. b) calculated from feed ratio. c) from NMR. d) from GPC.

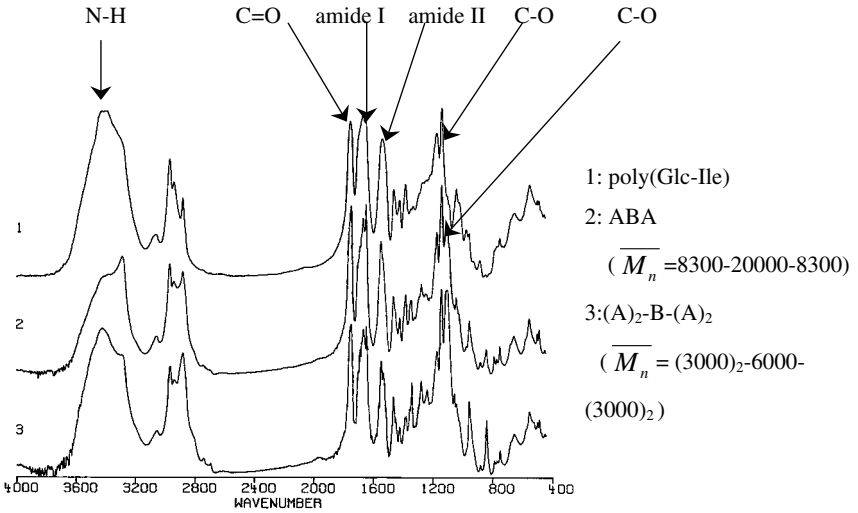

Fig. 15. IR spectra of the homopolymer poly(Glc-Ile) and of the block copolymers 3 and 8 (Tab. 11).

The IR spectra of poly(Glc-Ile) and the block copolymers (No. 3 and 8, Tab.11) are shown in Fig. 15. The strong absorption band at 3410 cm^{-1} (Fig.15 (2) and (3)) is assigned to the stretching band of the N-H bond in the poly(Glc-Ile) blocks. The band at 1760 cm^{-1} is due to C=O stretching mode of the ester group, and the band at 1652 cm^{-1} to the bending vibration of the N-H bond and stretching mode of the C-N bond of the CONH group. The amide II band appears at 1541 cm^{-1}. The characteristic absorption band of PEO appears at 1112 cm^{-1} (Fig. 15 (2) and (3)). When the IR spectra of poly(Glc-Ile) and block copolymers with a lower content of PEO (for example No.2 in Tab. 11, not shown in Fig. 15) are compared, no significant differences are found, because the characteristic absorption band of the PEO block overlaps with the absorption band of the C-O bond in the poly(Glc-Ile) block.

Thermal analysis of block copolymers

The DSC curves of ABA triblock copolymers upon first heating are presented in Fig 16. They display two distinct endotherms that correspond to the melting transition of each constituent block. The first endothermic peak (T_m = 39.8 - 54 °C) is attributed to the melting of the crystalline PEO phase. The second endotherm (about 97 °C) corresponds to melting of the

poly(Glc-Ile) phase. The DSC results demonstrate that microphase separation takes place in the copolymers.

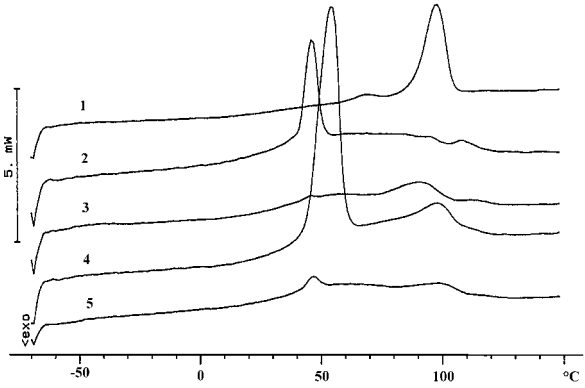

curve 1: No. 2 (Tab. 12)
curve 2: PGI/EO2 (Tab. 3)
curve 3: PGI/EO1 (Tab. 3)
curve 4: No. 3 (Tab. 12)
curve 5: No. 4 (Tab. 12)

Fig. 16. DSC thermograms of ABA triblock copolymers.

Curve 2 in Fig. 16 represents the melting of an ABA type block copolymer with the same length of the PEO block ($\overline{M_n}_{(PEO)}$=6000) as in curve 3, but with a shorter poly(Glc-Ile) block ($\overline{M_n}_{(poly(Glc\text{-}Ile))}$ = 13000). In this case, the crystallinity of the PEO block is significantly higher in comparison with the PEO endotherm in curve 3. This indicates that the crystallinity of the PEO block decreases greatly with increasing length of the poly(Glc-Ile) block. Comparing curve 3 and curve 4 it is seen that the crystallinity of the PEO block increases with increasing length of the PEO block when the length of the poly(Glc-Ile) block is constant.

Melting of the PEO block in the triblock copolymer was not observed when the weight fraction of PEO in the block copolymer is lower than 16% (curve 1 and curve 3 in Fig. 16). This indicates that the PEO block in these copolymers is amorphous.

Crystallinity and melting temperature of the PEO block (in Tab. 13) are considerably lower than those of the homopolymer. Tab. 13 shows that the endotherm of melting of the poly(Glc-Ile) block increases with increasing poly(Glc-Ile) block content. The melting temperature of the poly(Glc-Ile) block in the copolymers changes little with increasing length of the poly(Glc-Ile) block.

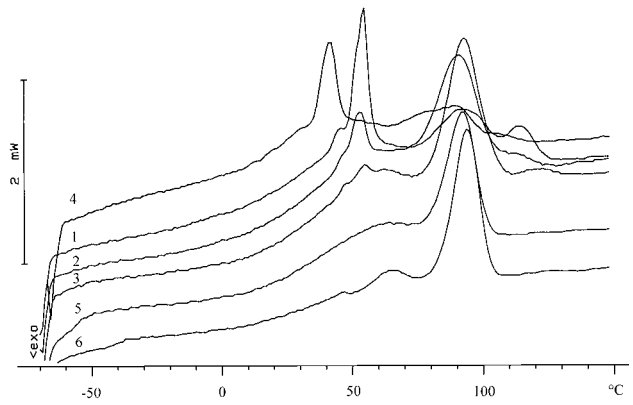

Fig. 17. DSC thermograms of block copolymers of poly(Glc-Ile)-PEO (Tab. 12).

Tab. 13. Crystallinity and melting point of PEO and poly(Glc-Ile) blocks upon first heating

No.	Type of PEO	PEO	PEO block			poly(Glc-Ile) block			
		in wt%	T_m/°C	ΔH/J/g	α_c/%	T_m/°C	ΔH/J/g[a)]	ΔH/J/g[b)]	T_g/°C
1		0				97.2	18.5	18.5	73.3
2	PEO1000	2.5	-	-	-	97.1	28.4	29.4	66
3	PEO20000	40.2	52.8	54.0	71.3	97.6	8.6	14.4	1.2
4	PEO20000	24.1	46.8	2.7	5.9	98.8	5.6	7.4	23
5	MPEO	25.0	54.6	18.0	38.2	93.8	13.7	18.3	22
6	$MPEO(OH)_2$	14.2	52.7	6.1	22.8	90.7	18.1	21.1	39
7	$MPEO(OH)_2$	7.7	-	-	-	92.6	19.2	20.8	55
8	$(HO)_2PEO(OH)_2$	33.0	36.7	10.6	17.0	-	-	-	-
9	$(HO)_2PEO(OH)_2$	7.9	-	-	-	92.7	19.5	21.2	56
10	$(HO)_2PEO(OH)_2$	4.3	-	-	-	93.7	23.7	24.8	62

a) endotherm of melting of the poly(Glc-Ile) block in the copolymer. b) ΔH/poly(Glc-Ile)%.

Fig. 17 allows comparison of DSC curves upon first heating of AB (curve 1), $(A)_2B$ (curve 2 and 3) and $(A)_2B(A)_2$ (curve 4,5 and 6) copolymers. The effect of the length of the poly(Glc-Ile) block on the crystallinity and T_m of the PEO block in $(A)_2B$ and $(A)_2B(A)_2$ type copolymers is the same as that in the ABA type copolymers. While the crystallinity and melting temperature of the PEO block in the $(A)_2B(A)_2$ type copolymer (No. 8 in Tab 13) are much smaller than those in the ABA type copolymer(No.3 in Tab. 13) when length and content of the PEO block are unchanged. Although the length of the PEO block ($\overline{M_n}$ =5000) in the $(A)_2B$ copolymer (No. 6 in Tab. 13) is shorter than that in the ABA copolymer ($\overline{M_n}$ =6000), the PEO block in the $(A)_2B$ copolymer exerts a degree of crystallinity of α_c =

22.8% with a T_m of 52.7 °C. The above results indicate that the mutual influence between poly(Glc-Ile) and PEO blocks is stronger in $(A)_2B(A)_2$ and ABA block copolymers than in AB diblock copolymers and $(A)_2B$ star shaped copolymers. In the latter two cases the restriction of crystallization of the PEO block is smaller (Fig. 16 and 17).

No crystallization and endothermic peaks for both blocks, PEO and poly(Glc-Ile), were observed upon cooling and second heating, respectively (not shown). The poly(Glc-Ile) block prevents the recrystallization of the PEO block upon cooling in all four types of block copolymers. T_g values of the copolymers observed upon second heating (Tab. 13) cover a wide range of temperature.

The DSC data suggest that the crystallizablility of the PEO blocks is effectively decreased upon attachment of longer poly(Glc-Ile) segments. Similar results were observed for PLLA-PEO-PLLA triblock copolymer with centered PEO segments by others[93,108].

Hydrophilicity of copolymers

The hydrophilicity of block copolymers was determined by measuring the static contact angles with water. The results listed in Tab. 14 clearly show that the static contact angle θ decreases with increasing PEO content in the block copolymers. For example, when the PEO content is 40.2 wt% the contact angle is 61° which is significantly smaller than that of the homopolymer poly(Glc-Ile) (θ = 81°).

Tab. 14. Static contact angle of poly(Glc-Ile)-PEO block copolymers

No.	Type of PEO	PEO (wt%)	θ (°)
1		0	81±2
2	PEO1000	2.5	78±3
3	PEO20000	40.2	61±4
4	PEO20000	24.1	73±2
5	MPEO	25.0	68±2
6	$MPEO(OH)_2$	14.2	78±3
7	$MPEO(OH)_2$	7.7	77±3
8	$(HO)_2PEO(OH)_2$	33.0	70±3
9	$(HO)_2PEO(OH)_2$	7.9	79±2
10	$(HO)_2PEO(OH)_2$	4.3	80±2

2.1.4 Synthesis and characterization of block copolymers with PEO and poly(Glc-Leu) sequences

The block copolymers were synthesized via polymerization of Cyclo(Glc-Leu) in the presence of PEO as the initiator and $Sn(oct)_2$ as a catalyst at 140 °C for 9 h. The copolymerization is illustrated in Scheme 6. The results of the copolymerization are listed in Tab. 15.

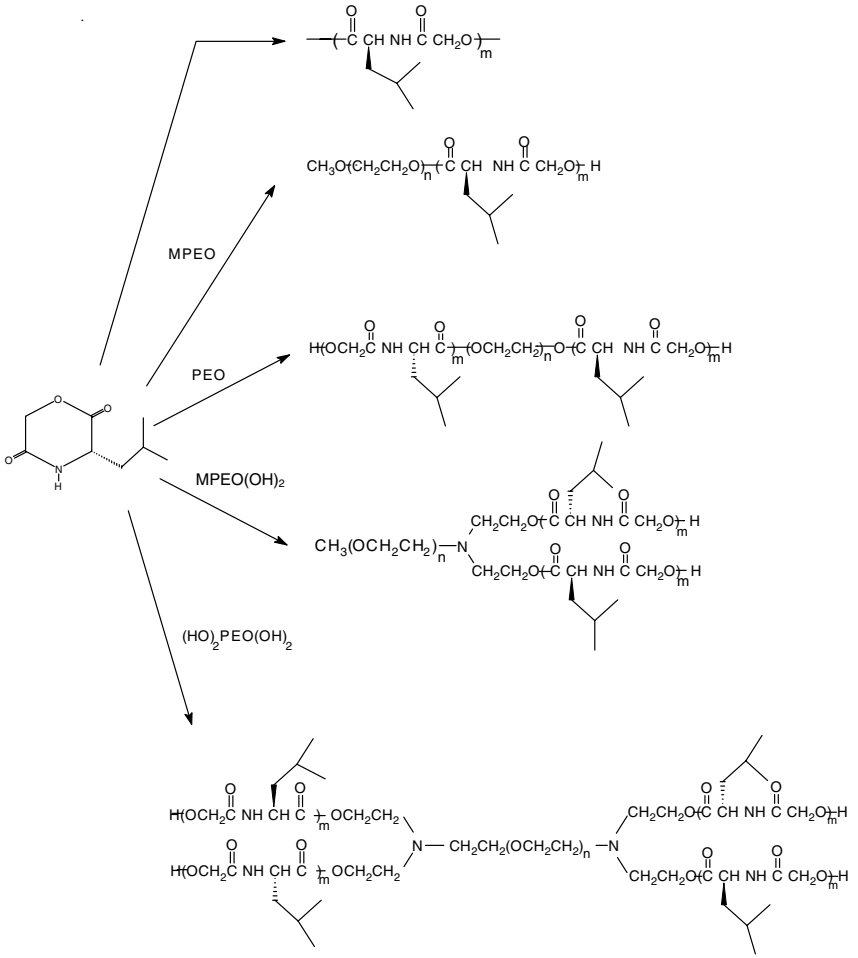

Scheme 6. Reaction scheme of the preparation of poly(Glc-leu)-PEO copolymers.

Tab. 15. Copolymerization of Cyclo(Glc-Leu) with PEO

No.	Type of PEO	PEO in 10^{-5}mol	OH[a)] in 10^{-5} mol	Cyclo(Glc-Leu) in 10^{-3} mol	[Cyclo(Glc-Leu)]/[OH]	Yield in %	Copolymer [b)]
1	PEO1000	2.6	5.2	2.9	56	70	ABA
2	PEO20000	2.7	5.4	3.2	59	91	ABA
3	PEO20000	2.3	4.6	5.4	117	90	ABA
4	MPEO5000	4.7	4.7	2.9	62	78	AB
5	MPEO5000	5.1	5.1	5.7	112	86	AB
6	$MPEO(OH)_2$	2.7	5.4	2.9	54	86	$(A)_2B$
7	$MPEO(OH)_2$	2.7	5.4	6.2	115	91	$(A)_2B$
8	$MPEO(OH)_2$	1.7	3.4	6.5	191	93	$(A)_2B$
9	$(HO)_2PEO(OH)_2$	4.4	17.6	4.3	24	85	$(A)_2B(A)_2$
10	$(HO)_2PEO(OH)_2$	1.6	6.4	3.0	47	90	$(A)_2B(A)_2$

a) hydroxyl group in PEO. b) A= poly(Glc-Leu); B=PEO.

The polymer obtained from precipitation in ether was purified by immersing in ethanol and deionized water, the solvent of PEO, to remove unreacted PEO. The ^{1}H-NMR spectra of the copolymers show that the ratio of the intensivity of the protons of poly(Glc-Leu) and PEO does not change before and after the immersion. This indicates that PEO is fully incorporated in the copolymer. The GPC of the copolymers shows no changes before and after the immersion and no peak of PEO. Since an equimolar ratio of hydroxy groups of PEO and $Sn(oct)_2$ was used it is assumed that all hydroxy groups of PEO initiate the polymerization of Cyclo(Glc-Leu).

It is not possible to detect any signal assignable to OCH_2CH_2OH carbon atoms belonging to HO-ended PEO groups. This finding shows that PEO hydroxyl end groups are totally esterified and that neither residual PEO nor poly(Glc-Leu)/PEO diblock copolymers for PEO-bifuncational initiators was present in the final products, nor poly(Glc-Leu) /PEO triblock copolymers for PEO tertrafunctional initiators, at least within the experimental limits of NMR spectroscopy. Furthermore, the hydroxyl end groups of the block copolymers were esterified with TFAA, and then analyzed by NMR. It was found that the chemical shift of the methylene protons of CH_2OH end-groups of poly(Glc-Leu) changed from 3.85 ppm to 4.30 ppm when the block copolymers were treated with TFAA. The ^{19}F NMR spectrum shows that there is only one kind of end groups. Therefore, the structure of the obtained block copolymers follows from the structure of PEO initiators.

Tab. 16. Composition and molecular weight of poly(Glc-Leu)-PEO block copolymers

No.[a]	$\overline{M_n}$ [b] $\times 10^{-4}$	poly(Glc-Leu)/PEO in wt% [b]	$\overline{M_n}$ [c] $\times 10^{-4}$	$\overline{M_w}$ [c] $\times 10^{-4}$	$\overline{M_w} / \overline{M_n}$ [c]
1	1.44	93/7	1.29	2.22	1.72
2	3.8	47/53	3.70	4.41	1.19
3	5.9	66/34	5.15	7.79	1.51
4	1.3	62/38	1.30	2.21	1.70
5	2.2	77/23	2.25	3.11	1.38
6	2.2	76/24	1.94	2.85	1.47
7	3.9	87/13	1.30	2.20	1.69
8	6.0	92/8	2.00	2.90	1.45
9	1.9	68/32	1.88	3.10	1.65
10	2.1	72/28	2.00	3.17	1.59

a) block copolymers are the same as in Tab. 15. b) from NMR. c) from GPC.

The composition of the block copolymers was determined by means of ^{1}H NMR spectroscopy from the intensity ratio of the signals originating from the PEO block and from the poly(Glc-Leu) block. The data (Tab. 15 and Tab. 16) and results of NMR demonstrate that block copolymers are obtained by the ring-opening copolymerization of Cyclo(Glc-Leu) with monofunctional MPEO5000, bifunctional PEO6000, PEO20000 and MPEO(OH)$_2$, and tetrafunctional (HO)$_2$PEO(OH)$_2$ as macroinitiators in high yield (70-93%).

Thermal analysis of block copolymers

The DSC curves of diblock and triblock copolymers upon first heating are presented in Fig 18. They display two distinct endotherms that correspond to the melting transition of each constituent block. The first endothermic peak (T_m = 44.4 - 51.9 °C) is attributed to the melting of the PEO crystalline phase. The second endotherm (about 190 °C) corresponds to melting of the poly(Glc-Leu) phase. The DSC results demonstrate that microphase separation takes place in the copolymers.

Curve 2 in Fig. 18 represents the melting of a diblock copolymer with the same length of the PEO block ($\overline{M_n}_{(PEO)}$ = 5000) as in curve 3, but with a shorter poly(Glc-Leu) block ($\overline{M_n}_{(poly(Glc-Leu))}$ = 8000). The crystallinity of the PEO block in curve 2 is significantly higher in comparison with the PEO endotherm in curve 3. This indicates that the crystallinity of the PEO block decreases greatly with increasing length of the poly(Glc-Leu) block. T_m of the PEO block in the triblock copolymer was not observed when the weight fraction of PEO in the block copolymer is lower than 7 wt% (curve 1 in Fig. 18). The PEO block is amorphous

because of the low molecular weight and the low weight fraction of PEO1000 in the block copolymer.

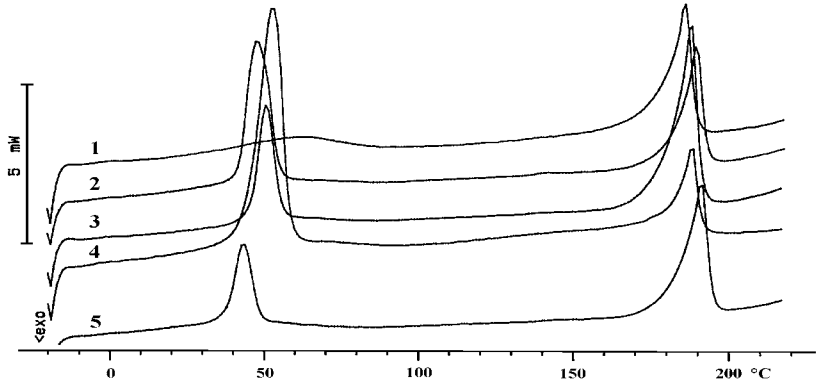

Fig. 18. DSC thermograms of AB and ABA copolymers, A=poly(Glc-Leu), B=PEO.

curve 1: $\overline{M_n}$=6500-1000-6500 (ABA); curve 2: $\overline{M_n}$=8000-5000 (AB); curve 3: $\overline{M_n}$=17000-5000 (AB); curve 4: $\overline{M_n}$=9000-20000-9000 (ABA); curve 5: $\overline{M_n}$=19500-20000-19500 (ABA).

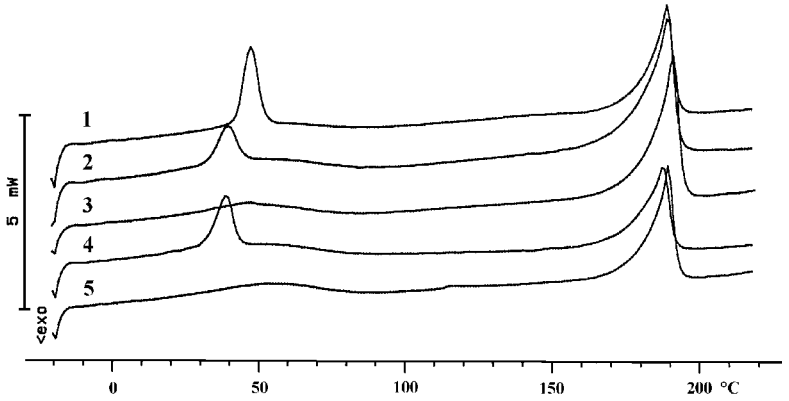

Fig. 19. DSC thermograms of $B(A)_2$ and $(A)_2B(A)_2$ block copolymers, A=poly(Glc-Leu), B=PEO.

curve 1: $\overline{M_n}$ = 5000-$(8500)_2$ ($B(A)_2$); curve 2: $\overline{M_n}$ = 5000-$(17000)_2$ ($B(A)_2$); curve 3: $\overline{M_n}$ = 5000-$(27500)_2$ ($B(A)_2$); curve 4: $\overline{M_n}$ =$(3200)_2$-6000-$(3200)_2$ ($(A)_2B(A)_2$); curve 5: $\overline{M_n}$ = $(3800)_2$-6000-$(3800)_2$ ($(A)_2B(A)_2$).

Crystallinity and melting temperature of the PEO block are (Tab. 17) are considerably lower than those of the homopolymer. Tab. 17 shows that the endotherm of melting of the poly(Glc-Leu) block increases with increasing poly(Glc-Leu) block content. The melting temperature of the poly(Glc-Leu) block in the copolymers changes little with increasing length of the poly(Glc-Leu) block.

Tab. 17. Crystallinity and melting point of PEO and poly(Glc-Leu) blocks upon first heating

No.	Type of PEO	PEO[a)]	PEO block			poly(Glc-Leu) block		
		in wt%	T_m/°C	ΔH/J/g	α_c/%	T_m/°C	ΔH/J/g	T_g/°C [b)]
1	PEO1000	7	-	-	-	186.4	48.9	39.0
2	PEO20000	53	51.9	83.8	83.9	188.5	25.5	-
3	PEO20000	34	44.4	37.0	57.8	191.5	37.2	81.0
4	MPEO5000	38	47.3	54.2	75.7	189.4	36.1	87.4
5	MPEO5000	23	49.5	23.4	54.0	188.0	46.0	-
6	$MPEO(OH)_2$	24	47.5	20.6	45.6	188.4	43.8	-
7	$MPEO(OH)_2$	13	39.6	10.6	43.3	188.3	50.5	-
8	$MPEO(OH)_2$	8	-	-	-	190.3	51.2	95.8
9	$(HO)_2PEO(OH)_2$	32	38.6	19.9	15.5	188.4	44.6	-
10	$(HO)_2PEO(OH)_2$	28	-	-	-	189.6	47.5	-

a) wt% of the PEO block in block copolymers, estimated by ^{1}H NMR spectroscopy.
b) upon second heating.

Fig. 19 allows comparison of DSC curves upon first heating of $B(A)_2$ (curve 1, 2 and 3) and $(A)_2B(A)_2$ (curve 4 and 5) copolymers. The effect of the length of the poly(Glc-Leu) block on the crystallinity and T_m of the PEO block in $(A)_2B$ and $(A)_2B(A)_2$ type copolymers is the same as that in the ABA type copolymer. The crystallinity and melting temperature of the PEO block in $(A)_2B(A)_2$ type copolymer (No. 9 and 10 in Tab. 17) are much smaller than those in ABA type copolymer. This indicates that the influence of poly(Glc-Leu) blocks on PEO blocks is stronger in $(A)_2B(A)_2$ than in the other block copolymers.

2.1.5 Synthesis and characterization of copolymers with PDLLA and polydepsipeptide sequences with functional groups

Polydepsipeptides were reported to be synthesized by ring-opening polymerization of morpholine-2,5-diones with different alkyl substituents. Copolymerization of morpholine-2,5-diones with DLLA or CL provided a series of biodegradable polyester amides with a wide range of chemical and physical properties. Based on these results, the ring-opening polymerization of morpholine-2,5-diones with functional groups will be considered in the following study. The use of trifunctional α-amino acids like S-aspatic acid (Asp), S-lysine (Lys), R-cysteine (Cys) and S-tyrsine (Tyr) in the synthesis of morpholine-2,5-diones offers a synthetic route to biodegradable polymers with pendant carboxylic acid, amino, thiol and hydroxy groups, respectively. Different α-amino acids residues with protected side-chain functional groups were incorporated into morpholine-2,5-diones, which were polymerized in a ring-opening fashion, followed by deprotection of the pendant functional groups.

Monomer synthesis

The synthesis of morpholine-2,5-diones with pendant functional groups, i.e. Cyclo[DLLA-Asp(OBzl)], Cyclo[DLLA-Glu(OBzl)], Cyclo[DLLA-Lys(Z)], Cyclo[DLLA-Cys(*p*NBzl)], Cyclo[DLLA-Tyr(Bzl)] was performed as shown in Scheme 7 and 8. In order to avoid side reactions, the pendant functional groups of the trifunctional amino acid residues had to be temporarily blocked by protecting groups which are stable to the projected reactions outlined in Scheme 7 and 8. Moreover, the protective groups have to be stable during the ring-opening polymerization of the morpholine-2,5-diones. Subsequently the protective groups must be selectively removed without cleavage of ester and/or amide bonds of the polymer main chains. On the basis of literature the benzyl ester was selected as the protective group for the β- and γ-carboxylic acid function of Asp and Glu, respectively[39]. The benzyl group was also used as a protective group for the hydroxy function of Tyr. The ε-amino group of the Lys was protected by the benzyloxycarbonyl group. Feijen[39] reported the *p*-methoxybenzyl group was used as protective group for Cys; however, the removal of the *p*-methoxybenzyl group is performed with trifluoromethanesulfonic acid. The deprotection condition might cause ester and/or amide bond cleavage in the polymer main chain. The molecular weight of the polymer decreases extremely after deprotection. The *p*-nitrobenzyl group was selected as the protective group for thiol group of Cys in the following study. The protective groups could easily are removed by means of catalytic hydrogenation.

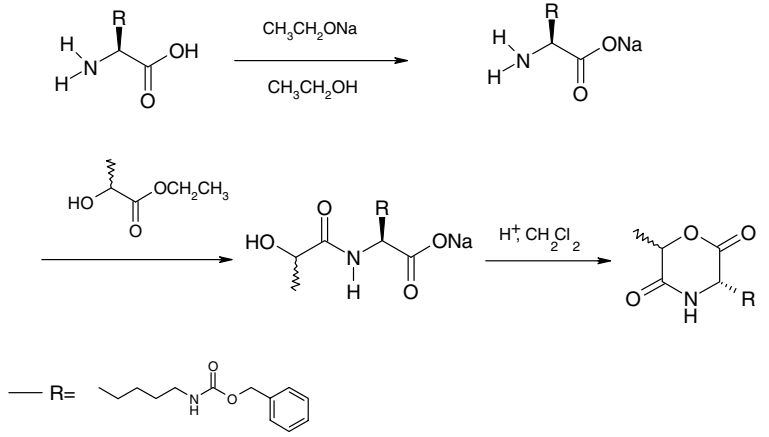

Scheme 7. Reaction scheme of the preparation of Cyclo(DLLA-Lys(Z)).

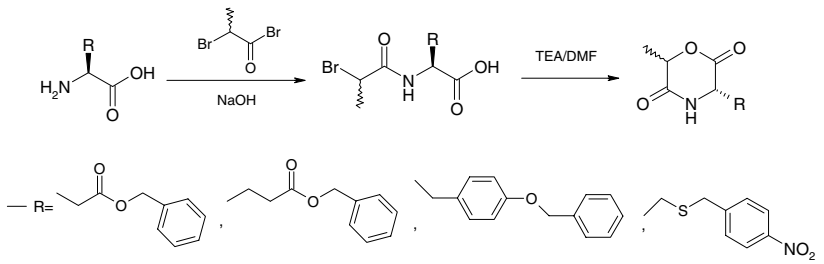

Scheme 8. Reaction scheme of the preparation of Cyclo(DLLA-Asp(OBzl)), Cyclo(DLLA-Glu(OBzl)), Cyclo(DLLA-Tyr(Bzl)) and Cyclo(DLLA-Cys(*p*NBzl)).

Cyclo[DLLA-Lys(Z)] was prepared in 25% yield by intramolecular cyclization of N^{α}-2(R,S)-[hydroxy-propionyl]-N^{ε}-(benzyloxylcarbonyl)-(S)-lysine. Attempts to synthesize Cyclo[DLLA-Asp(OBzl)] and Cyclo[DLLA-Glu(OBzl)] failed. Most probably transesterification reactions at the protective benzyl ester groups of β-benzyl-N-[2(R,S)-hydroxy-propionyl]-(S)-aspartate and γ-benzyl-N-[2(R,S)-hydroxy-propionyl]-(S)-glutamate occur during the cyclization procedure. Cyclo[DLLA-Asp(OBzl)], Cyclo[DLLA-Glu(OBzl)] and Cyclo[DLLA-Tyr(Bzl)] were synthesized according to Scheme 8 with TEA in a large amount of DMF for 3 h at 100 °C. Purification of the obtained morpholine-2,5-diones with functional groups was carried out by column chromatography on silica gel using ethyl acetate

as an eluent, followed by recrystallization from ethyl acetate/hexane (1/3 v/v). However, purified Cyclo[DLLA-Asp(OBzl)] was obtained by crystallization of the reaction mixture from toluene without column chromatography. The yield of the protected morpholine-2,5-diones was low. It is suggested that the intramolecular cyclization occurs in competition with the intermolecular reaction even at high dilution.

Cyclo[DLLA-Cys(*p*NBzl)] was prepared by treatment of N-[2(R,S)-bromopropionyl]-S-*p*-nitrobenzyl-(R)-cysteine with TEA in DMF for 17 h at room temperature. When the reaction was carried out at 100 °C for 3 h, partial deprotection of the thiol group resulted in the formation of several side products.

Polymer synthesis

The polymerization conditions used in the ring-opening polymerization of protected morpholine-2,5-diones and DLLA or CL were selected on the basis of earlier work on the ring-opening polymerization of morpholine-2,5-diones[8,30]. The results are summarized in Tab. 18.

Tab. 18. Copolymerization of morpholine-2,5-diones with protected functional groups and DLLA or CL[a)]

No.	Morpholine-2,5-dione	Co-monomer	F_M [b)] in %	Yield in %	f_M [c)] in %	$\overline{M_n}$ $\times 10^{-4}$	$\overline{M_w}$ $\times 10^{-4}$	$\overline{M_w}/\overline{M_n}$
1	Cyclo[DLLA-Asp(OBzl)]	Cyclo(Glc-Ile)	10	16	6.3	1.10	1.60	1.45
2	Cyclo[DLLA-Asp(OBzl)]	DLLA	2.5	90	1.5	5.50	11.5	2.09
3	Cyclo[DLLA-Asp(OBzl)]	DLLA	5	88	2.8	1.80	4.10	2.28
4	Cyclo[DLLA-Asp(OBzl)]	DLLA	7	37	3.3	1.50	2.40	1.60
5	Cyclo[DLLA-Asp(OBzl)]	DLLA	16.7	77	4.4	4.75	8.79	1.85
6	Cyclo[DLLA-Asp(OBzl)]	DLLA	19.2	70	4.9	1.88	2.61	1.39
7	Cyclo[DLLA-Asp(OBzl)]	CL	7.6	84	5.2	0.765	4.17	5.45
8	Cyclo[DLLA-Lys(Z)]	DLLA	7.2	76	3.4	0.54	1.47	2.72
9	Cyclo[DLLA-Tyr(Bzl)]	DLLA	10.7	63	6.3	3.25	5.64	1.73
10	Cyclo[DLLA-Glu(OBzl)]	DLLA	5.7	48	1.9	0.45	0.77	1.71
11	Cyclo[DLLA-Glu(OBzl)]	DLLA	8.5	35	3.4	0.43	0.82	1.91
12	Cyclo[DLLA-Glu(OBzl)]	DLLA	16.5	22	4.3	0.25	0.42	1.68
13[d)]	Cyclo[DLLA-Asp(OBzl)]	DLLA	11.5	70	4.7	1.40	3.93	2.81
14[e)]	Cyclo[DLLA-Asp(OBzl)]	DLLA	11.5	72	5.7	1.13	1.64	1.45

a) polymerizations were carried out in the bulk at 140 °C using stannous octoate as a catalyst, mole ratio M/I=125, t_p = 24 h, except for No. 1 and 4 t_p = 9 h.
b) mole fraction of morpholine-2,5-dione with protected functional group in the feed.
c) mole fraction of morpholine-2,5-dione with protected functional group in copolymer was determined by ^{1}H NMR.
d) 30 wt% PEO8000 as an initiator.
1) 45 wt% PEO8000 as an initiator.

Tab. 18 shows that the yield and molecular weight of the copolymers decreases with increasing F_M. The mole fraction of depsipeptide units in the copolymers is lower than that in the feed of the copolymerization. Apparently, this is due to the low reactivity of morpholine-2,5-diones. An increase in steric hindrance and stability of the ring structure with an increase in the number and size of ring substituents might decrease the reactivity. Moreover, the introduction of an additional functional group in the morpholine-2,5-diones might result in an additional reduction of the reactivity, caused by an interaction between catalyst and pendant functional group.

Tab. 19. Charaterization of poly(DLLA-co-Asp(Obzl)) copolymers and poly(DLLA-co-Asp(Obzl))-*b*-PEO block copolymers before and after deprotection

No.	Polymer	f_M [a)] in %	$\overline{M_n}$ $\times 10^{-4}$ [a)]	$\overline{M_w}$ $\times 10^{-4}$ [a)]	f_M [b)] in %	$\overline{M_n}$ $\times 10^{-4}$ [b)]	$\overline{M_w}$ $\times 10^{-4}$ [b)]
1	Poly(DLLA-co-Asp)	1.5	5.5	11.5	1.5	5.1	10.4
2	Poly(DLLA-co-Asp)	2.8	1.8	4.1	2.7	1.5	3.3
3	Poly(DLLA-co-Asp)-*b*-PEO	4.7	1.4	3.93	4.5	1.27	2.80
4	Poly(DLLA-co-Asp)-*b*-PEO	5.7	1.13	1.64	5.4	0.96	1.55

a) copolymer before deprotection. b) copolymer after deprotection.

The benzyl protecting groups of poly[DLLA-co-Asp(OBzl)] and poly[DLLA-co-Asp(OBzl)]-*b*-PEO block copolymers were removed by catalytic hydrogenation using palladium/carbon as a catalyst. ^{1}H NMR analysis of the resulting copolymers demonstrated the complete removal of the protecting groups by the absence of the proton signals of benzyl group at 7.4 ppm (Fig. 20 and Fig 21). The f_M values and molecular weight of the deprotected copolymers are somewhat lower compared to the values of the corresponding protected copolymers (Tab. 19). The catalytic hydrogenation appeared to be a selective and facile method to remove the pendant benzyl protecting groups.

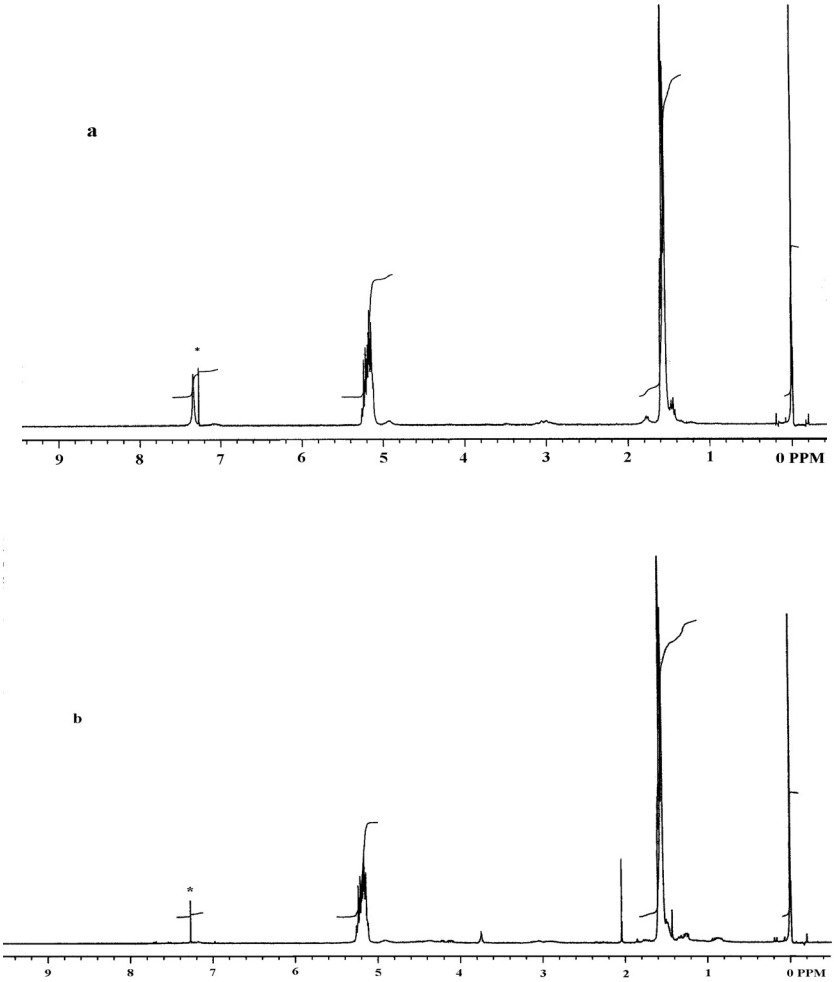

Fig. 20. ^{1}H NMR spectrum of copolymer poly[DLLA-co-Asp(OBzl)] (a) and poly[DLLA-co-Asp] ($CDCl_3$) (b). a: before deprotection, b: after deprotection, * = $CDCl_3$ peaks.

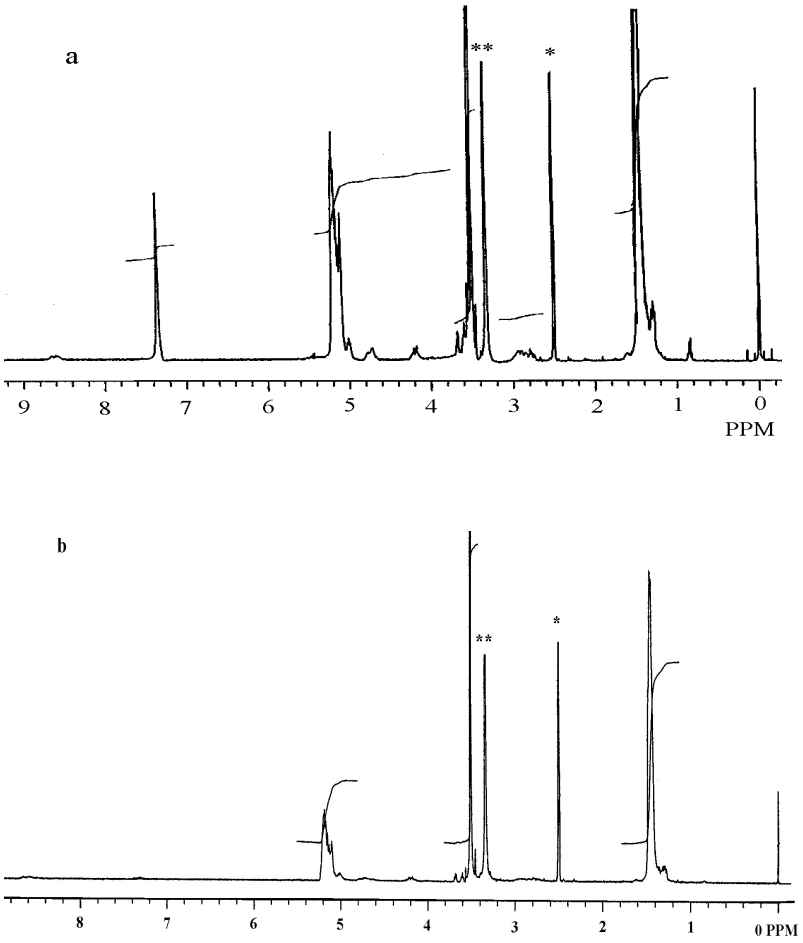

Fig. 21. ^{1}H NMR of poly(DLLA-co-Asp(OBzl))-*b*-PEO block copolymer before and after deprotection (DMSO-d-6).

a: before deprotection, b: after deprotection, * = DMSO-d-6 peaks, ** = water peaks.

Thermal analysis of block copolymers

The DSC curves of the triblock copolymers before deprotection obtained upon first and second heating are presented in Fig. 22. The curves upon first heating show one endotherm that corresponds to the melting of PEO block. Upon cooling from 200 to −70 °C, poly[DLLA-co-Asp(OBzl)]-*b*-PEO (No.14) recrystallizes with one exotherm ΔH = 66.1 J/g at 11.9 °C (not shown), while no transition was observed upon cooling for poly[DLLA-co-Asp(OBzl)]-*b*-PEO (No.13). One endothermic peak was observed upon second heating for poly[DLLA-co-Asp(OBzl)]-*b*-PEO (No.14).

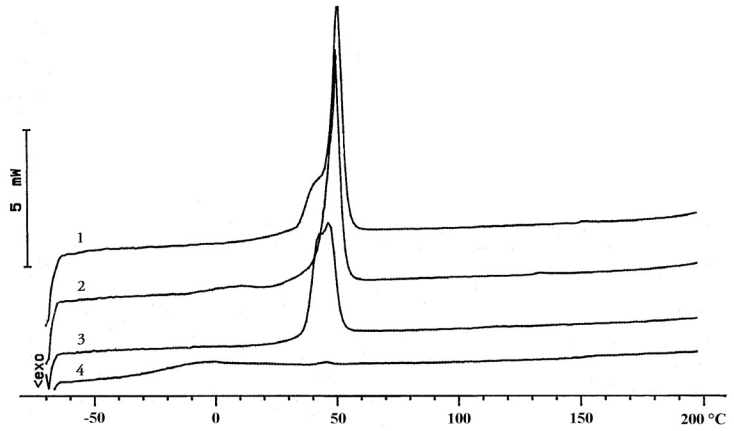

Fig. 22. DSC thermograms of poly[DLLA-co-Asp(OBzl)]-*b*-PEO copolymers.
Curve 1 and 2: first heating and second heating of poly[DLLA-co-Asp(OBzl)]-*b*-PEO (No.14, Tab. 18), respectively, Curve 3 and 4: first heating and second heating of poly[DLLA-co-Asp(OBzl)]-*b*-PEO (No.13, Tab. 18), respectively.

Fig. 23 shows the DSC curves of triblock copolymers after deprotection upon first and second heating. The results are similar to those before deprotection. However, compared with those before deprotection, the protected block copolymers have lower crystallization and melting temperature. Crystallinity and melting temperature of PEO block are considerably lower than those of PEO (Tab. 20).

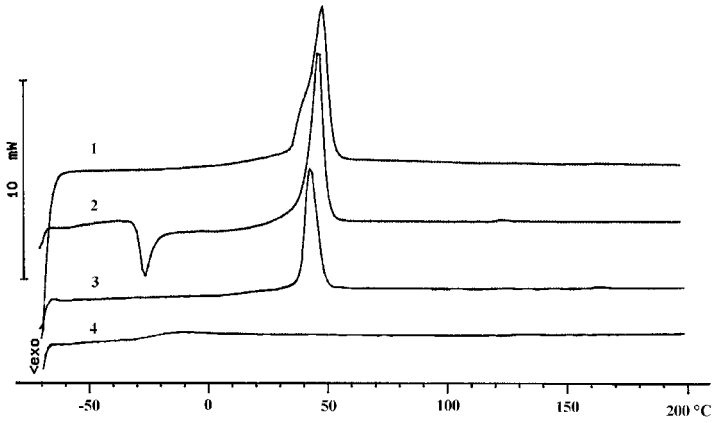

Fig. 23. DSC thermograms of poly(DLLA-co-Asp)-*b*-PEO copolymers.
Curve 1 and 2: first heating and second heating of poly(DLLA-co-Asp)-*b*-PEO (No.4, Tab. 19), Curve 3 and 4: first heating and second heating of poly(DLLA-co-Asp)-*b*-PEO (No.3, Tab. 19).

Tab. 20. Crystallinity and melting point of PEO block in triblock copolymers

Polymer	PEO in wt%	1st heating T_m/°C	ΔH/J/g	α_c/%	Cooling T_c/°C	ΔH/J/g	2nd heating T_m/°C	ΔH/J/g	α_c/%
PEO8000	100	58	188.5	100	20.9	187.8	57.3 .	177.7	94.3
Poly[DLLA-co-Asp(OBzl)]-*b*-PEO	38.0	46.0	51.5	71.9	-	-	45.3	0.6	0.8
Poly[DLLA-co-Asp(OBzl)]-*b*-PEO	53.7	50.2	82.5	81.5	11.9	66.1	49.0	.68.9	68.1
Poly(DLLA-co-Asp)-*b*-PEO	39.5	42.0	55.5	74.5	-	-	T_g= -25.1 °C		
Poly(DLLA-co-Asp)-*b*-PEO	55.6	47.5	94.7	90.4	-16.5	27.2	45.1 -25.4 [a)]	76.0 15.1 [a)]	72.5

a) crystallization at second heating.

Mechanical properties

Tab. 21 shows mechanical properties of poly(DLLA-co-Asp)-*b*-PEO. Compared with a PDLLA homopolymer, poly(DLLA-co-Asp)-*b*-PEO has a lower Young ' s modulus and lower elongation at break. The properties are controlled both by the PEO center block and the two end blocks poly(DLLA-co-Asp). For poly(DLLA-co-Asp)-*b*-PEO (No.4, Tab. 19), the mechanical properties can not be tested because it is too brittle. This may result from the high weight fraction of PEO in the block copolymer and the low molecular weight of the block copolymer.

Tab. 21. Mechanical properties of block copolymers

Sample No.	Young' s modulus in N/cm^2	Stress at break in MPa	Stress at yield in MPa	Elongation at yield in %	Elongation at break in %
PDLLA	201	42.7	88.2	11	480
poly(DLLA-co-Asp)-*b*-PEO (39.5%)	183	1.5	6.8	7	42
poly(DLLA-co-Asp)-*b*-PEO(59.6%)	-	-	-	-	-

2.1.6 New block copolymers based on depsipeptides, DLLA or LLA, and PEO

PLA, PGA, PCL and their copolymers constitute the most promising bioresorbable materials in the field of surgery and pharmaceutics. Recently, a new family of triblock copolymers based on PEO has attracted the attention of investigators. This is largely due to the unique properties that the PEO moiety can confer, namely, solubility in water and many organic solvents, lack of toxicity, rapid clearance from body, lack of immunogenicity, high mobility and large exclusion volume in water, and FDA approval for internal consumption. When coupled to another molecule, many of these properties are transferred to the conjugate product. Copolymerization of LA or GA with PEO alters the flexibility and hydrophilicity of these materials, thus extending their applicability.

Because the PEO block is soluble in water while the end blocks are not, the resulting copolymers inevitably form micellar structures in water and are thus potential candidates for carriers in controlled drug-delivery systems. In the following study, some new ABA triblock copolymers will be synthesized and characterized, where the B block is PEO8000 and two end A blocks are random copolymers of DLLA or LLA and morpholine-2,5-diones.

Synthesis of new ABA triblock copolymers

The new ABA triblock copolymers were synthesized via ring-opening polymerization of DLLA or LLA with morpholine-2,5-diones in the presence of PEO8000 as an initiator and stannous octoate as a catalyst at 140 °C for 9 h. The following scheme shows the general reaction (Scheme 9):

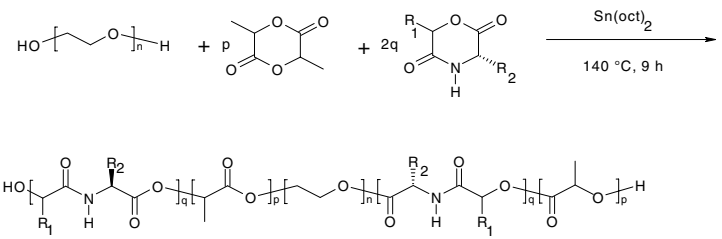

Scheme 9. Reaction scheme of the preparation of block copolymers based on depsipeptides, DLLA or LLA and PEO.

Since the two terminal hydroxy groups of the PEO essentially have equal reactivity toward monomers it acts as a macroinitiator for the ring-opening polymerization of morpholine-2,5-diones and DLLA or LLA. The mechanism of this polymerization can be explained by the mechanism of hydroxy-bearing species initiating lactone polymerization. Because the ^{1}H NMR signals of each monomer residue are distinguished and well separated, the molar ratio in the block copolymers is determined according to ^{1}H NMR. Tab. 22 and 23 show the yield, composition and molecular weight of the block copolymers.

Tab. 22. Copolymerization of morpholine-2,5-diones, DLLA or LLA with PEO in the presence of $Sn(oct)_2$ catalyst at 140 °C for 9 h

No.	Morpholine-2,5-dione	Comonomer	LA/MD [a)]	W_{PEO} [b)] in wt%	Yield [c)] in %	Block copolymer
1	-	DLLA	1:0	15	92	PDLLA-PEO
2	-	LLA	1:0	15	97	PLLA-PEO
3	Cyclo(Glc-Val)	DLLA	5:1	15	88	PDLLA-Glc-Val-EO-1
4	Cyclo(Glc-Val)	DLLA	1:1	15	78	PDLLA-Glc-Val-EO-2
5	Cyclo(Glc-Val)	DLLA	5:1	30	90	PDLLA-Glc-Val-EO-3
6	Cyclo(Glc-Val)	DLLA	5:1	45	91	PDLLA-Glc-Val-EO-4
7	Cyclo(LLA-Ile)	DLLA	5:1	15	93	PDLLA-Ile-EO-1
8	Cyclo(LLA-Ile)	DLLA	1:1	15	86	PDLLA-Ile-EO-2
9	Cyclo(LLA-Ile)	DLLA	5:1	30	61	PDLLA-Ile-EO-3
10	Cyclo(LLA-Ile)	DLLA	5:1	45	77	PDLLA-Ile-EO-4
11	Cyclo(LLA-Ile)	-	0:1	15	40	P(LLA-Ile)-PEO
12	Cyclo(LLA-Ile)	LLA	5:1	15	80	PLLA-Ile-EO-1
13	Cyclo(LLA-Ile)	LLA	1:1	15	60	PLLA-Ile-EO-2
14	Cyclo(LLA-Ile)	LLA	5:1	30	87	PLLA-Ile-EO-3
15	Cyclo(LLA-Ile)	LLA	5:1	45	85	PLLA-Ile-EO-4
16	Cyclo(LLA-Gly)	DLLA	5:1	15	86	PDLLA-Gly-EO-1
17	Cyclo(LLA-Gly)	DLLA	1:1	15	91	PDLLA-Gly-EO-2
18	Cyclo(LLA-Gly)	DLLA	5:1	30	94	PDLLA-Gly-EO-3
19	Cyclo(LLA-Gly)	DLLA	5:1	45	97	PDLLA-Gly-EO-4
20	Cyclo(LLA-Gly)	-	0:1	15	70	P(LLA-Gly)-PEO
21	Cyclo(LLA-Gly)	LLA	5:1	15	83	PLLA-Gly-EO-1
22	Cyclo(LLA-Gly)	LLA	1:1	15	86	PLLA-Gly-EO-2
23	Cyclo(LLA-Gly)	LLA	5:1	30	87	PLLA-Gly-EO-3
24	Cyclo(LLA-Gly)	LLA	5:1	45	76	PLLA-Gly-EO-4
25	Cyclo(Glc-Leu)	LLA	5:1	15	83	PLLA-Glc-Leu-EO-1
26	Cyclo(Glc-Leu)	LLA	1:1	15	57	PLLA-Glc-Leu-EO-2
27	Cyclo(Glc-Leu)	LLA	5:1	30	83	PLLA-Glc-Leu-EO-3
28	Cyclo(Glc-Leu)	LLA	5:1	45	61	PLLA-Glc-Leu-EO-4
29	Cyclo(Glc-Leu)	-	0:1	15	84	P(Glc-Leu)-PEO

a) mole ratio of morpholine-2,5-diones and DLLA or LLA in the feed.
b) PEO weight fraction in the feed.
c) calculated according to $W_{polymer}$/(Weight of PEO + Weight of MD) × 100%.

Tab. 23. Compositions and molecular weight of triblock copolymers

No.	Block copolymer	LA/MD/EO [a]	$\overline{M_{n,F}}$ [b] $\times 10^{-4}$	$\overline{M_{n,f}}$ [c] $\times 10^{-4}$	$\overline{M_n}$ [d] $\times 10^{-4}$	$\overline{M_w}$ [d] $\times 10^{-4}$	$\overline{M_w}/\overline{M_n}$ [d]
1	PDLLA-PEO	76/0/24	5.3	5.00	2.31	4.55	1.97
2	PLLA-PEO	62/0/38	5.3	2.97	1.79	3.32	1.85
3	PDLLA-Glc-Val-EO-1	67/5/26	5.3	3.79	4.64	5.25	1.13
4	PDLLA-Glc-Val-EO-2	46/20/34	5.3	2.31	1.43	3.12	2.18
5	PDLLA-Glc-Val-EO-3	47/6/47	2.7	2.45	1.65	2.18	1.32
6	PDLLA-Glc-Val-EO-4	32/5/63	1.8	1.65	1.37	1.69	1.23
7	PDLLA-Ile-EO-1	67/8/25	5.3	4.90	4.62	5.25	1.14
8	PDLLA-Ile-EO-2	46/21/33	5.3	3.96	2.92	5.14	1.76
9	PDLLA-Ile-EO-3	48/2/50	2.7	2.15	1.85	2.45	1.32
10	PDLLA-Ile-EO-4	35/2/63	1.8	1.58	1.44	1.73	1.20
11	P(LLA-Ile)-PEO	0/18/82	5.3	1.54	1.07	1.29	1.21
12	PLLA-Ile-EO-1	62/2/45	5.3	2.70	2.54	3.80	1.50
13	PLLA-Ile-EO-2	57/6/37	5.3	3.11	2.06	2.79	1.35
14	PLLA-Ile-EO-3	42/1.5/56.5	2.7	1.82	1.66	2.02	1.22
15	PLLA-Ile-EO-4	33/2/65	1.8	1.50	1.32	1.49	1.13
16	PDLLA-Gly-EO-1	69/6/25	5.3	4.68	3.07	4.97	1.62
17	PDLLA-Gly-EO-2	59/19/22	5.3	5.12	3.51	6.32	1.80
18	PDLLA-Gly-EO-3	52/5/43	2.7	2.51	2.60	3.40	1.31
19	PDLLA-Gly-EO-4	37/3/60	1.8	1.65	1.41	1.63	1.16
20	P(LLA-Gly)-PEO	0/61/39	5.3	4.61	3.27	4.74	1.45
21	PLLA-Gly-EO-1	66/7/27	5.3	4.90	1.79	4.00	2.23
22	PLLA-Gly-EO-2	49/24/27	5.3	5.06	1.17	2.73	2.33
23	PLLA-Gly-EO-3	49/6/45	2.7	2.49	1.45	2.00	1.38
24	PLLA-Gly-EO-4	31/4/65	1.8	1.60	1.30	1.77	1.36
25	PLLA-Glc-Leu-EO-1	67/5/28	5.3	4.54	1.07	2.02	1.89
26	PLLA-Glc-Leu-EO-2	44/22/34	5.3	4.55	2.07	4.54	2.19
27	PLLA-Glc-Leu-EO-3	46/5/49	2.7	2.29	1.58	1.88	1.19
28	PLLA-Glc-Leu-EO-4	30/3/67	1.8	1.51	1.07	1.68	1.57
29	P(Glc-Leu)-PEO	56/44	5.3	4.74	0.81	1.63	2.01

a) mole fraction of lactyl/morpholine-2,5-dione/ethyloxide(LA/MD/EO) in the copolymer, determined by ^{1}H-NMR spectroscopy.
b) calculated by mole fraction in the feed.
c) molecular weight of triblock copolymers was estimated by ^{1}H NMR spectroscopy.
d) molecular weight of triblock copolymers was measured by GPC with DMAc as solvent.

The results shown in Tab. 22 and 23 demonstrate that the triblock copolymers are obtained by ring-opening polymerization of LLA or DLLA with morpholine-2,5-diones. The block copolymers were characterized by means of ^{1}H NMR and IR. The results and discussion are similar to the above discussion in Section 2.1.1-2.1.5.

Thermal analysis of triblock copolymers

The melting and crystallization behavior of the triblock copolymers with different composition was investigated by means of DSC. All samples were first heated above the melting temperature, then cooled to −70 °C at a rate of 10 °C/min and finally heated at 10 °C/min from -70 to 200 °C or 220 °C.

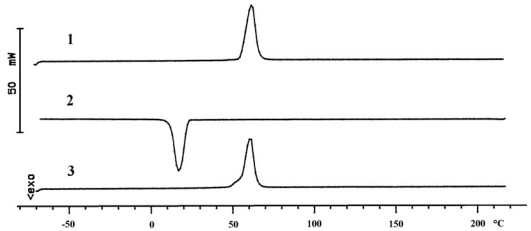

Fig. 24. DSC thermograms of PEO8000, Curve 1: first heating, Curve 2: cooling, Curve 3: second heating.

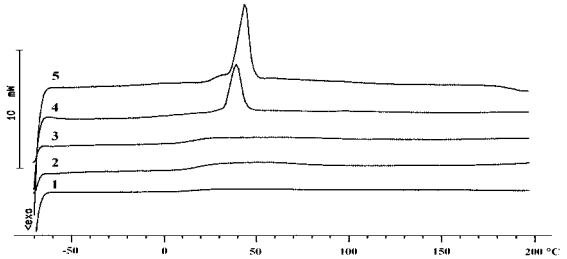

Fig. 25. DSC thermograms of PDLLA-Glc-Val-EO upon first heating, Curve 1: PDLLA-PEO, Curve 2: PDLLA-Glc-Val-EO-2, Curve 3: PDLLA-Glc-Val-EO-1, Curve 4: PDLLA-Glc-Val-EO-3, Curve 5: PDLLA-Glc-Val-EO-4.

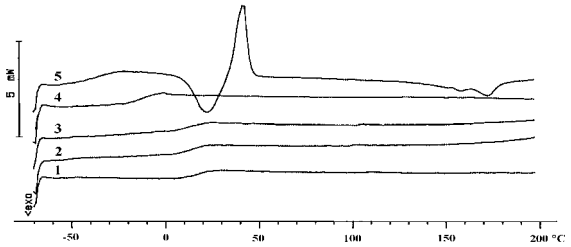

Fig. 26. DSC thermograms of PDLLA-Glc-Val-EO upon second heating, Curve 1: PDLLA-PEO, Curve 2: PDLLA-Glc-Val-EO-2, Curve 3: PDLLA-Glc-Val-EO-1, Curve 4: PDLLA-Glc-Val-EO-3, Curve 5: PDLLA-Glc-Val-EO-4.

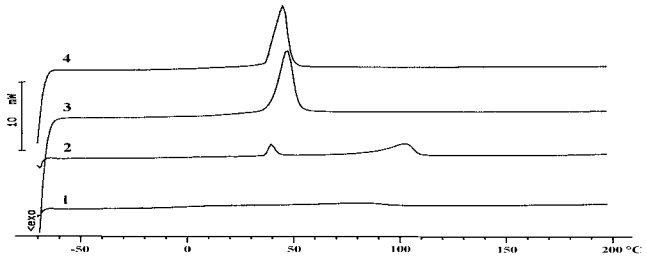

Fig.27. DSC thermograms of PDLLA-Ile-EO upon first heating, Curve 1: PDLLA-Ile-EO-1, Curve 2: PDLLA-Ile-EO-2, Curve 3: PDLLA-Ile-EO-3, Curve 4: PDLLA-Ile-EO-4.

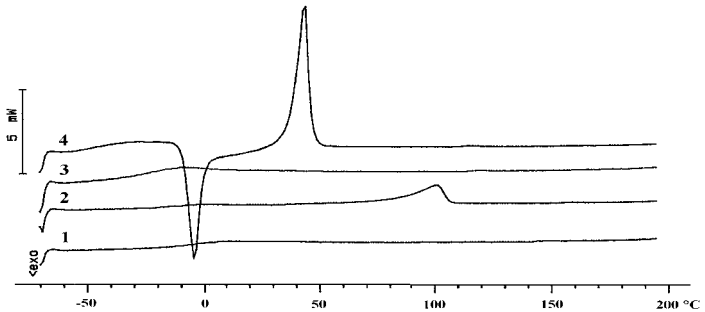

Fig.28. DSC thermograms of PDLLA-Ile-EO upon second heating, Curve 1: PDLLA-Ile-EO-1, Curve 2: PDLLA-Ile-EO-2, Curve 3: PDLLA-Ile-EO-3, Curve 4: PDLLA-Ile-EO-4.

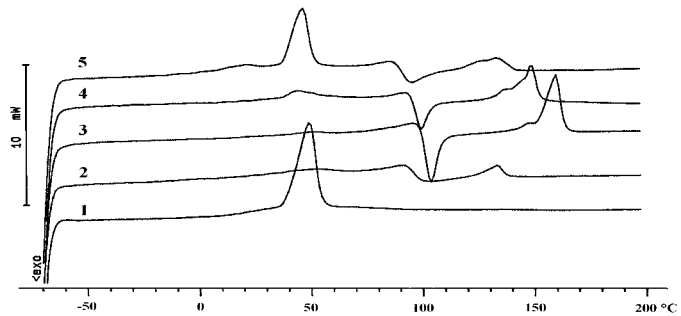

Fig. 29. DSC thermograms of PLLA-Ile-EO upon first heating, Curve 1: P(LLA-Ile)-EO, Curve 2: PLLA-Ile-EO-2, Curve 3: PLLA-Ile-EO-1, Curve 4: PLLA-Ile-EO-3, Curve 5: PLLA-Ile-EO-4.

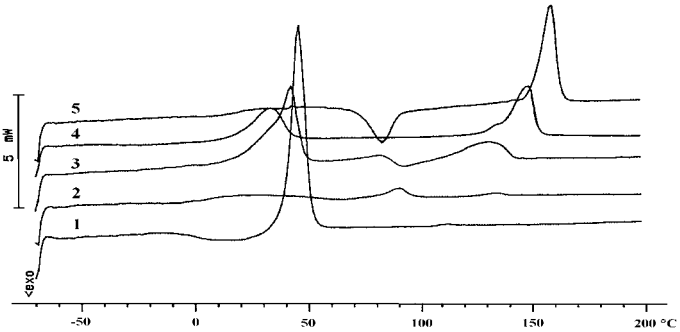

Fig. 30. DSC thermograms of PLLA-Ile-EO upon second heating, Curve 1: P(LLA-Ile)-EO, Curve 2: PLLA-Ile-EO-2, Curve 3: PLLA-Ile-EO-4, Curve 4: PLLA-Ile-EO-3, Curve 5: PLLA-Ile-EO-1.

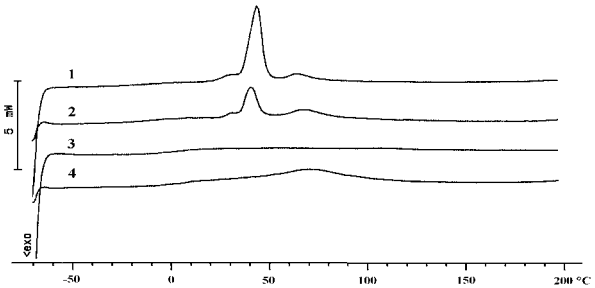

Fig. 31. DSC thermograms of PDLLA-Gly-EO upon first heating, Curve 1: PDLLA-Gly-EO-4, Curve 2: PDLLA-Gly-EO-3, Curve 3: PDLLA-Gly-EO-1, Curve 4: PDLLA-Gly-EO-2 .

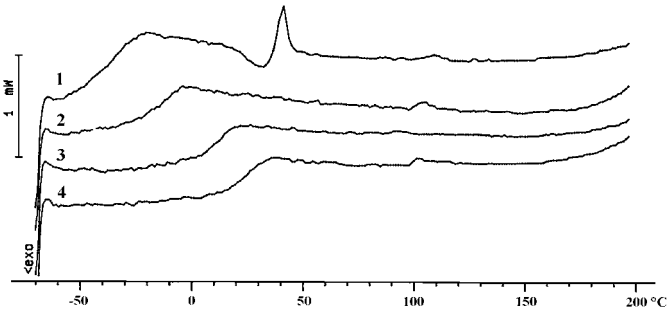

Fig. 32. DSC thermograms of PDLLA-Gly-EO upon second heating, Curve 1: PDLLA-Gly-EO-4, Curve 2: PDLLA-Gly-EO-3, Curve 3: PDLLA-Gly-EO-1, Curve 4: PDLLA-Gly-EO-2.

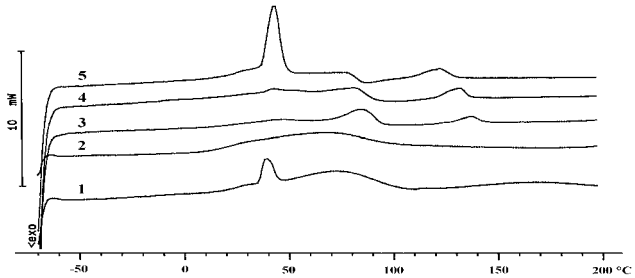

Fig. 33. DSC thermograms of PLLA-Gly-EO upon first heating, Curve 1: P(LLA-Gly)-PEO, Curve 2: PLLA-Gly-EO-2; Curve 3: PLLA-Gly-EO-1, Curve 4: PLLA-Gly-EO-3; Curve 5: PLLA-Gly-EO-4.

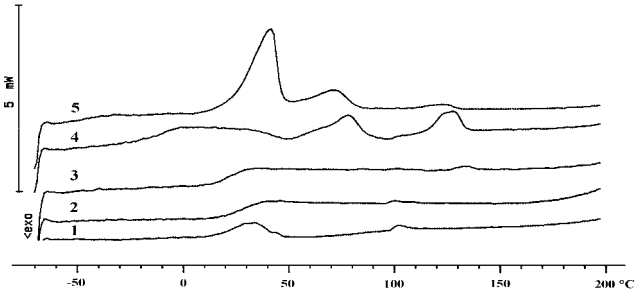

Fig. 34. DSC thermograms of PLLA-Gly-EO upon second heating, Curve 1: P(LLA-Gly)-PEO, Curve 2: PLLA-Gly-EO-2; Curve 3: PLLA-Gly-EO-1, Curve 4: PLLA-Gly-EO-3; Curve 5: PLLA-Gly-EO-4.

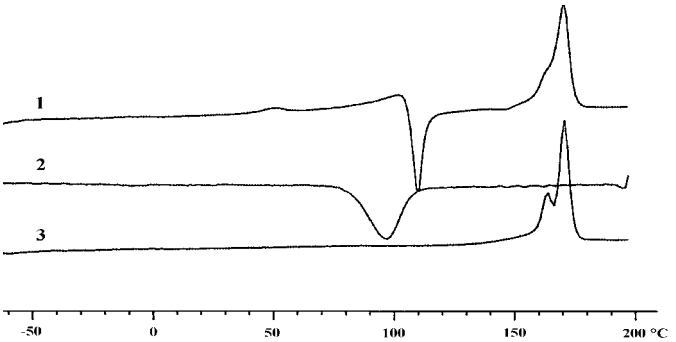

Fig. 35. DSC thermograms of PLLA-PEO, Curve 1: first heating, Curve 2: cooling, Curve 3: second heating.

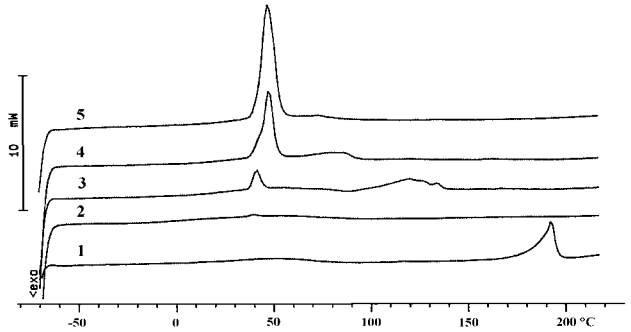

Fig. 36. DSC thermograms of PLLA-Glc-Leu-EO upon first heating, Curve 1: P(Glc-Leu)-PEO, Curve 2: PLLA-Glc-Leu-EO-2, Curve 3: PLLA-Glc-Leu-EO-1, Curve 4: PLLA-Glc-Leu-EO-3, Curve 5: PLLA-Glc-Leu-EO-4.

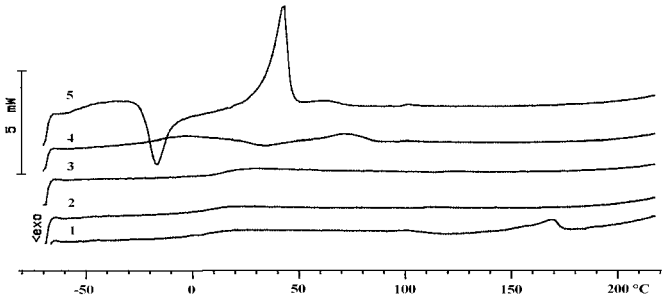

Fig. 37. DSC thermograms of PLLA-Glc-Leu-EO upon second heating, Curve 1: P(Glc-Leu)-PEO, Curve 2: PLLA-Glc-Leu-EO-2, Curve 3: PLLA-Glc-Leu-EO-1, Curve 4: PLLA-Glc-Leu-EO-3, Curve 5: PLLA-Glc-Leu-EO-4.

Tab. 24. Melting point and ΔH of block copolymers

No.[a]	PEO wt%	in PEO block [b] T_m/°C	ΔH/J/g	Copolymer block[b] T_m/°C	ΔH/J/g	T_g [b] /°C	PEO block [c] T_m/°C	ΔH/J/g	Copolymer block[c] T_m/°C	ΔH/J/g	T_g [c] /°C
1	16.0	-	-	-	-	18.0	-	-	-	-	16.4
2	26.9	51.1	2.1	170.7	45.9	-	-	-	170.6	49.0	-
3	21.1	-	-	-	-	15.4	-	-	-	-	14.0
4	34.6	44.1	25.7	-	-	-	-	-	-	-	14.2
5	32.6	39.0	30.9	-	-	-	-	-	-	-	-15.1
6	48.5	43.4	57.7	-	-	-	41.5	22.1	-	-	-
7	16.3	broad	11.6	-	-	-4.1	-	-	-	-	-1.5
8	20.2	39.3	9.2	102.3	37.4	-	-	-	101.2	23.5	-4.1
9	37.2	46.5	59.8	-	-	-	-	-	-	-	-24.1
10	50.6	47.0	76.7	-	-	-	44.3	66.1	-	-	-
11	51.9	47.9	56.9	-	-	-	45.4	61.1	-	-	-
12	29.6	-	-	159.2	28.4	-	-	-	158.0	31.8	19.6
13	25.7	-	-	90.7	13.1	-	19.6	11.4	90.8	5.1	-
				132.7	6.7				132.8	1.0	
14	43.9	44.0	7.7	147.7	25.0	-	33.5	24.1	147.8	26.5	-
15	53.3	45.9	29.3	132.7	10.1	-	42.5	39.7	82.6	5.5	-
									130.4	14.2	
16	17.1	-	-	-	-	5.0	-	-	-	-	13.1
17	15.6	-	-	69.7	50.3	0.0	-	-	101.4	0.4	24.6
18	31.9	40.3	20.0	68.6	14.1	-	-	-	-	-	-
19	48.5	43.4	52.3	65.1	4.3	-	41.8	3.5	-	-	-
20	17.3	39.2	10.1	75.5	28.4	-	33.7	6.8	101.3	1.0	-
21	16.3	-	-	83.7	15.2	-	-	-	135.1	1.1	22.1
				137.4	6.0						
22	15.8	-	-	65.0	broad	-	-	-	100.2	0.5	26.5
23	32.1	42.9	1.0	81.4	7.7	-	-1.4	17.3	77.9	11.6	-
				131.6	10.0				126.9	8.3	
24	50.0	42.3	43.1	122.3	8.5	-	41.6	28.2	72.1	6.4	-
									123.5	1.5	
25	17.6	41.6	6.8	120.0	21.3	-	-	-	-	-	15.0
26	17.6	39.4	1.1	-	-	-	-	-	-	-	6.2
27	34.9	47.1	35.8	86.1	8.0	-	-4.9	6.9	71.0	6.6	-
28	53.0	46.6	65.1	-	-	-	42.4	43.7	-	-	-
29	16.9	-	-	191.8	42.3	-	-	-	167.7	7.5	2.5

a) block copolymers are the same as in Tab. 23. b) upon first heating. c) upon second heating.

Fig. 24-37 show the DSC thermograms of the block copolymers at first and second heating. The melting temperature and ΔH are summarized in Tab. 24. The influence of copolymer blocks on the crytallization of PEO is similar to that of polydepsipeptides on the crystallization of PEO in ABA triblock copolymers as discussed in the above section 2.1.1. PEO8000 exerts a peak of first melting(T_m = 58 °C, ΔH = 195 J/g) and crystallization on cooling (T_c = 20.9 °C). The endotherm of the second melting was found at 57.3 °C (ΔH =

177.7 J/g) (Fig. 24). In Fig. 25, Curve 4 and 5 show only one endotherm that corresponds to the melting of the PEO block. The other curves show no endotherm. This indicates that the copolymer blocks of poly[DLLA-co-(Glc-Val)] do not crystallize.

Fig. 27 shows that Curve 3 and 4 have only one endotherm that corresponds to the melting of the PEO block, while Curve 2 exerts two distinct endotherms that correspond to the melting of PEO and poly(LLA-Ile). The higher the mole ratio of Cyclo(LLA-Ile) to DLLA the more enriched is poly(LLA-Ile) in the block copolymer.

Fig. 29 shows that the PLLA-enriched microstructure crystallizes when the block copolymer is prepared with a mole ratio of Cyclo(LLA-Ile) to LLA of 1:5. The random Ile units in the block copolymer result in decreasing the melting temperature of the PLLA blocks. The melting temperature decreases from 170.7 °C (LA/Cyclo(LLA-Ile) = 1:0) to 90.7 °C (LA/ Cyclo(LLA-Ile) = 1:1). Since the copolymer PLLA-Ile-EO-2 has a short PLLA sequence the lamella formation is restricted. The crystallinity and melting temperature of the PLLA block are low.

Fig. 31 shows that curve 1 and 2 have two distinct endotherms that correspond to the melting of the PEO and the poly(LLA-Gly) block. This indicates that the poly(LLA-Gly)-enriched microstructure is formed during the copolymerization even if the mole ratio of DLLA/Cyclo(LLA-Gly) is very high (5:1). The difference in polymerization activity between Cyclo(LLA-Gly) and DLLA may result in the formation of poly(LLA-Gly)-enriched blocks.

Fig. 33 shows that curve 3-5 have two distinct endotherms, beside the endotherm of PEO, that corresponding the melting of PLLA and poly(LLA-Gly). It is interesting to find that only a broad transition is observed for PLLA-Gly-EO-2. When the mole ratio of LLA/Cyclo(LLA-Gly) is 1:1, the copolymerization of Cyclo(LLA-Gly) and LLA results in a copolymer which does not crystallize. Fig. 36 shows a similar result.

Mechanical properties

Fig. 38 compares the typical stress-strain diagrams of the block copolymers. Tab. 25 shows average values of some mechanical properties of the block copolymers from five measurements per sample.

The results show that the block copolymers which were prepared with 45% PEO in the feed are very brittle, this results from the low molecular weight and high crystallinity of the PEO block. In general, for all of these block copolymers, increasing PEO molar ratios lead to a

decrease in molecular weight of the polylactide/depsipeptide block and a higher crystallinity in the PEO block.

The area under the stress-strain curve indicates the toughness of the material. Toughness is related to impact strength and indicates the energy that a material can absorb before breaking. Toughness is directly proportional to elongation at break. An increase in the amount of poly(Glc-Val) in the block copolymers PDLLA-Glc-Val-EO decreases elongation at break and toughness, while Young's modulus increases. Similar results were reported by Knüffermann in the study on the mechanical properties of poly[(DLLA-(Glc-Val)][8]. Except PDLLA-Ile-EO-1, the copolymers PDLLA-Ile-EO are brittle materials. A similar relationship between the stress and strain has been found in the study on PDLLA-Gly-EO block copolymers. However, the influence of the depsipeptide unit in PDLLA-Gly-EO block copolymers on the elongation at break and Young's modulus is stronger than that in PDLLA-Glc-Val-EO, i.e., the elongation at break of PDLLA-Gly-EO-2 decreases from 560% (PDLLA-Gly-EO-1) to 34%, while the Young's modulus increases from 23 to 450 MPa.

It is interesting to find that, for PLLA-Ile-EO, PLLA-Gly-EO and PLLA-Glc-Leu-EO, the influence of depsipeptide unit in block copolymers on the elongation at break and Young's modulus is completely different from that in PDLLA-Glc-Val-EO, PDLLA-Gly-EO. Compared with PLLA-Ile-EO-1, PLLA-Gly-EO-1 and PLLA-Glc-Leu-EO-1, PLLA-Ile-EO-2, PLLA-Gly-EO-2 and PLLA-Glc-Leu-EO-2 have higher elongation at break but lower Young's modulus. The effect is more significant with increasing amount of poly(LLA-Ile) and poly(Glc-Leu) in the block copolymers, for example, the elongation at break and Young's modulus of PLLA-Glc-Leu-EO-2 are 550% and 22 MPa, respectively. The elongation at break is larger by a factor of 4.5 than that of PLLA-Glc-Leu-EO-1, while Young's modulus decreases from 177 MPa to 22 MPa. Such a finding is somehow unexpected, because poly(LLA-Ile), poly(Glc-Leu) and poly(LLA-Gly) are semicrystalline polymers. It must be pointed out that PLLA is a semicrystalline polymer, while PDLLA is a amorphous polymer. When Cyclo(LLA-Ile), Cyclo(Glc-Leu) or Cyclo(LLA-Gly) were copolymerized with DLLA in the presence of PEO, polydepsipeptide units as rigid structures improve Young's modulus and at the same time decrease the elongation at break as expected. PLLA-PEO is a brittle block copolymer, due to the high crystallinity of the PLLA block. When the morpholine-2,5-diones as co-monomers are introduced into the PLLA block, the crystallinity of PLLA decreased significantly. That the copolymer block (poly[LLA-(Glc-Leu)]) in PLLA-Glc-Leu-EO-2 does not crystallize, while in PLLA-Glc-Leu-EO-1 it

crystallizes slightly (Tab. 24). This lower crystallinity in the blocks results in a higher elongation at break and a lower Young ' s modulus.

The weight fraction of PEO, the molecular weight of the block copolymers and the crystallinity affect the mechanical properties significantly. This means that block copolymers with different mechanical properties can be prepared by selecting of monomers and their mole ratio, controlling the weight fraction of PEO and the molecular weight of the block copolymers.

Tab. 25. Mechanical properties of block copolymers based on depsipeptides, DLLA or LLA and PEO

No.[a)]	Young' s modulus in N/cm^2	Stress at break in MPa	Stress at yield in MPa	Elongation at yield in %	Elongation at break in %
1	62	6.5	6.2	15	550
2	-	10.1	-	-	2.5
3	8.6	7.9	3.9	26	510
4	48	5.2	3.9	12	402
5	95	4.7	-	-	10
6	-	-	-	-	-
7	6.1	1.9	0.7	40	780
8	-	-	-	-	0.9
9	-	-	-	-	-
10	-	-	-	-	-
11	-	-	-	-	-
12	288	22	-	-	37
13	76	9.2	9.0	37	400
14	97	7.0	8.9	19	83
15	-	-	-	-	1.2
16	23	4.4	1.8	18	560
17	450	2.0	14	5	34
18	100	0.6	5.5	9	37
19	-	-	-	-	-
20	-	-	-	-	1.1
21	339	14	-	-	15
22	255	1.4	14	8	84
23	156	6	11	17	90
24	-	-	-	-	1.1
25	177	10	11	40	100
26	22	1.5	1.7	17	550
27	23	2.5	4	60	150
28	97	6	-	-	33
29	-	-	-	-	-

a) block copolymes are the same as in Tab. 23.

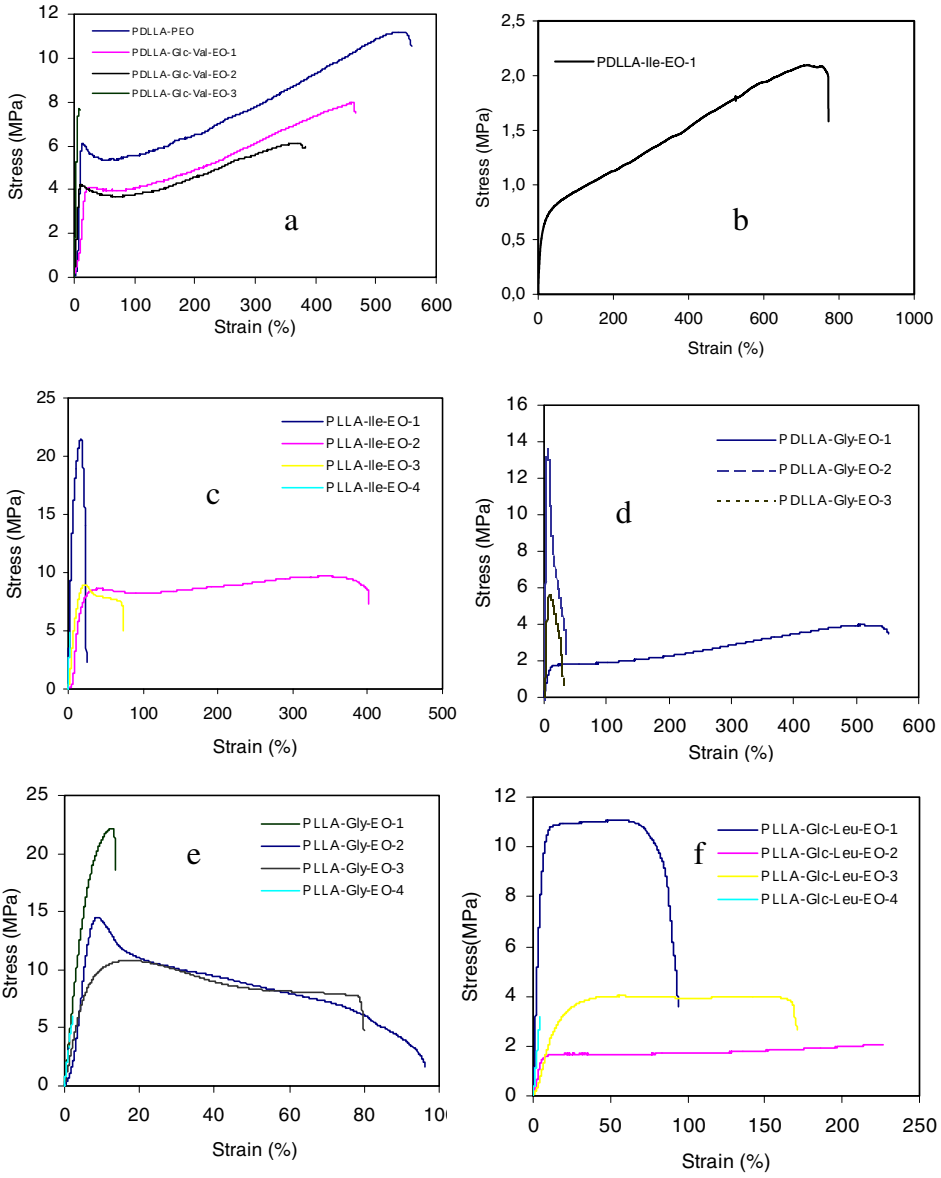

Fig. 38. Stress-strain diagrams of block copolymers based on depsipeptides, DLLA or LLA and PEO.

2.1.7 Degradation of block copolymers based on depsipeptides, DLLA or LLA, and PEO

The synthesis and degradation of random copolymers of DLLA or CL with Cyclo(DLLA-Gly) were studied by Helder et al.[29,35,38,39,40]. Their results indicate that the copolymers degrade faster than their individual homopolymers do. Similarly, the crystallinity, degradability and some other properties of polydepsipeptides may be changed by the incorporation of DLLA or LLA into polydepsipeptides-PEO block copolymers. In this part the hydrolytic degradability of the block copolymers, which were prepared in Section 2.1.6, was studied. The *in vitro* degradation behavior of compression moulded samples was determined at 37 °C and pH 7.0 in phosphate buffer. Several variables were measured to characterize the degradation behavior, including (1) water absorption, (2) weight loss, (3) molecular weight reduction, and (4) ^{1}H NMR spectrum.

Hydrophilicity of copolymers

The hydrophilicity of block copolymers was determined by measuring the static contact angles. The results listed in Tab. 26 clearly show that the static contact angle θ decreases with increasing PEO content in the block copolymer. However, the values of the static contact angles of PLLA-Ile-EO-4 and PLLA-Glc-Leu-EO-4 are higher than those of PLLA-Ile-EO-3 and PLLA-Glc-Leu-EO-3, respectively. When the block copolymers have higher PEO content, the surface of the polymer film is wetted very quickly by water, and water is adsorbed. In this case, it is difficult to exactly measure the static contact angle.

Tab. 26. Static contact angle and molecular weight of the block copolymers after degradation

No. [a]	PEO in wt%	θ in degree	$\overline{M_{n,7}}/\overline{M_n}$ [b] in %	$\overline{M_{n,14}}/\overline{M_n}$ [c] in %	$(\overline{M_w}/\overline{M_n})_7$ [d]	$(\overline{M_w}/\overline{M_n})_{14}$ [e]
1	16.0	51±1	67.9	54.5	1.90	3.06
2	26.9	67±2	67.1	54.2	3.01	4.29
3	21.1	55±1	65.5	56.2	2.41	2.50
4	34.6	56±2	68.9	51.5	1.89	1.94
5	32.6	43±2	47.6	40.7	1.89	2.53
6	48.5	40±2	67.7 [f]	50.1 [b]	1.57 [f]	1.88 [b]
7	16.3	72±2	50.7	34.6	1.92	2.10
8	20.2	53±2	36.7	25.4	1.54	2.37
9	37.2	66±2	80.5	67.0	1.70	1.63
10	50.6	62±2	81.3 [g]		1.21 [g]	
11	51.9	89±2	88.1	84.5	1.22	1.11
12	29.6	51±5	66.1	50.7	2.29	3.26
13	25.7	50±3	65.5	45.5	1.59	3.36
14	43.9	45±5	72.9	56.6	1.32	1.96
15	53.3	60±3	93.1	79.2	1.43	1.58
16	17.1	77±1	39.4	25.3	2.50	2.57
17	15.6	90±1	51.1	n.d.	2.54	n.d.
18	31.9	45±2	34.7	23.3	1.97	3.57
19	48.5	40±1	68.2 [g]	n.d.	1.49 [g]	n.d.
20	17.3	36±2				
21	16.3	62±2	41.7	31.9	3.41	3.41
22	15.8	76±2	45.2	n.d.	3.35	n.d.
23	32.1	38±1	47.1	38.5	2.15	2.76
24	50.0	34±1	73.1		1.30	
25	17.6	64±1	45.1	32.6	3.58	5.76
26	17.6	90±2	37.0	24.8	2.67	3.26
27	34.9	55±2	35.5	31.3	2.73	3.49
28	53.0	84±3	77.5	91.5	1.81	1.34
29	16.9	74±1	27.6		2.74	

a) block copolymers are the same as in Tab. 23. b) molecular weight decrease after degradation for 7 days in buffer. c) molecular weight decrease after 14 days d) molecular weight distribution after degradation for 7 days. e) molecular weight distribution after degradation 14 days. f) degradation for 1 day. g) degradation for 3 days.

Water absorption

For degradation studies film specimens with 1.5 cm^2 surface area and approximate identical weights (60 - 90 mg) were obtained from plates prepared by compression moulding. The specimens were incubated in 5 mL of Na_2HPO_4/KH_2PO_4 buffer (pH 7.0) at 37 °C in a shaking incubator operating at a frequency of 60 rpm. At the end of each immersion period, the

specimens were take out, washed with distilled water three times, and dried at room temperature in a desiccator *in vacuo* over P_2O_5 for 14 days.

The water absorption was determined by using the equation:

Water Absorption = $(W_s - W_d) \times 100\% / W_d$

where W_d and W_s are the weight of the dried sample and the weight of the swollen sample at a given time.

Fig. 39(a-f) shows that water adsorption increases gradually with increasing degradation time. In general, water adsorption is mainly proportional to the weight fraction of PEO in the block copolymers. With increasing weight fraction of PEO, the hydrophilicity is improved and the water adsorption ability is elevated significantly. The crystallinity of the copolymer blocks affects the water adsorption ability. From Fig. 39(f), it is seen that water adsorption of PLLA-Glc-Leu-PEO-1 is much lower than that of PLLA-Glc-Leu-PEO-2, although the weight fraction of PEO in these two block copolymers is equal. As mentioned in Section 2.1.6, the crystallinity of poly(LLA-(Glc-Leu)) copolymer block in PLLA-Glc-Leu-PEO-2 decreases with increasing depsipeptide content. The crystalline regions of poly(LLA-(Glc-Leu)) (not in PEO) are more resistant to water adsorption, the amorphous block absorbs water more rapidly. The water adsorption ability of P(Glc-Leu)-PEO is smaller than that of PLLA-Glc-Leu-EO-1; this is due to the higher crystallinity of polydepsipeptide block.

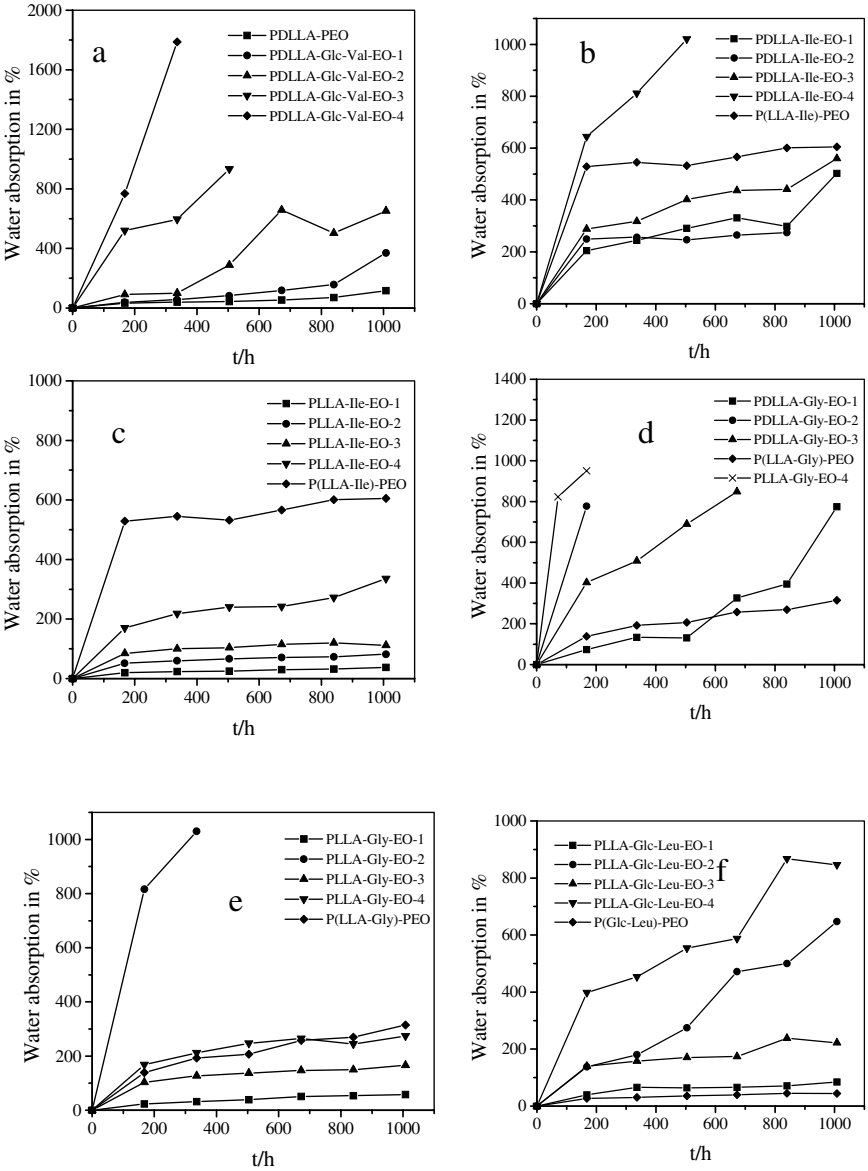

Fig. 39. Water adsorption of block copolymers based on depsipeptides, DLLA or LLA and PEO

Weight loss

The weight loss behavior as presented in Fig. 40(a-f) reveals that the weight loss rates are very different for different block copolymers. The degradation occurs in the bulk by random chain scission. Once the average molecular weight of the sample decreases to a certain level or the weight fraction of PEO is higher than a certain value in the degraded block copolymers, chains become soluble and weight loss is observed. The block copolymers based on depsipeptides, DLLA and PEO lose their weight faster than the block copolymers which are based on depsipeptides, LLA and PEO. This is due to the higher crystallinity of copolymer blocks in PLLA/depsipetide-PEO. For the same kind of block copolymers, the weight loss rate depends on the weight fraction of PEO in the block copolymers and the starting molecular weight.

The weight of the PLLA-PEO sample (Fig. 40 f) remains steady through 6 weeks since the molecular weight had not gone below the critical value where the oligomers would be soluble in the buffer. The weight decrease of PLLA-Glc-Leu-EO-1 is much faster than that of PLLA-PEO. This result indicates that the additional depsipeptide units change the degradation behavior significantly. PLLA-PEO block copolymer shows a higher melting temperature and heat of fusion than PLLA-Glc-Leu-EO block copolymers. Smaller, less perfect crystallites in the block copolymers degrade more quickly than the larger defect-free crystallites of PLLA-PEO; therefore, the weight of PLLA-Glc-Leu-EO-1 decreases more quickly. Poly(LLA-(Glc-Leu)) blocks in PLLA-Glc-Leu-EO-2 are amorphous and should be degradable much faster than PLLA-Glc-Leu-EO-1. However, in the first 4 weeks of degradation, the results are completely the contrary as expected, after 4 weeks, they are as expected. Another factor that influences the weight loss rate is the hydrophilicity of the block copolymers. The solubility of the degraded block copolymer of PLLA-Glc-Leu-EO-2 is different from that of PLLA-Glc-Leu-EO-1, because the mole ratio of LLA to depsipeptide is different. The “critical value” (beyond critical value degradation product is soluble in water) of molecular weight for PLLA-Glc-Leu-EO-2 might be higher than that for PLLA-Glc-Leu-EO-1. After 4 weeks of degradation, PLLA-Glc-Leu-EO-2 degrades below the critical value and the weight decreases much fast.

The results of the weight loss for other block copolymers shown in Fig. 40 (a-e) can be explained by a similar way.

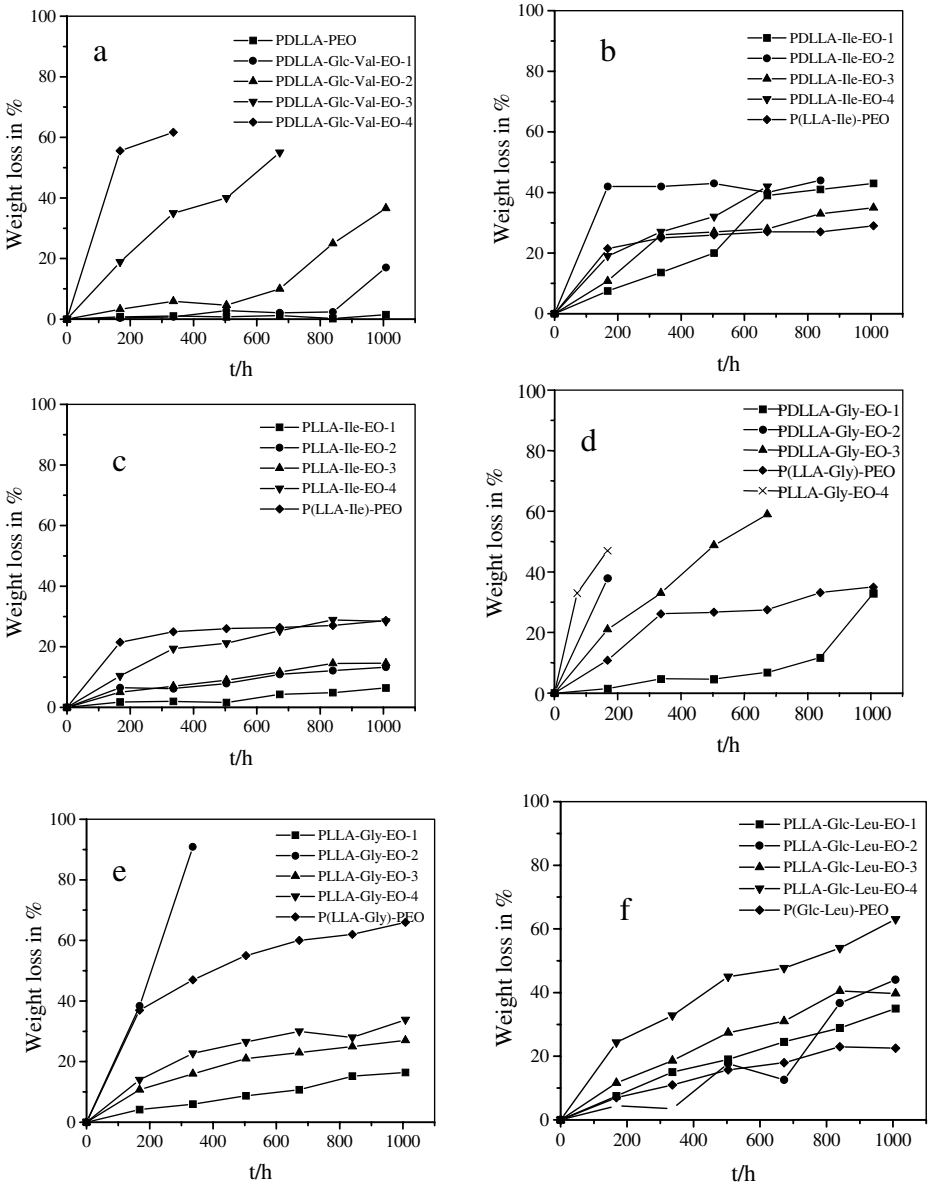

Fig. 40. Weight loss during degradation of block copolymers based on depsipeptides, DLLA or LLA and PEO

Decrease of molecular weight

Block copolymers based on depsipeptides, DLLA or LLA, and PEO degrade through hydrolysis of ester groups. The hydrolysis is autocatalyzed by carboxylic acid end groups. For semicrystalline PLLA-Glc-Leu-EO, PLLA-Gly-EO, PLLA-Ile-EO and PDLLA-Gly-EO, degradation occurs in two steps. In the first step, water diffuses into the amorphous region and the PEO region quickly and then hydrolysis begins. The second stage is the hydrolysis of the crystalline region[109)]. With amorphous PDLLA-Glc-Val-EO and PDLLA-Ile-EO (the crystallinity of the PEO blocks is not considered, because PEO absorbs water quickly), only the first stage occurs. The degradation rate depends on chemical structure, molecular weight and its distribution, morphological structure, dimension of the testing sample, and hydrolysis conditions.

The molecular weight and its distribution of the block copolymers after degradation in buffer at 37 °C for 7 days and 14 days were determined by means of GPC. The results are summarized in Tab. 26. The molecular weight decreases quickly, while polydispersity index increases (Tab. 26).

From results of degradation and mechanical properties studies, it is found that block copolymers based on depsipeptides, DLLA or LLA and PEO with different properties, i.e., crystallinity, mechanical properties, degradation rate, water absorption, are synthesized by selecting proper co-monomers from morpholine-2,5-diones, DLLA and LLA, controlling the mole ratio in the feed, and varying the relative amount of PEO. The block polymers might satisfy different requirements for different applications.

2.2 CaH_2 as a co-initiator for the ring-opening polymerization of 3(S)-isopropyl-morpholine-2,5-dione in the presence of PEO

PEO presents outstanding physico-chemical and biological properties, including hydrophilicity, solubility in water and in organic solvents, lack of toxicity, and absence of antigenicity and immunogenicity, which allows PEO to be used for many biomedical and biotechnological applications. Considerable effort has been focused on the preparation of polyester-PEO di- and triblock copolymers using a monohydroxy or α,ω-dihydroxy poly(ethylene oxide) as an initiator for the polymerization of lactones[95-97]. Copolymerization offered the possibility of varying the hydrophilic/hydrophobic and soft/hard segment ratio and thus, constitutes a very attractive means to modulate the basic properties of each homopolymer. It was reported that lactide can lead to PLA/PEO/PLA triblock copolymers when polymerization is performed in the presence of PEO and NaH[110]. The reaction proceeds quite rapidly and is completed within 5 min at 20 °C. However, slight racemization and formation of PLA homopolymers is observed. Rashkov et al. reported that the reaction between PEO and L-lactide in the presence of CaH_2 proceeds smoothly within 14 h at 140-145 °C without racemization. But after 96 h there is racemization[93,111].

Stannous octoate is one of the most effective catalysts that produce both high yields and high molecular weights in the preparation of polydepsipeptides[46]. However, stannous octoate, like many other catalysts, is more or less cytotoxic[112]. Furthermore, difficulties in removal of the catalyst from the resulting polymer limits its utilization in many cases.

The synthesis and characterization of PEO bearing poly(Glc-Val) sequences at both ends using CaH_2 as a co-initiator is investigated in this study. CaH_2 is selected because it is known as a PLA co-initiator and it is not supposed to lead to toxic impurities in the final product.

Synthesis and characterization of poly(Glc-Val)-b-PEO-b-poly(Glc-Val) copolymers

Block copolymers poly(Glc-Val)-*b*-PEO-*b*-poly(Glc-Val) (PGV/EO) were synthesized by polymerization of Cyclo(Glc-Val) in the presence of PEO6000 with CaH_2 as a co-initiator at 140 °C for 24 or 96 h (Scheme 10). The copolymerizations with mole fractions of Cyclo(Glc-Val), $F_{Cyclo(Glc\text{-}Val),}$ ranging from 14 to 65% in the feed, and the corresponding mole fractions of Cyclo(Glc-Val) in the block copolymers, $f_{Cyclo(Glc\text{-}Val)}$, are listed in Tab. 27 and 28. The composition of the triblock copolymers was determined by ^{1}H NMR spectroscopy from the

intensity ratio of the signals from the PEO block at δ =3.51 ppm (s; 4H, CH_2CH_2) and from the poly(Glc-Val) block at δ = 0.88-0.95 ppm (m; 6H, $2CH_3$) according to the following equation: $f_{Cyclo(Glc-Val)} = \frac{I_{CH_3}/6}{I_{CH_3}/6 + I_{CH_2}/4}$,

where I_{CH_3} and I_{CH_2} are the intensity of the signals originating from poly(Glc-Val) and PEO, respectively (Fig. 41, 42).

Tab. 27. Copolymerization of Cyclo(Glc-Val) with PEO in the presence of CaH_2 at 140 °C

No.	PEO in g	Cyclo(Glc-Val) in g	$F_{Cyclo(Glc-Val)}$ [a] in %	M/OH[b]	Reaction time in h	Yield[c] in %	Racemization in %[d]
PGV/EO1	0.6507	0.3764	14	12	24	52	13
PGV/EO2	0.5873	0.6976	25	24	24	61	12
PGV/EO3	0.3993	0.9064	39	46	24	37	12
PGV/EO4	0.4000	0.9070	39	46	96	55	41
PGV/EO5	0.2913	0.9840	46	68	96	43	42
PGV/EO6	0.2717	1.300	57	92	96	57	43
PGV/EO7	0.1420	0.9349	65	131	96	63	45

a) mole fraction of Cyclo(Glc-Val) in the feed, $F_{Cyclo(Glc-Val)}$ = [Cyclo(Glc-Val)]/([Cyclo(Glc-Val)] + [EO]) × 100%.
b) M/OH = [Cyclo(Glc-Val)]/[OH].
c) calculated according to W/(Weight of PEO + Weight of Cyclo(Glc-Val)) × 100%.
d) calculated according to ^{1}H NMR.

Tab. 28. Compositions and molecular weight of triblock copolymers

No.	$F_{Cyclo(Glc-Val)}$ in %	$f_{Cyclo(Glc-Val)}$ [a] in %	$\overline{M_n}$,f [b] $\times 10^{-3}$	$\overline{M_n}$ [c] $\times 10^{-3}$	$\overline{M_w}$ [c] $\times 10^{-3}$	$\overline{M_w}/\overline{M_n}$ [c]
PGV/EO1	14	9.3	8.2	8.8	14.7	1.67
PGV/EO2	25	16	10.1	10.2	16.7	1.64
PGV/EO3	39	17	10.4	10.7	15.1	1.41
PGV/EO4	39	31	16.1	15.8	21.3	1.35
PGV/EO5	46	41	20.6	24.0	28.4	1.18
PGV/EO6	57	47	24.9	27.8	34.4	1.24

a) mole fraction of Cyclo(Glc-Val) in the copolymer, determined by ^{1}H NMR spectroscopy.
b) molecular weight of triblock copolymers was estimated by ^{1}H NMR spectroscopy.
c) molecular weight of triblock copolymers was measured by GPC with DMAc as solvent.

The data demonstrate that the block copolymers poly(Glc-Val)-*b*-PEO-*b*-poly(Glc-Val) are obtained by ring-opening polymerization of Cyclo(Glc-Val) with hydroxytelechelic PEO6000 in yields from 37% to 63%. The yield of polymerization in the presence of PEO and CaH_2 as a co-initiator at 140 °C for 24 h is lower than that obtained in the presence of PEO and $Sn(oct)_2$ as a catalyst at 140 °C for 9 h.

The reaction mechanism for block copolymerization of Cyclo(Glc-Val) initiated by PEO in the presence of CaH_2 is not well understood. One possibility is that the ring-opening reaction is initiated through the formation of $(RO)_2Ca$ under the polymerization conditions (Scheme 10).

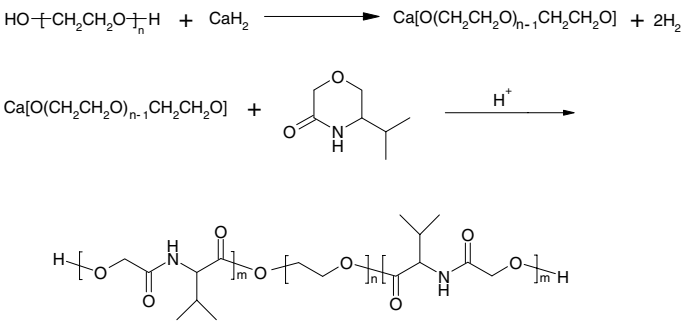

Scheme 10. Reaction mechanism of CaH_2 as a co-initiator for the ring-opening polymerization of 3(S)-isopropyl-morpholine-2,5-dione in the presence of PEO

The IR spectra of block copolymers PGV/EO1, PGV/EO3 and PGV/EO6 are shown in Fig. 43. The strong absorption band at 3390 cm^{-1} is assigned to the stretching band of N-H group in the poly(Glc-Val) blocks. The band at 1750-1758 cm^{-1} is due to C=O stretching mode of the ester group, and the band at 1680 cm^{-1} to the bending vibration of the N-H bond and the stretching mode of the C-N bond of the CONH group. The amide II band appears at 1540 cm^{-1}. The characteristic absorption band of PEO in the block copolymer appears at 1114 cm^{-1}. This indicates that the IR spectra of the block copolymers show absorption bands related to both PEO and poly(Glc-Val) blocks. The position and the relative intensity of the carbonyl stretching vibration depend on the length of poly(Glc-Val). The longer the poly(Glc-Val) block, the higher the relative intensity as referred to the C-H stretching band of the PEO block centered at 2887 cm^{-1}, and the longer the wavenumber (C=O), which shifted from 1750 cm^{-1} in the case of PGV/EO1 to 1758 cm^{-1} for PGV/EO7. Similar results were observed for PLA/PEO block copolymers[93,111]. The bands at 963 and 843 cm^{-1} are known to be characteristic of the crystalline phase of PEO[113]. In the IR spectra of the block copolymers shown in Fig. 43 absorption maxima characteristic of the crystalline phase of PEO are observed for PGV/EO1 and PGV/EO3 which suggests that PEO blocks within the copolymers are crystalline.

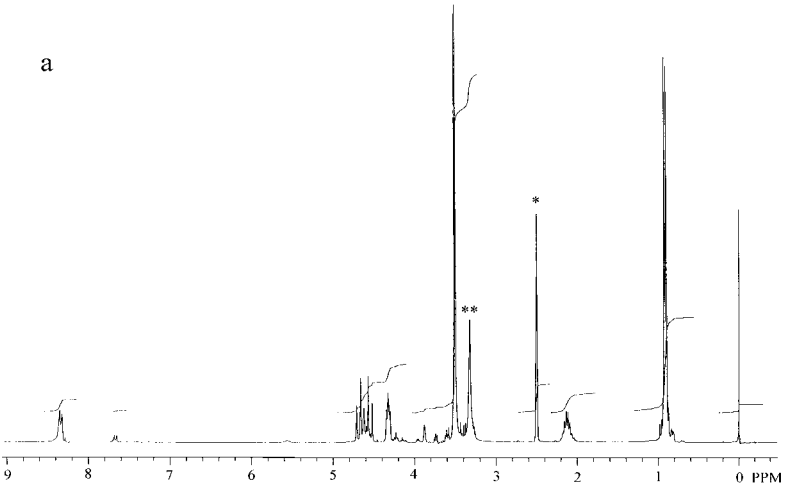

Fig. 41. ^{1}H NMR spectrum of PGV/EO3 in DMSO-d-6/TMS; * = DMSO-d-6 peaks, ** = H_2O peaks.

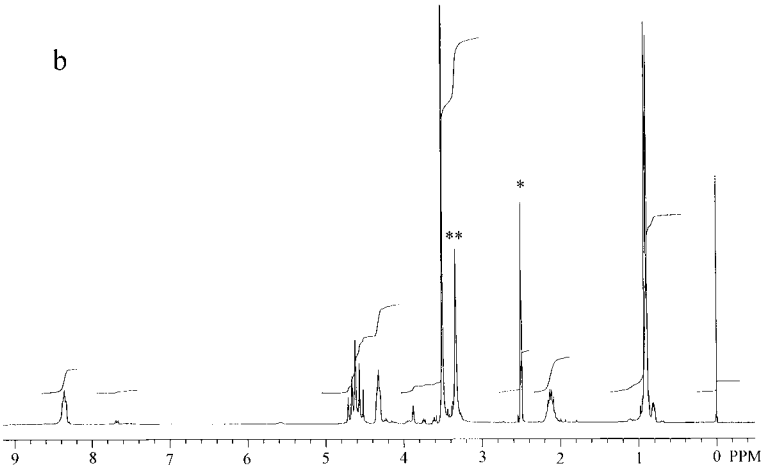

Fig. 42. ^{1}H NMR spectrum of PGV/EO4 in DMSO-d-6/TMS; * = DMSO-d-6 peaks, ** = H_2O peaks.

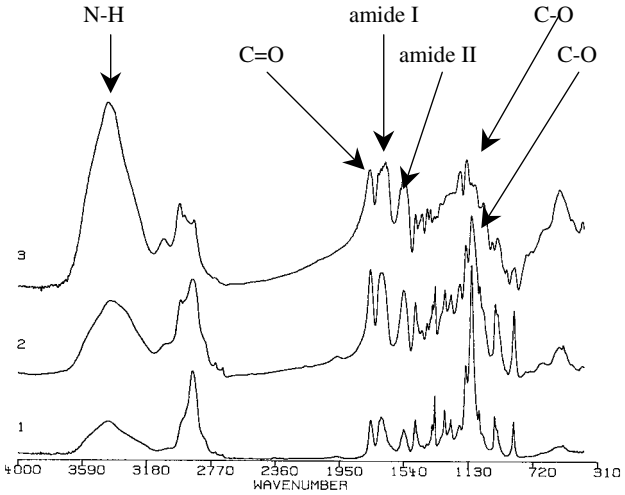

Fig. 43. IR of block copolymers PGV/EO1 (1), PGV/EO3 (2) and PGV/EO6 (3).

Fig. 41 and Fig. 42 show the ^{1}H NMR spectra of the block copolymers PGV/EO3 and PGV/EO4, respectively. The resonance line at 3.51 ppm originates from the methylene protons in the PEO blocks, the resonance at 8.36 ppm from the amide proton, the shifts at 0.92-0.99, 2.01-2.20 and 4.24-4.38 ppm from the S-valine residue in the poly(Glc-Val) block, and the shift at 4.50-4.73 ppm (AB-system, ^{AB}J = 14.6 Hz, 2H, CH_2-1, isotactic diad) from the glycolate residue in the poly(Glc-Val) block. In the ^{1}H NMR spectrum of the block copolymers there is a singlet at 4.62 ppm (s, 2H, CH_2-1, syndiotactic diad), which is evidence for the racemization of the S-valine residue during copolymerization of Cyclo(Glc-Val) with PEO in the presence of CaH_2[46]. On the other hand, no racemization of the S-valine residue was observed during polymerization of Cyclo(Glc-Val) in the presence of $Sn(oct)_2$ ([Cyclo(Glc-Val)]/[$Sn(oct)_2$] = 125, T_p=140 °C, t_p = 9 h)[46]. In the study on polymerization of 3(S)-isobutyl-morpholine-2,5-dione in the presence of PEO with $Sn(oct)_2$, racemization of the S-leucine residue did not occur as discussed above in Section 2.1.2. The intensity of the resonance at 4.62 ppm of PGV/EO4 is stronger than that of PGV/EO3 (Fig. 41, 42), which indicates that racemization in PGV/EO4 is more pronounced than that of PGV/EO3. The racemization of the S-valine residue during copolymerization of Cyclo(Glc-Val) with PEO in the presence of CaH_2 was determined from the ^{1}H NMR spectrum and is listed in Tab.27. It is seen that more than 40% of the S-valine residue racemized at 140 °C within 96 h, while about 12% occurred within 24 h. The reasons for the racemization are high reaction temperature,

long reaction time and basic reaction conditions. The deprotonation of Cyclo(Glc-Val) is the main source of racemization. Cyclo(Glc-Val) is much sensitive to racemization because the delocalization of the negative charge in a cyclic molecule is favored by entropy (Scheme 11). Kricheldorf et al. reported a similar racemization mechanism of L-lactide during the anionic polymerization of L-lactide[114,115].

Scheme 11. Racemization mechanism of Cyclo(Glc-Val) during the polymerization

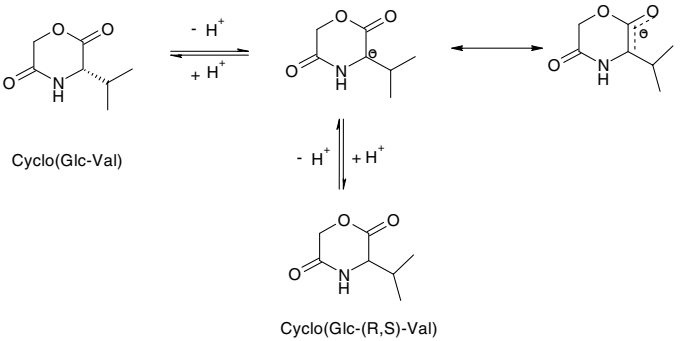

Besides the main resonances in the ^{1}H NMR spectrum of the block copolymers, there are many small characteristic peaks: a doublet at 7.68 ppm due to NH proton of the terminal amide unit, a broad singlet at 5.57 ppm ascribed to the proton of the end group $\underline{HO}CH_2$, a singlet peak at 3.9 ppm due to the α-methylene protons of the terminal hydroxyl group, a multiplet at 4.1-4.2 ppm due to α-methylene protons of poly(Glc-Val)-connecting EO units (poly(Glc-Val)-COO$\underline{CH}_2$-), a multiplet at 4.20-4.25 ppm due to – OOC$\underline{CH}$(CH(CH$_3$)$_2$)-NHCOCH$_2$OH in the end groups of poly(Glc-Val), and a multiplet at 0.80-0.85 ppm due to the protons of CH_3 end groups.

A typical ^{13}C NMR spectrum of PGV/EO5 is shown in Fig. 44 and reveals the presence of the different carbon atoms belonging to poly(Glc-Val) and PEO. For the poly(Glc-Val) blocks, there is no major difference between chemical shift values of the homopolymer and block copolymers, except for the resonances of CO groups. The chemical shifts at 166.6 ppm and 170.5 ppm, which also appear in ^{13}C NMR spectrum of poly(Glc-Val) prepared with Sn(oct)$_2$ as the catalyst at 140 °C for 9 h, are due to carbonyl carbon atoms of ester groups and of amide groups in syndiotactic diads, respectively. The resonance at 172.5 ppm is due to carbonyl carbon atoms at end groups. The resonance at 170.7 ppm is due to carbonyl carbon atoms of amide groups in isotactic diads, which indicates the racemization of the S-valine

residue during the ring-opening polymerization of Cyclo(Glc-Val) in the presence of CaH_2, in agreement with ^1H NMR results mentioned above. Furthermore, resonances at 62.1, 56.7, 30.0, 17.7 ppm are not single peaks. Every major resonance is overlapped by a small resonance which appears at almost the same chemical shift of the major resonance. This is also due to the racemization of the S-valine residue.

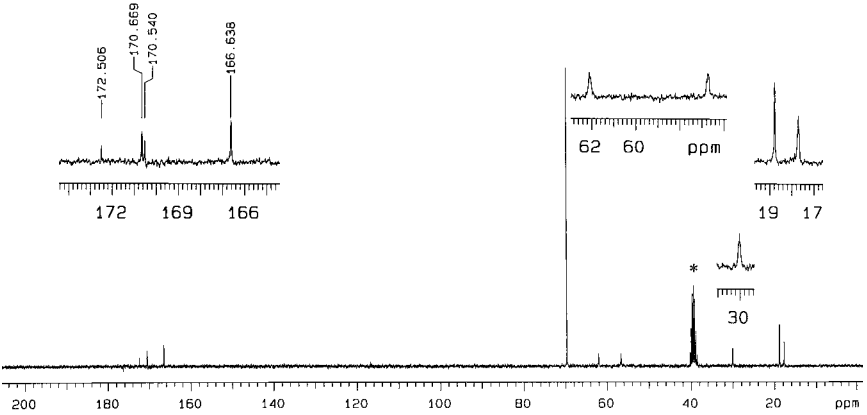

Fig. 44. ^{13}C NMR spectrum of PGV/EO5 in DMSO-d-6/TMS; * = DMSO peaks.

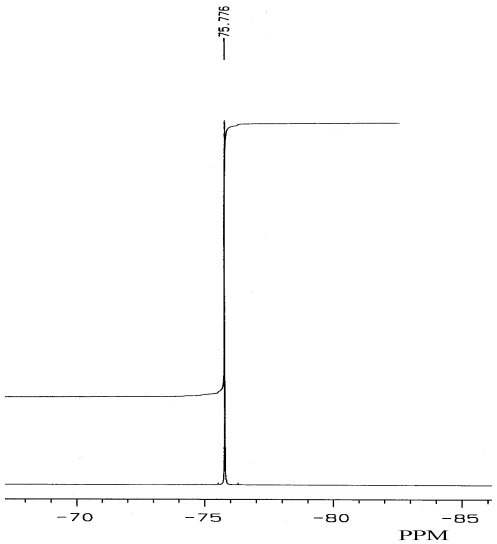

Fig. 45. ^{19}F NMR spectrum of PGV/EO5

It was found that all CH_2OH end-groups of PEO were esterified with Cyclo(Glc-Val) as determined by analysis with TFAA[101)] . The ^{19}F NMR spectrum of block copolymer treated with TFAA shows that only one peak appears at – 75.78 ppm (Fig. 45). It is worth to note the absence of a resonance at – 75.35 ppm which was due to PEO treated with TFAA. This indicates that all of the hydroxyl end groups of PEO initiated ring-opening polymerization of Cyclo(Glc-Val), at least within the limits of ^{19}F NMR sensitivity.

The block copolymerization was further confirmed by GPC measurements. In every case GPC results of the block copolymers show a monomodal distribution, indicating that PEO molecules had completely reacted with Cyclo(Glc-Val). Similar results were observed for the copolymerization of PEO with LA and GA by others[93,111)].

Thermal analysis of block copolymers

The DSC curves of the triblock copolymers obtained upon first heating are presented in Fig. 46. Curve 1-6 show one endotherm that corresponds to the melting of the PEO block. Curve 7 shows a broad transition around 60 °C that belongs to the glass transition and relaxation phenomena of amorphous poly(Glc-Val) block in the copolymer, the PEO block being in the amorphous state in the block copolymer with a long poly(Glc-Val) block, as shown by X-ray diffractometry. The crystallinity of the PEO block is calculated from the enthalpy of melting with respect to the PEO content. Crystallinity and melting temperature of the PEO block (Tab. 29) are considerably lower than those of the PEO homopolymer. The PEO block does not crystallize upon cooling after the first heating when the weight fraction of the poly(Glc-Val) block in the triblock copolymer is more than 41% (PGV/EO2). However, the PEO block crystallizes upon the second heating at about 15 °C, and then melts at about 47 °C, when the weight fraction of the PEO block in the triblock copolymer is between 37-59%. When the weight fraction of PEO is less than 30%, the PEO block does not crystallize upon cooling or second heating.

The T_m of the PEO block in the copolymer was not observed when the weight fraction of PEO in the block copolymer is lower than 16% (PGV/EO7). This indicates that the PEO block in PGV/EO7 is amorphous since the long poly(Glc-Val) block hinders the crystallization of the PEO block.

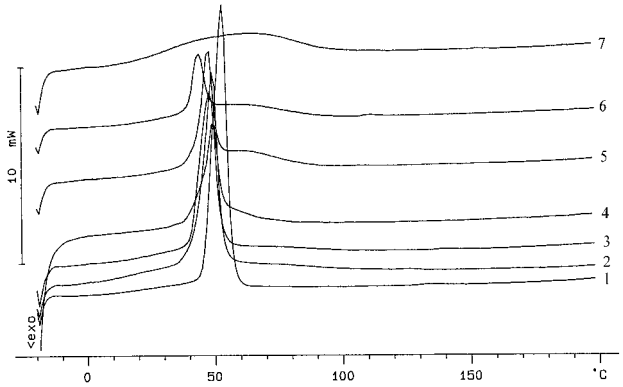

curve 1 PGV/EO1;
curve 2 PGV/EO2;
curve 3 PGV/EO3;
curve 4 PGV/EO4;
curve 5 PGV/EO5;
curve 6 PGV/EO6;
curve 7 PGV/EO7

Fig. 46. DSC thermograms of copolymers of PGV/EO and PEO6000

Tab. 29. Crystallinity and melting point of the PEO block in PGV/EO triblock copolymers

No.	PEO	1st heating			Cooling		2nd heating		
	in wt%	T_m/°C	ΔH/J/g	α_c/%	T_c/°C	ΔH/J/g	T_m/°C	ΔH/J/g	α_c/%
PEO6000	100	60.6	184.0	97.7	36.3	174.5	60.3	183.9	97.6
PGV/EO1	73	51.2	123.2	89.6	15.5	93.5	48.4	95.8	69.7
PGV/EO2	59	46.9	82.5	74.2	11.5[a)]	59.7[a)]	46.8	66.6	59.9
PGV/EO3	58	47.6	77.3	70.7	14.5[a)]	57.8[a)]	47.7	63.8	58.4
PGV/EO4	37	48.2	46.2	66.3	15.1 [a)]	39.6 [a)]	34.1	39.6	56.8
PGV/EO5	29	47.1	35.3	64.6	-	-	-	-	-
PGV/EO6	24	43.5	20.8	46.0	-	-	-	-	-
PGV/EO7	16	-	-	-	-	-	-	-	-

a) upon second heating.

2.3 Enzyme-catalyzed ring-opening polymerization of morpholine-2,5-diones

2.3.1 Lipase-catalyzed ring-opening polymerization of morpholine-2,5-dione derivatives: A route to the synthesis of poly(ester amide)s

Recently, enzymatic polymerizations have received much attention as a new methodology of polymer syntheses[9,10]. Enzymatic syntheses of aliphatic polyesters have been studied extensively[116-125]. Medium-size lactones (6- and 7-membered) as well as macrocyclic lactones (12-, 13-, and 16-membered) are polymerized with lipases as catalysts yielding the corresponding polyesters[121-124] . Macrolides with small ring strain, which hence show low anionic polymerizability, were found to be polymerized much faster with lipases than CL[123-124]. This is due to a favored transition state of the macrolide to open the ring[125]. Although the enzymatic ring-opening polymerization of lactones and cyclic carbonates was studied in detail by many researchers, the enzymatic polymerization of morpholine-2,5-diones to the best of our knowledge has not been reported so far.

The enzymatic polymerization of 3(S)-isopropyl-morpholine-2,5-dione was carried out in bulk in the presence of lipases as catalysts. Four lipases of different origin, i.e., lipases derived from *Porcine pancres* (PPL), *Pseudomonas species* (PS), *Pseudomonas cepacia* (PC), and *C. Antarctica* (Novozym-435), the latter immobilized on polymeric beads, were employed. Polymerization results are given in Tab 30. PPL and PS catalyze the polymerization both at 100 and 130 °C, i.e., they remain active at the given temperatures for polymerization. However, no polymerization was observed at 130°C in the presence of PC or Novozym-435. In the control experiment (without enzyme) Cyclo(Glc-Val) was recovered unchanged (entry 12 and 13).

The lipase PPL was mainly employed as a catalyst yielding a polymer with high molecular weight in high yields. We extended the method to the polymerization of other morpholine-2,5-diones with PPL as a catalyst. The enzymatic polymerization of morpholine-2,5-diones was carried out in bulk. Polymerization results are given in Tab. 31.

Tab. 30. Ring-opening polymerization of Cyclo(Glc-Val) with/without lipase

Entry	Lipase	wt%	Temp. in °C	Time in h	Conv. [a] in %	$\overline{M_n}$ [b] $\times 10^{-3}$	$\overline{M_w}/\overline{M_n}$ [b]
1	PPL	10	100	72	62.6	10.1	1.06
2	PPL	28.4	100	72	80.3	7.4	1.23
3	PPL	33.5	100	72	89.7	7.0	1.28
4	PPL	1.5	130	72	54.2	11.5	1.78
5	PPL	10	130	72	85.7	8.7	1.46
6	PS	1.5	100	72	12.2	17.5	1.50
7	PS	4.7	100	168	73.8	12.5	3.33
8	PC	10	100	72	20.8	4.50	1.84
9	PC	10	130	168	0		
10	Novo-435	10	100	72	5.6		
11	Novo-435	10	130	168	0		
12	blank	0	100	168	0		
13	blank	0	130	168	0		

a) determined by means of ^{1}H NMR. b) determined by means of GPC using DMAc as eluent and polystyrene standards for calibration.

Tab. 31. Ring-opening polymerization of morpholine-2,5-diones with/without lipase PPL

Entry	Monomer	PPL[a] in wt%	Temp. in °C	Time in h	Conv. [a] in %	$\overline{M_n}$ [b] $\times 10^{-3}$	$\overline{M_w}/\overline{M_n}$ [b]
1	Cyclo(Glc-Val)	1	120	72	21	15.2	1.06
2	Cyclo(Glc-Val)	10	120	72	92	14.3	1.07
3	Cyclo(Glc-Val)	0	120	72	0		
4	Cyclo(Glc-(R)-Val)	10	120	72	90	12.2	1.14
5	Cyclo(Glc-(R)-Val)	0	120	72	0		
6	Cyclo(Glc-(R,S)-Val)	10	120	72	90	12.0	1.15
7	Cyclo(Glc-(R,S)-Val)	0	120	72	0		
8	Cyclo(DLLA-Val)	10	120	72	9	6.9	1.16
9	Cyclo(DLLA-Val)	0	120	72	0		
10	Cyclo(Glc-Leu)	10	130	72	40	9.9	1.14
11	Cyclo(Glc-Leu)	0	130	72	0		
12	Cyclo(Glc-Ile)	1	120	72	11	7.8	1.10
13	Cyclo(Glc-Ile)	10	110	72	79	10.7	1.07
14	Cyclo(Glc-Ile)	10	110	144	90	11.5	1.09
15	Cyclo(Glc-Ile)	0	120	72	0		
16	Cyclo(LLA-Gly)	1	120	72	8	9.2	1.05
17	Cyclo(LLA-Gly)	1	120	144	22	12.3	1.06
18	Cyclo(LLA-Gly)	1	100	72	12	9.4	1.08
19	Cyclo(LLA-Gly)	10	100	72	76	12.0	1.05
20	Cyclo(LLA-Gly)	0	120	72	0		
21	Cyclo(DLLA-Gly)	10	120	72	34	9.3	1.04
22	Cyclo(DLLA-Gly)	0	120	72	0		

a) determined by means of ^{1}H NMR. b) determined by means of GPC using DMAc as eluent and polystyrene standards for calibration.

The results show that PPL remains active at the given temperatures (100 - 130 °C) of polymerization[24]. In the control experiment (in the absence of the enzyme) monomers were recovered unchanged (entry 3,5,7,9,11,15,20 and 22 in Tab. 31). After 72h incubation of Cyclo(Glc-Val) at 120 °C with deactivated PPL, 70% of the monomer was converted to low-molecular weight material with $\overline{M_n}$ around 1000 (Tab. 32). The active PPL catalyzed the ring-opening polymerization with a conversion of 92%, and a molecular weight of 14300, as well as a low molecular weight fraction with a molecular weight of 2000-2500. The low molecular weight fraction might result from the ring-opening polymerization catalyzed by the denatured PPL. BSA and glycine also catalyze the ring-opening polymerization, however, only oligomers are obtained ($\overline{M_n}$ <1000). This indicates that the ring-opening polymerization is an enzymatically catalyzed reaction*.

Tab. 32. Ring-opening polymerization of Cyclo(Glc-Val) with different catalysts [a]

Entry	Catalyst	Conv. in % [b]	$\overline{M_n}$ [c]
1	PPL	92	14300
2	deactivated PPL	70	1000
3	BSA [d]	13	500
4	glycine	60	900

a) catalyst 10 wt%, polymerization temperature 120 °C, polymerization time 72 h.
b) determined by means of ^{1}H NMR.
c) determined by means of GPC using DMAc as eluent and polystyrene standards for calibration.
d) BSA: albumin bovine fraction V.

The conversion of morpholine-2,5-diones increases with increasing lipase concentration (entry 1 and 2, 18 and 19 in Tab. 31). With increasing polymerization time the conversion of morpholine-2,5-dione derivatives increases as well as the molecular weight of the resulting polymers (entry 13 and 14, 16 and 17 in Tab. 31).

The behavior of Cyclo(Glc-Val), Cyclo(Glc-(R)-Val) and Cyclo(Glc-(R,S)-Val) is similar with respect to molecular weight and molecular weight distribution of the polymers formed (entry 2, 4 and 6) and significantly different from that of Cyclo(LLA-Gly) and Cyclo(DLLA-Gly) (entry 19 and 21). This indicates that the configuration of the amino acid moieties, i.e., R, S, or R,S, in the monomers does not affect the enzyme-catalyzed ring-opening polymerization of morpholine-2,5-diones. The conversion of morpholine-2,5-diones

* The melting point of morpholine-2,5-diones is above 96 °C. This temperature determines the minimum temperature for polymerizations in the melt. In 1,4-dioxane as a solvent polymerization is observed at 60 °C, although with low yield. It should be noted that deactivated PPL does not show activity for the hydrolysis of an ester group (according to the method recommended by Sigma Chemical Co.) nor for the polymerization of morpholine-2,5-diones.

decreases significantly when methyl substituents are introduced into the hydroxyl acid residues (entry 2 and 8). The configuration of the lactic acid residue in the monomer strongly affects the polymerization behavior. The reason may be that the enzyme-catalyzed polymerization of morpholine-2,5-dione derivatives takes place at the ester group of the morpholine-2,5-dione derivatives and that the steric effect of the methyl group is the reason for the decreased activity. Further, PPL might favor the polymerization of 6(S)-methyl-morpholine-2,5-dione compared with 6(R,S)-methyl-morpholine-2,5-dione.

The ^{1}H NMR spectra (DMSO-d-6) of poly(Glc-Val), poly(Glc-(R)-Val) and poly(Glc-(R,S)-Val) show five main resonances. The resonance centered at about $\delta = 4.6$ ppm results from the overlap of an AB-system of isotactic diads ((S,S) and (R,R) diads) at 4.54 and 4.69 ppm with the singlet at 4.62 ppm for the diasteromeric syndiotactic diads ((R,S) and (S,R) diads). The presence of the singlet at 4.62 or 4.63 ppm is evidence for the racemization of the (R)- or (S)-valine residue during enzymatic polymerization of Cyclo(Glc-Val) and Cyclo(Glc-(R)-Val). Beside the main resonances, there are three small characteristic peaks: a doublet at 7.60 ppm for poly(Glc-Val) and at 7.68 ppm for poly(Glc-(R)-Val) and poly(Glc-(R,S)-Val) due to the NH proton of the terminal unit, a broad singlet at about 5.57 ppm ascribed to the hydroxyl end group, and a peak at 3.9 ppm due to the α-methylene protons of the terminal hydroxyl group. The ^{13}C-NMR spectra of poly(Glc-Val), poly(Glc-(R)-Val) and poly(Glc-(R,S)-Val) show mainly 7 resonance lines, 170.7, 166.6, 62.1, 56.7 30.0, 18.8 and 17.7 ppm due to NH$\underline{C}$O, $\underline{C}$OO, O$\underline{C}$H$_2$CO, NH$\underline{C}$HCO, $\underline{C}$H(CH$_3$)$_2$, CH(C$\underline{H}_3$)$_2$, and CH(C$\underline{H}_3$)$_2$, respectively. There are two small characteristic peaks besides the main resonances of the carbonyl carbon, a peak at 172.0 ppm due to the carbonyl carbon of the carboxylic acid and a peak at 170.6 ppm ascribed to carbonyl carbon atoms in the isotactic diad, which indicates the racemization of the amino acid residue during enzymatic ring-opening polymerization. These data indicate that the enzymatic polymerization of Cyclo(Glc-Val), Cyclo(Glc-(R)-Val) and Cyclo(Glc-(R,S)-Val) produces poly(glycolic acid-*alt*-valine) with a carboxylic acid group at one end and a hydroxyl group at the other one.

Tab. 33 shows the IR spectra of poly(Glc-Val), poly(Glc-(R)-Val) and poly(Glc-(R,S)-Val). A strong absorption band at about 3300 cm^{-1} is assigned to the stretching band of the N-H group. The band at 1752 cm^{-1} is due to the C=O stretching mode of the ester group, the band at 1673 cm^{-1} to the bending mode of the N-H bond and the stretching mode of the C-N bond of the amide group. The amide II band appears at 1538 cm^{-1}.

Tab. 33. Characteristic IR frequencies of poly(Glc-Val) [a)]

Polymer [b)]	NH stretching vibration	Amide I	Amide II (trans)	C=O	C-O-C
Poly(Glc-Val)	3370	1677	1538	1753	1146
Poly(Glc-(R)-Val)	3330	1673	1538	1752	1147
Poly(Glc-(R,S)-Val)	3320	1673	1536	1752	1147

a) in the solid state as KBr pellets; ν-values in cm^{-1}.
b) polymers were prepared with 10 wt% PPL, 120 °C, 72 h.

Tab. 34. Specific rotations ($[\alpha]_D^{25}$) of polymers

Polymer	$[\alpha]_D^{25}$ [a,b)] (°)	$[\alpha]_D^{25}$ [c,d)] (°)
poly((Glc-Val)	14	43
poly(Glc-(R)-Val)	- 2	-9
poly(Glc-(R,S)-Val)	0	0
poly(Glc-Leu)	-12 [d)]	-28 [d)]
Poly(Glc-Ile) [b)]	21	61
poly(LLA-Gly) [b)]	32 [d)]	64 [d)]
poly(DLLA-Gly)	0 [d)]	0 [d)]

a) polymers were prepared with 10 wt% PPL, 120 °C, 72 h.
b) c=0.20 g/dL, $CHCl_3$ as solvent.
c) c=0.20 g/dL, DMSO as solvent.
d) polymers were prepared with 1/125 mol% $Sn(oct)_2$, 140 °C, 9 h.
e) polymers were prepared with 10 wt% PPL, 100 °C, 144 h.

The specific rotations of polymers which were prepared via the ring-opening polymerization of morpholine-2,5-diones in the presence of PPL or $Sn(oct)_2$ as a catalyst are given in Tab. 34. Poly(Glc-(R,S)-Val) and poly(DLLA-Gly) have the specific rotation of 0°, because they are prepared from the racemate. The specific rotations of poly(Glc-Val), poly(Glc-(R)-Val), poly(Glc-Leu) and poly(Glc-Ile) prepared via PPL catalyzed ring-opening polymerization are significantly smaller than those of polymers prepared via $Sn(oct)_2$-catalyzed polymerization. This is caused by the enhanced racemization of the amino acids residues during enzymatic polymerization. The racemization of 6(S)-methyl-morpholine-2,5-dione is also observed during the PPL-catalyzed polymerization. This indicates that R-, S-amino acids and S-lactic acid residues are racemized during PPL catalyzed ring-opening polymerization of morpholine-2,5-diones.

2.3.2 Lipase-catalyzed ring-opening polymerization of 3(S)-isopropyl-morpholine-2,5-dione

Screening of Enzymes

Screening results using selected commercial lipases for the bulk polymerization of Cyclo(Glc-Val) are given in Tab. 35. The reactions were carried out at 100 °C in bulk for 72 or 168 h. In all cases, the enzymes and the monomer were dried under vacuum (10^{-3} mbar) over P_2O_5 at room temperature for 24 h. Except for the lipase Novo-435, all the other lipases studied are effective for Cyclo(Glc-Val) polymerization. Polymerizations catalyzed with lipases PPL, PS and CR result in Cyclo(Glc-Val) conversions of ca. 50%. $\overline{M_n}$ values of poly(Glc-Val) range from 3500 to 12000. Although Novo-435 is efficient in catalyzing the ring-opening polymerization of caprolactone at 60 °C[126], the heat stability of Novo-435 is very poor. Therefore it failed to polymerize the cyclic depsipeptide. Since the initial experiments with PPL give high molecular weight polymers as well as high conversion, and this lipase is very cheap, it was selected for further studies herein.

Tab. 35. Ring-opening polymerization of Cyclo(Glc-Val) with/without lipase

Entry	Lipase[a]	wt%	Temp. in °C	Time in h	Conv.[b] in %	$\overline{M_n}$[b] $\times 10^{-3}$	$\overline{M_w}/\overline{M_n}$[b]
1	PPL	1.5	100	72	3.2	6.1	1.10
2	PPL	5	100	72	26.2	10.4	1.05
3	PPL	10	100	72	53.6	11.0	1.08
4	PS	1.5	100	72	12.2	17.5	1.50
5	PS	4.7	100	168	73.8	12.5	3.33
6	PC	10	100	72	20.8	4.50	1.84
7	CR	10	100	72	46.3	3.50	1.99
8	Novo-435	10	100	72	5.6		
9	blank	0	100	168	0		

a) CR: lipase type VII from *Candida rugosa*.
b) determined by means of GPC using DMAc as eluent and polystyrene standards for calibration.

The lipase-catalyzed ring-opening polymerization of Cyclo(Glc-Val) produces a high molecular weight fraction and a low molecular weight fraction, which is readily removed by reprecipitation using chloroform as a good solvent and ether as a poor solvent. During the polymerization, the molecular weight of the high molecular weight fraction gradually increases with reaction time; the molecular weight of the low molecular weight fraction,

however, remains unchanged. In the following discussion, we focus on the effects of the reaction conditions on the high molecular weight fraction.

Characterization of poly(Glc-Val)

The ^{1}H-NMR spectrum (DMSO-d-6, Fig. 47) shows five main resonances: a doublet at 8.35 ppm due to the NH proton, a quintet at 4.54 and 4.69 ppm due to OC$\underline{H}_2$CO (AB-system, ^{AB}J = 14.8 Hz, isotactic diad), a singlet at 4.62 ppm due to OC$\underline{H}_2$CO (syndiotactic diad), a multiplet at 4.33 ppm due to NHC$\underline{H}$CO, and resonance lines at 2.12 and 0.91 ppm ascribed to C$\underline{H}(CH_3)_2$ and CH(C$\underline{H}_3)_2$. Beside the main resonances, there are three small charateristic peaks: a doublet at 7.60 ppm due to the NH proton of the terminal amide unit, a broad singlet at 5.57 ppm ascribed to the end group $\underline{H}OCH_2$, and a peak at 3.9 ppm due to the α-methylene protons of the terminal hydroxyl group. The resonance centered at 4.62 ppm results from the overlap of an AB-system in isotactic diads ((S,S) and (R,R) diad) at 4.54 and 4.69 ppm with the singlet at 4.62 ppm for the diasteromeric syndiotactic diads ((R,S) and (S,R) diad) (cf. Scheme 12)[46]. ^{1}H NMR proves that no racemization of the valine residue occurs in the unreacted Cyclo(Glc-Val) under the conditions of polymerization. The presence of the singlet at 4.62 ppm is evidence for the racemization of the valine residue in the polymer. The specific rotation of poly(Glc-Val) (entry 5, in Tab. 35) is only 14.6° (2.056g/dl, $CHCl_3$), but the specific rotation of poly(Glc-Val) prepared by Sn(oct)$_2$ is 44° (0.2g/dl, $CHCl_3$). The ^{13}C-NMR spectrum shows 7 main resonance lines at 170.7, 166.6, 62.1, 56.7 30.0, 18.8 and 17.7 ppm due to NH$\underline{C}$O, $\underline{C}$OO, O$\underline{C}H_2$CO, NH$\underline{C}$HCO, $\underline{C}H(CH_3)_2$, CH($\underline{C}H_3)_2$, and CH($\underline{C}H_3)_2$, respectively.

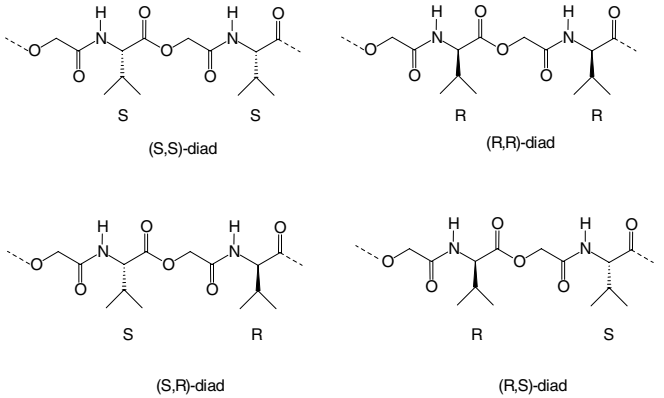

Scheme 12. Diads in poly(Glc-Val).

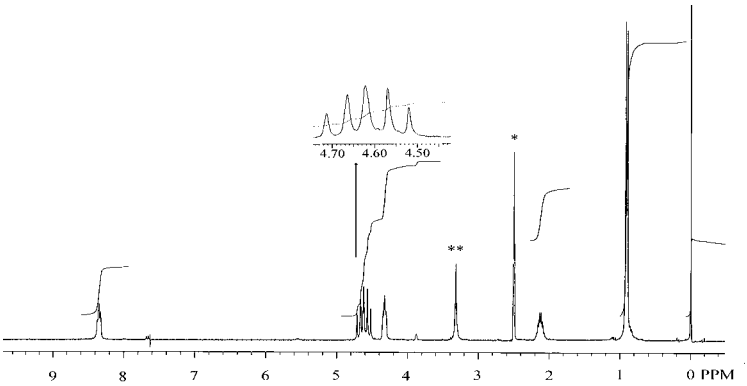

Fig. 47. ^{1}H-NMR of poly(Glc-Val) (entry 5, in Table 1), * DMSO peaks, ** H_2O peaks.

The IR spectrum of poly(Glc-Val) shows a strong absorption band at 3370 cm^{-1} which is assigned to the stretching band of the N-H group. The band at 1753 cm^{-1} is due to the C=O stretching mode of the ester group, and the band at 1677 cm^{-1} to the bending mode of the N-H band and the stretching mode of the C-N bond of the amide group. The amide II band appears at 1538 cm^{-1}.

The thermal behaviour of poly(Glc-Val) was investigated by means of DSC. The sample was first heated to 200 °C, then cooled at a rate of 10 °C/min to -70 °C and finally heated at 10 °C/min from -70 to 200 °C. The DSC curve of poly(Glc-Val) shows a glass transition ($T_{g(1st\ heating)}$ = 56 °C and $T_{g\ (2nd\ heating)}$ = 75 °C), but no melting peak. This result corresponds to that obtained for poly(Glc-Val) prepared with $Sn(oct)_2$ as a catalyst[30] and indicates that poly(Glc-Val) is amorphous.

Effect of reaction time and concentration of PPL for PPL catalyzed polymerization

The polymerization of the cyclic depsipeptide Cyclo(Glc-Val) in the melt at 100°C with four different concentrations of PPL was studied with respect to the dependence of the monomer conversion and the molecular weight on reaction time. Samples were drawn at different times, dissolved in chloroform, filtered to remove insoluble enzyme, then kept under reduced pressure to give the crude polymer, and analyzed by means of GPC (DMAc as eluent). From the ratio of the areas under the elution curve for the polymer and monomer the conversion was calculated.

The apparent rate of polymerization increases with concentration of the enzyme PPL. Fig. 48 shows the results obtained for four PPL concentration. For a concentration of 5 wt% and 10

wt% a conversion of about 70% is reached after 5 d and 7 d, respectively, while for 1 wt% and 0.5 wt% the conversion is less than 15% even after 11 d.

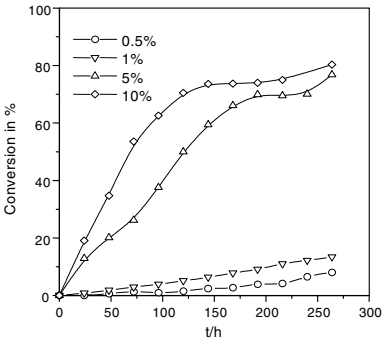

Fig. 48. Dependence of monomer conversion on time.
Polymerization temperature T_p = 100 °C.

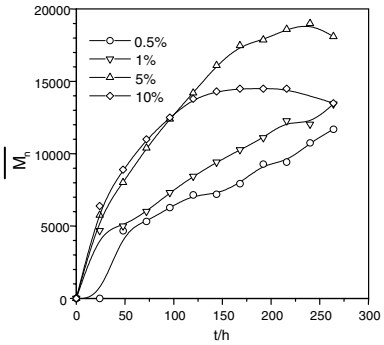

Fig. 49. Dependence of the number average molecular weight $\overline{M_n}$ on time.

The dependence of the number average molecular weight $\overline{M_n}$ on time and PPL concentration reveals two important features:

(i) High concentration of PPL (10 wt%) results in the highest $\overline{M_n}$ value (<4 d); with decreasing concentration of PPL poly(Glc-Val) of lower molecular weight is obtained.

(ii) Increasing polymerization time (and conversion) leads for high PPL concentrations (10 wt%) first to an increase in $\overline{M_n}$ and later to a decrease. For the polymerization experiments with 0.5 and 1 wt% PPL an increase of $\overline{M_n}$ is observed up to a polymerization time of 11 d. Analysis of the GPC traces for polymerization with 10 wt% PPL reveals that for polymerization times longer than 6 d $\overline{M_n}$ decreases, while in the same time the polydispersity index Q increases and at long polymerization times a most probable distribution is obtained (Q increases from 1.09 (24 h) to 1.51 (264 h)).

Effect of reaction temperature for PPL catalyzed polymerization

Ring-opening bulk polymerizations of Cyclo(Glc-Val) catalyzed with PPL were performed at 100, 110, 120 and 130 °C for 168 h. Monomer conversion and molecular weight were determined by means of GPC with DMAc as eluent every 24 h. Fig. 50 shows that monomer conversion increases with increasing reaction temperature from 100 to 130 °C. The relationship of conversion and reaction time is a straight line. This means that PPL is not

deactivated during the polymerization even at 130 °C; at least the domain of PPL, which catalyzes the ring-opening polymerization of Cyclo(Glc-Val), is heat stable.

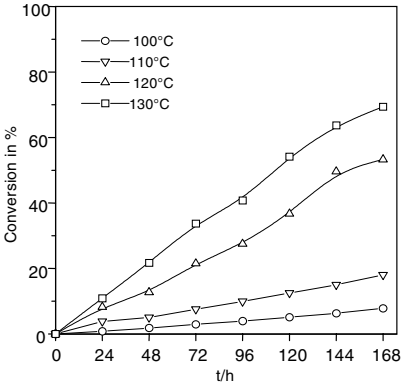

Fig. 50. Dependence of monomer conversion on time. PPL/M = 1 wt%.

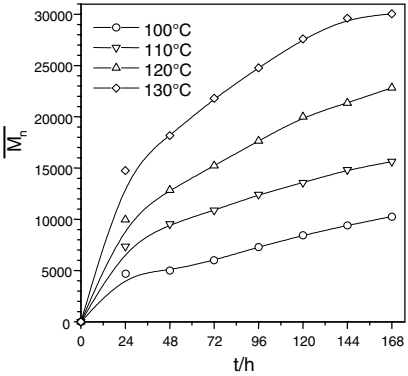

Fig. 51. Dependence of molecular weight on time.

Fig. 51 shows that the reaction temperature is a critical parameter which regulates the molecular weight of poly(Glc-Val). It is seen that an increase in reaction temperature from 100 to 130 °C results in an increase of $\overline{M_n}$. Thus, the highest molecular weights were observed by conducting the polymerization at 130 °C (for the same reaction time). In studies of Kobayashi for lipase-catalyzed polymerizations of 12-dodecanolide, increasing the reaction temperature leads to increased $\overline{M_n}$ [124], too. $\overline{M_n}$ > 30000 results when carrying out polymerizations at 130 °C with 5 wt% PPL. In other words, to achieve high molecular weights of poly(Glc-Val) the concentration of PPL and the polymerization temperature must be carefully adjusted.

An important effect of increased reaction temperature is monomer and polymer diffusion[123]. As the polymerization temperature is increased from 100 to 130 °C, the diffusion of the monomer is enhanced, leading to higher molecular weight products.

Fig. 52 shows GPC traces recorded for reactions conducted for 168 h at 100, 110, 120 and 130 °C. For polymerizations conducted at 100 °C, $\overline{M_w} / \overline{M_n}$ is 1.08 and the GPC trace suggests a unimodal molecular weight distribution ($\overline{M_n}$ = 10200). However, reactions carried out at 110, 120 and 130 °C show a bimodal distribution. For the high molecular weight component $\overline{M_n}$ is 15600 ($\overline{M_w} / \overline{M_n}$ =1.07, 110 °C), 22800 ($\overline{M_w} / \overline{M_n}$ =1.06, 120 °C) and 30000 ($\overline{M_w} / \overline{M_n}$ =1.16, 130 °C). Similarly, for the low molecular weight

component $\overline{M_n}$ is 3200 ($\overline{M_w}$ / $\overline{M_n}$ =1.23, 110 °C), 4300 ($\overline{M_w}$ / $\overline{M_n}$ =1.38, 120 °C) and 5200 ($\overline{M_w}$ / $\overline{M_n}$ =1.56, 130 °C). In studies of Bisht for the lipase-catalyzed polymerization of trimethylene carbonate, increasing reaction temperature also leads to a bimodal distribution[127].

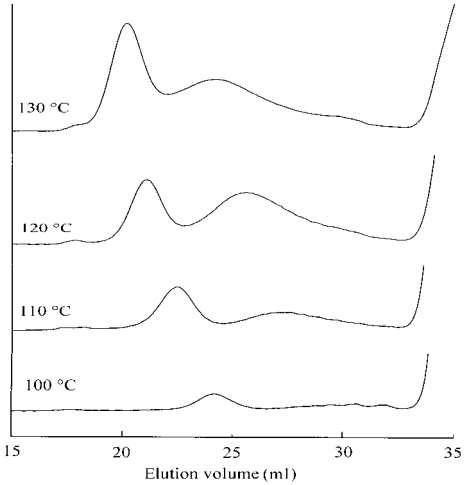

Fig. 52. GPC traces of poly(Glc-Val) obtained with 1 wt% of PPL after 168h.

Effect of water content

The role of water in enzyme catalyzed polymerizations of lactones and cyclic carbonates was discussed in detail[85]. The water content for PPL catalyzed Cyclo(Glc-Val) polymerizations conducted at 100°C for 24, 48 and 72 h was varied. The monomer conversion as a function of the water content (wt%) is plotted in Fig. 53. Increasing water content results in enhanced polymerization rate. For example, by increasing the water content from 1.1 to 4.4 wt%, monomer conversion increases from 11.4 to 50.4% within 48 h. Interestingly, a small increase in water content from 0 to 1.1 wt% results in a rather large increase in monomer conversion, i.e., from 2.9 to 23%. These observations are similar to those made for PS-30 catalyzed polymerizations of ω-pentadecalactone and can be explained in a similar fashion[128]. However, when the water content is increased to 8.4 wt%, the conversion is less than that for a water content of 4.4 wt% (reaction time 48 and 72 h). 3(S)-Isopropyl-morpholine-2,5-dione can be reacted with water to form *N*-(α-hydroxy acetyl)-*S*-valine. The conversion of Cyclo(Glc-Val) is 94% with 8.4% water content within 72 h at 100 °C (according to ^{1}H NMR results). By increasing the water content, polymerization rates are

increased due to an increase in the number of propagating chain ends (Scheme 13). Also, increased water content in the system may result in an enhanced enzyme activity[32].

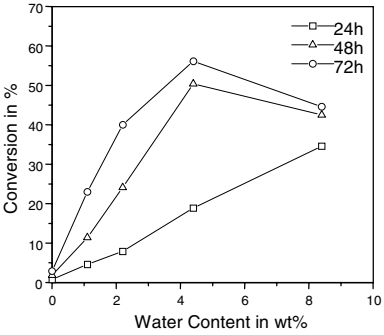

Fig.53. Variation in monomer conversion as a function of water content (wt%) for polymerization conducted at 100 °C .

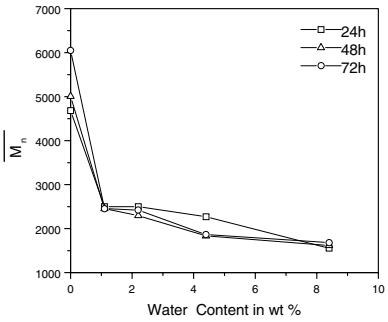

Fig. 54. Variation in poly(Glc-Val) molecular weight as a function of water content (wt%) for polymerization conducted at 100 °C.

The water content was also found to be important in controlling the molecular weight. The effects of water content on $\overline{M_n}$ are shown in Fig. 54 for reactions conducted for 24, 48 and 72 h at 100 °C. $\overline{M_n}$ increases from 2450 to 5000 by decreasing the water content from 1.1 to 0 wt%. MacDonald et al. reported that $\overline{M_n}$ of poly(CL) which was prepared via PPL-catalyzed CL polymerization is given by the ratio [M]/[I] where [M] and [I] are the monomer and initiator (for example water, ethanol) concentration, respectively[85]. When water was the sole initiator, only a fraction of the water present reacted to initiate chains. However, as the water content in the polymerization increased, the portion of water which reacted to initiate chains also increased. It is possible that by further drying of PPL using a different protocol or vacuum for a longer time (> 24 h) significantly higher molecular weights are obtained. However, this increase in molecular weight is accompanied by a decrease in polymerization rate.

Proposed mechanism

The mechanism for lipase-catalyzed Cyclo(Glc-Val) ring-opening polymerization proposed is shown in Scheme 13. It is based on: (i) poly(Glc-Val) with a carboxylic acid group at one end and a hydroxy group at the other end; (ii) the effect of water on $\overline{M_n}$ of poly(Glc-Val); and (iii) mechanisms proposed previously for lipase-catalyzed ring-opening polymerizations of lactones and cyclic carbonates[85,129]. Initiation involves (i) the reaction of Cyclo(Glc-Val)

with the lipase to form the lipase-Cyclo(Glc-Val) enzyme-activated-monomer (EAM) complex and (ii) the reaction of EAM with water to form N-(α-hydroxy acetyl)-S-valine. Propagation as defined by the presence of an ester function involves the formation of dimer by reaction of the EAM with N-(α-hydroxy acetyl)-S-valine, Trimer synthesis by reaction of dimer with EAM, and subsequent propagation reactions to form high molecular weight chains. It is important to note that, in the proposed model, it is assumed that the serine residue is the catalytically essential region, where the enzyme reacts with the Cyclo(Glc-Val) ester function by attacking the carbonyl group. This would result in the formation of an EAM complex which contains highly reactive serine residues as generally accepted for lipases which catalyze the hydrolysis of triglycerides[130].

Initiation:

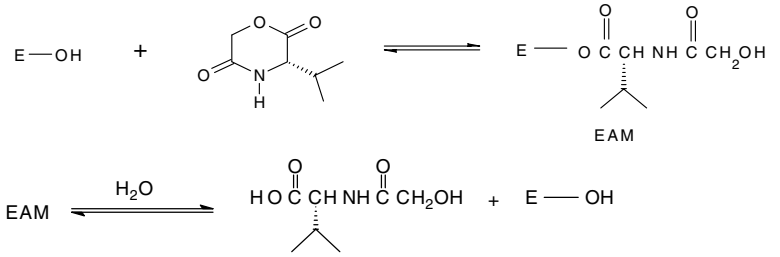

Propagation:

Dimerization:

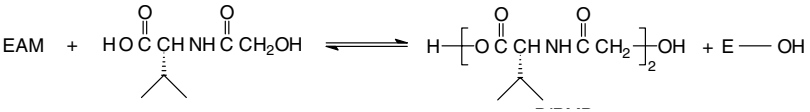

Trimerization:

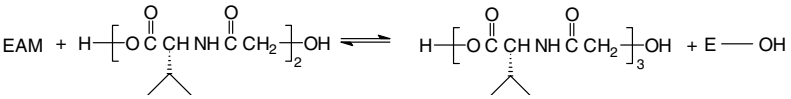

Polymerization:

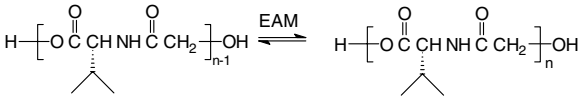

Scheme 13. Mechanism for lipase-catalyzed ring-opening polymerization of Cyclo(Glc-Val).

2.3.3 Lipase-catalyzed ring-opening polymerization of 6(S)-methyl-morpholine-2,5-dione

Screening of enzymes

Screening results using selected commercial lipases for the bulk polymerization of Cyclo(LLA-Gly) are given in Tab. 36. The reactions were carried out at 100 °C in bulk for 72 or 144 h. In all cases, the enzymes and the monomer were dried under vacuum (10^{-3} mbar) over P_2O_5 at room temperature for 24 h.

Tab. 36. Ring-opening polymerization of 6(S)-methyl-morpholine-2.5-dione with/without lipase

Entry	Lipase[a)]	wt%	Temp. in °C	Time in h	Conv.[b)] in %	$\overline{M_n}$ [b)]	$\overline{M_w}$ / $\overline{M_n}$ [b)]
1	PPL	1	100	72	10	9400	1.08
2	PPL	5	100	72	48	12600	1.05
3	PPL	5	100	144	68	15100	1.07
4	PPL	10	100	72	77	12100	1.05
5	PPL	10	100	144	88	12700	1.07
6	MJ	10	100	72	40	6900	2.94
7	PC	10	100	72	70	8200	2.64
8	CR	10	100	72	75	9800	1.04
9	Novo-435	10	100	72	0		
10	$Sn(oct)_2$	1/125[c)]	140	9	75[d)]	19600	1.44
11	blank	0	100	168	0		
12	blank	0	130	168	0		

a) MJ: lipase from *Mucor javanicus*.
b) determined by means of GPC using DMAc as eluent and polystyrene standards for calibration.
c) molar ratio of $Sn(oct)_2$ to monomer.
d) polymer yield in wt% based on monomer.

Except for lipase Novo-435, all the other lipases studied are effective for Cyclo(LLA-Gly) polymerization. However, a significant difference between the enzymes was observed with respect to monomer conversion and molecular weight of the polymer. Polymerizations catalyzed with 10 wt% of the lipases PPL, PC and CR result in Cyclo(LLA-Gly) conversions of ca. 75%. $\overline{M_n}$ values of poly(LLA-Gly) ranged from 8200 to 12100. MJ showed lower catalytic activity for the polymerization of Cyclo(LLA-Gly). The monomer conversion and molecular weight of the resulted polymer are significantly lower. Since the initial result with PPL gives high molecular weight polymers as well as high conversion, and this lipase is very cheap, it was selected for further studies herein.

Characterization of poly(LLA-Gly)

The ^{1}H NMR spectrum (DMSO-d-6, Fig. 55) of poly(LLA-Gly) which was prepared via $Sn(oct)_2$ catalyzed ring-opening polymerization of Cyclo(LLA-Gly) shows four resonances: a doublet at 8.49 ppm due to the NH proton, a quartet at 5.03-5.08 ppm due to the proton of OC<u>H</u>CO, a multiplet at 3.95 ppm due to protons of NHC<u>H</u>$_2$CO, and a doublet at 1.35 ppm ascribed to protons of C<u>H</u>$_3$. The ^{1}H NMR spectrum of poly(LLA-Gly) which was prepared via PPL catalyzed ring-opening polymerization of Cyclo(LLA-Gly) also shows these four main resonances. Beside the main resonances, there are 4 small characteristic peaks**:** a triplet at 8.10 ppm due to the NH proton of the terminal amide unite, a broad singlet at 5.63 ppm ascribed to the proton of the end group <u>H</u>OCH, a doublet peak at 3.85 ppm due to methylene protons in the end group C<u>H</u>$_2$COOH, and a doublet peak at 1.22 ppm due to C<u>H</u>$_3$ protons of the terminal group. Moreover, a peak at about 3.9 ppm due to methine proton of the terminal hydroxyl group is overlapped with the main multiplet of protons of NHC<u>H</u>$_2$CO. The multipet resonance at 3.95 ppm in Fig. 55(a) is more complex than that in Fig. 55(b). This is due to the overlap of (S,S), (S,R), (R,S) and (R,R) diads which result from the racemization of Cyclo(LLA-Gly) during the PPL-catalyzed polymerization. The ^{13}C NMR spectrum shows 5 main resonance lines at 170.3, 168.7, 69.7, 40.3 and 17.4 ppm due to NH<u>C</u>O, <u>C</u>OO, O<u>C</u>H(CH$_3$)CO, NH<u>C</u>H$_2$CO and <u>C</u>H$_3$, respectively. There are four small characteristic peaks beside the main peaks: a peak at 175.1 ppm due to the carbonyl carbon of the carboxylic acid, a peak at 169.0 ppm ascribed to carbonyl carbon atoms in isotactic diads, which indicates the racemization of the L-lactic residue during the ring-opening polymerization of Cyclo(LLA-Gly) in the presence of PPL, a peak at 67.0 ppm ascribed to the <u>C</u>H carbon of the hydroxy group and a peak ascribed to the CH_3 carbon of the terminal group. Therefore, the polymer prepared via PPL catalyzed polymerization of Cyclo(LLA-Gly) has a carboxylic acid group at one end and a hydroxyl group at the other end.

The IR spectrum of poly(LLA-Gly) shows a strong absorption band at 3400 cm^{-1} which is assigned to the stretching band of the N-H group (Fig. 56). The band at 1757 cm^{-1} is due to the C=O stretching mode of the ester group, and the band at 1669 cm^{-1} to the bending mode of the N-H band and the stretching mode of the C-N bond of the amide group. The amide II band appears at 1541 cm^{-1}. The IR spectrum of poly(LLA-Gly) which was prepared in the presence of PPL is similar to that of poly(LLA-Gly) which was prepared in the presence of $Sn(oct)_2$ as a catalyst.

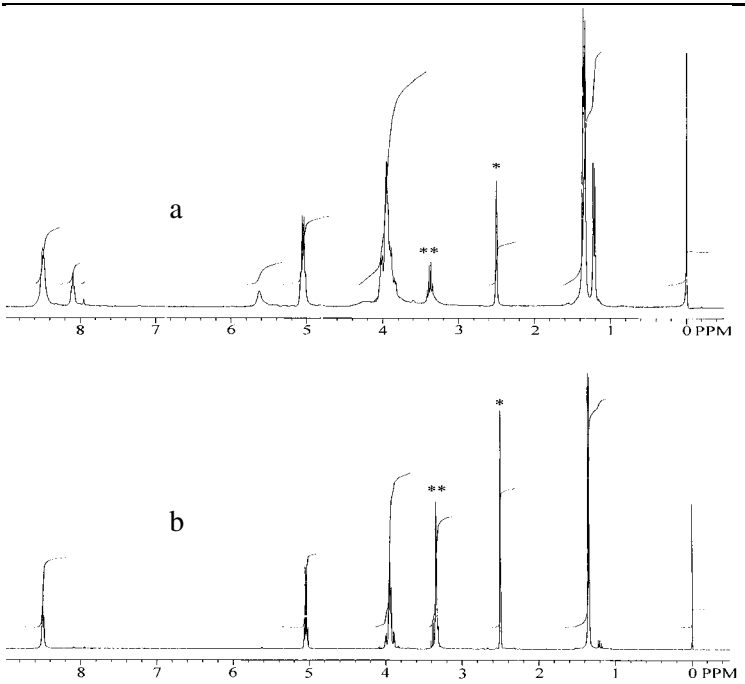

Fig. 55. ^{1}H-NMR of poly(LLA-Gly), a: poly(LLA-Gly) (entry 5, in Tab. 36), b: (entry 10, in Tab. 36). * DMSO peaks, ** H_2O peaks.

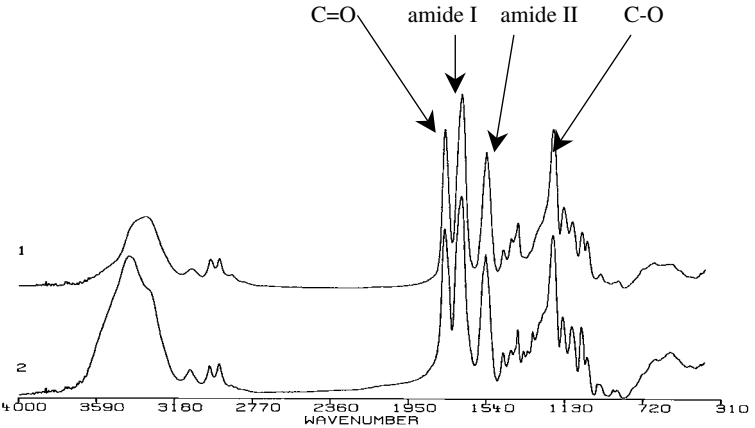

Fig. 56. IR of poly(LLA-Gly), 1: poly(LLA-Gly) (entry 5, in Tab. 36), 2 (entry 10, in Tab. 36).

The specific rotation of poly(LLA-Gly) prepared via PPL catalyzed ring-opening polymerization (entry 5 in Tab. 36) is 32°, which is significantly smaller than that of poly(LLA-Gly) prepared via $Sn(oct)_2$ catalyzed polymerization ($[\alpha]_D^{25} = 64°$). This is caused by the racemization of the amino acid residue during the PPL catalyzed polymerization.

The thermal behavior of poly(LLA-Gly) was investigated by means of DSC. The sample was first heated to 200 °C, then cooled at a rate of 10 °C/min to -70 °C and finally heated at 10 °C/min from -70 to 200 °C. The DSC curves of poly(LLA-Gly) show a melting peak upon first heating (Fig. 57), namely, T_m = 78 °C, ΔH = 99 J/g for poly(LLA-Gly) prepared via $Sn(oct)_2$ catalyzed polymerization, T_m = 72 °C, ΔH = 82 J/g for poly(LLA-Gly) prepared via PPL catalyzed polymerization. The racemization of Cyclo(LLA-Gly) during PPL catalyzed ring-opening polymerization results in lower melting temperature and melting endotherm. The cooling curves (not shown in Fig. 57) and second heating curves of poly(LLA-Gly) show only a glass transition ($T_{g(cooling)}$ = 56 °C and $T_{g\ (2nd\ heating)}$ = 71 °C for poly(LLA-Gly) prepared with $Sn(oct)_2$ catalyst, $T_{g(cooling)}$ = 56 °C and $T_{g\ (2nd\ heating)}$ = 59 °C for poly(LLA-Gly) prepared with PPL catalyst), there is no crystallization exotherm upon cooling nor a melting endotherm upon the second heating.

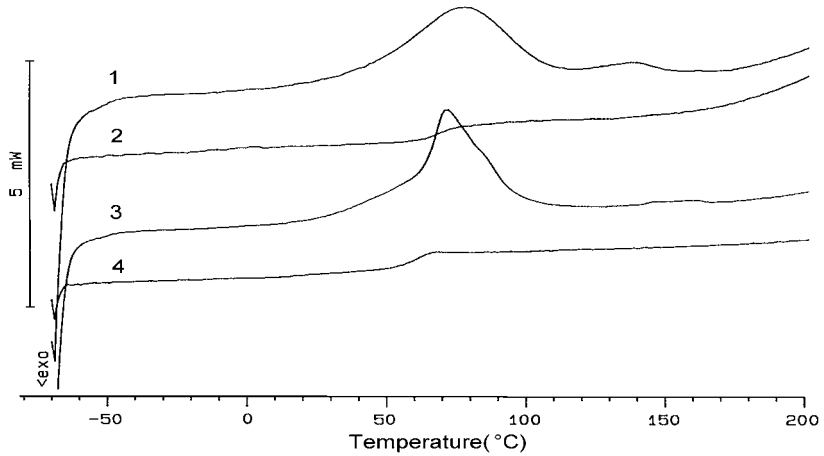

Fig. 57. DSC thermograms of poly(LLA-Gly).

Curve 1: first heating of poly(LLA-Gly) (entry 10, in Tab.36),
Curve 2: second heating of poly(LLA-Gly) (entry 10, in Tab.36),
Curve 3: first heating of poly(LLA-Gly) (entry 5, in Tab.36),
Curve 4: second heating of poly(LLA-Gly) (entry 5, in Tab.36).

Effect of concentration of PPL for PPL catalyzed polymerization

The polymerization of the cyclic depsipeptide Cyclo(LLA-Gly) in the melt at 100 °C with three different concentrations of PPL was studied with respect to the dependence of the monomer conversion and the molecular weight on reaction time. Samples were taken at different times, dissolved in DMF, filtered to remove insoluble enzyme, then kept under reduced pressure to give the crude polymer, and analyzed by means of ^{1}H-NMR and GPC (DMAc as eluent).

The apparent rate of polymerization increases with concentration of the enzyme PPL. Fig. 58 shows the results obtained for three PPL concentrations, for 5 wt% and 10 wt% a conversion of about 70% is reached after 6 d and 1 d, respectively, while for 1 wt% the conversion is less than 20% even after 6 d.

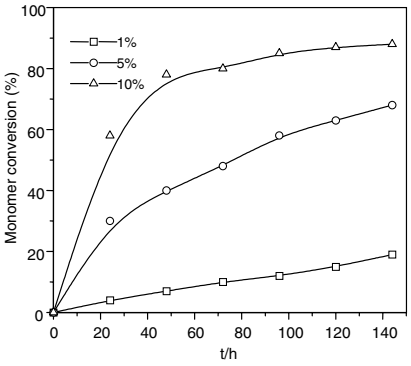

Fig. 58. Polymerization of Cyclo(LLA-Gly) in the bulk with PPL as a catalyst; dependence of monomer conversion on time. Polymerization temperature T_p = 100 °C.

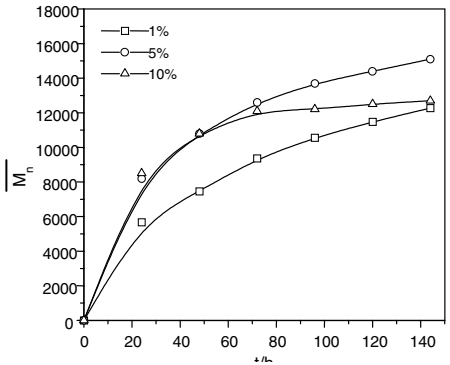

Fig. 59. Polymerization of Cyclo(LLA-Gly) in the bulk with PPL as a catalyst; dependence of the number average molecular weight $\overline{M_n}$ on time.

The dependence of the number average molecular weight $\overline{M_n}$ on time and PPL concentration reveals two important features:

(i) High concentration of PPL (Fig. 59, 5 wt%) results in high $\overline{M_n}$ value; with lower concentration of PPL (1 wt%) poly(LLA-Gly) of lower molecular weight is obtained. However, the molecular weight of the resulting polymer with 10 wt% PPL is lower than that obtained with 5 wt% PPL. The water in PPL may cause decreasing of molecular weight when the concentration of PPL is very high.

(ii) Increasing polymerization time (and conversion) leads to an increase in $\overline{M_n}$.

Effect of reaction temperature for PPL catalyzed polymerization

Ring-opening bulk polymerizations of Cyclo(LLA-Gly) catalyzed with 1 wt% PPL were performed at 100, 110, 120 and 130 °C for 144 h. Monomer conversion and molecular weight were determined by means of ^{1}H NMR and GPC with DMAc as eluent every 24 h. Fig. 60 shows that the monomer conversion increases slightly with increasing reaction temperature from 100 to 130 °C. The relationship of conversion and reaction time is linear. This means that the domain of PPL, which catalyzes the ring-opening polymerization of Cyclo(LLA-Gly), is heat stable. In the above study on the enzymatic polymerization of 3(S)-isopropyl-morpholine-2,5-dione it was found that the reaction temperature is a critical parameter which regulates the molecular weight of poly(Glc-Val). An increase in reaction temperature from 100 to 130 °C results in a significant increase of conversion and molecular weight. While, Fig. 60 and 61 show that the reaction temperature is not an important parameter which regulates the conversion of the monomer and the molecular weight of poly(LLA-Gly). It is seen that an increase in reaction temperature from 100 to 120 °C results in similar $\overline{M_n}$ values. However, the molecular weight of the polymer increases when the polymerization is carried out at 130 °C.

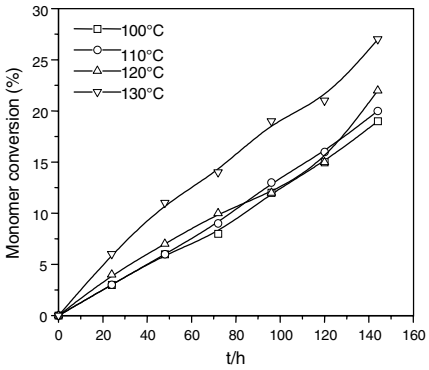

Fig. 60. Effect of polymerization temperature on monomer conversion for 1 wt% PPL catalyzed polymerization.

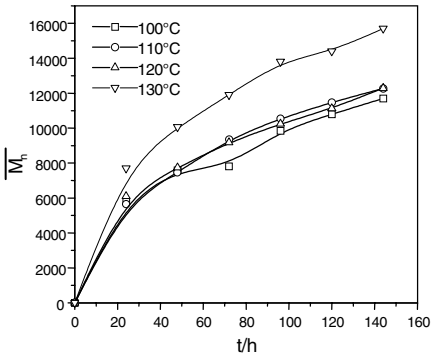

Fig. 61. Effect of polymerization temperature on poly(LLA-Gly) molecular weight for 1% PPL catalyzed polymerization.

Effect of water content

The water content for PPL catalyzed Cyclo(LLA-Gly) polymerizations conducted at 100 °C for 24, 48 and 72 h was varied. The monomer conversion as a function of the water content (wt%) is plotted in Fig. 62. Increasing water content results in enhanced polymerization rate. For example, by increasing the water content from 1.0 to 4.2 wt%, monomer conversion increases from 4 to 32 % within 24 h. This observation is similar to that made for PPL catalyzed 3(S)-isopropyl-morpholine-2,5-dione polymerization and can be explained in a similar fashion.

The water content was also found to be important in controlling the molecular weight. The effects of water content on $\overline{M_n}$ are shown in Fig. 63 for reactions conducted for 24, 48 and 72 h at 100 °C. $\overline{M_n}$ increases from 3100 to 9400 by decreasing the water content from 1.0 to 0.1 wt% (reaction time: 72 h).

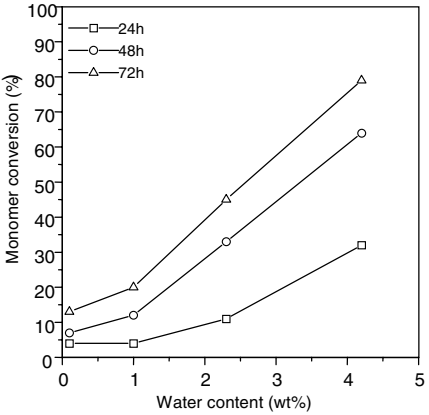

Fig. 62. Variation in monomer conversion as a function of water content for polymerization conducted at 100 °C.

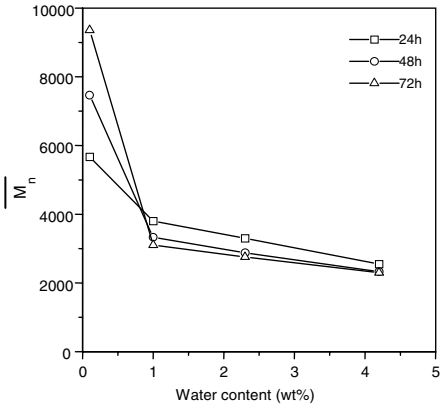

Fig. 63. Variation in poly(LLA-Gly) molecular weight as a function of water content for polymerization conducted at 100 °C.

2.3.4 Lipase-catalyzed ring-opening polymerization of 3(S)-*sec*-butyl-morpholine-2,5-dione

Screening of enzymes

Lipase-catalyzed ring-opening polymerization of 3(S)-*sec*-butyl-morpholine-2,5-dione in bulk was carried out as shown in the following Eq.

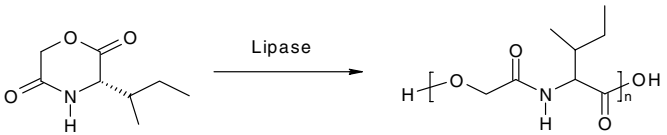

Screening results using selected commercial lipases for the bulk polymerization of Cyclo(Glc-Ile) are given in Tab. 37. The reactions were carried out at 110°C in bulk for 72 h or 144 h. In all cases, the enzymes and the monomer were dried in vacuum (10^{-3} mbar) over P_2O_5 at room temperature for 24 h.

Tab. 37. Ring-opening polymerization of Cyclo(Glc-Ile) with/without lipase

Entry	Lipase[a)]	wt %	Temp. in °C	Time in h	Conv. [b)] in %	$\overline{M_n}$ [b)]	$\overline{M_w}$ / $\overline{M_n}$ [b)]
1	PPL	1.5	110	72	2	4200	1.07
2	PPL	5	110	72	49	10600	1.09
3	PPL	5	120	144	92	19900	1.06
4	PPL	10	110	72	79	10700	1.07
5	MJ	10	110	72	33	3500	1.13
6	PC	10	110	72	70	5500	1.42
7	CR	10	110	72	6	8200	1.02
8	ES	10	110	72	11	3400	1.10
9	Novo-435	10	110	72	0		
10	blank	0	100	168	0		
11	blank	0	130	168	0		

a) *ES: Esperase 4,0T.*
b) determined by means of GPC using DMAc as eluent and polystyrene standards for calibration.

Except for lipase Novo-435, all the other lipases studied are effective for Cyclo(Glc-Ile) polymerization. However, a significant difference between the enzymes was observed with respect to monomer conversion and molecular weight of the polymer. Polymerizations catalyzed with 10 wt% of lipases PPL and PC result in Cyclo(Glc-Ile) conversions of ca. 70%. $\overline{M_n}$ values of poly(Glc-Ile) range from 5500 to 10700. Although Novo-435 is efficient

in catalyzing the ring-opening polymerization of ε-caprolactone at 60 °C, it failed to polymerize the cyclic depsipeptide at 110 °C because the heat stability of Novo-435 is very poor. MJ, CR and ES showed lower catalytic activity for the polymerization of Cyclo(Glc-Ile) than PPL and PC; monomer conversion and molecular weight of the resulting polymer were significantly lower than for PPL and PC.

Characterization of poly(Glc-Ile)

The ^{1}H NMR spectrum (DMSO-d-6, Fig. 64) shows five main resonance lines: a doublet at 8.35 ppm due to the NH proton, a multiplet at 4.5-4.7 ppm due to the protons of OCH_2CO, a multiplet at 4.37 ppm due to the proton of NHCHCO; the resonance lines at 1.84, 1.19-1.45 and 0.88 ppm are ascribed to protons of $CH(CH_3)CH_2CH_3$. Beside the main resonances, there are 4 small characteristic peaks**:** two doublets at 7.58 and 7.70 ppm due to the NH proton of the terminal amide units in $HOCH_2CONH$- and -$NHCH[CH(CH_3)CH_2CH_3]COOH$, respectively, a broad singlet at 5.57 ppm ascribed to the end group $HOCH_2$, and a peak at 3.88 ppm due to the α-methylene protons of the terminal hydroxy group. The multiplet resonance at 4.5-4.7 ppm results from the overlap of an AB-system in isotactic diads ((S,S) and (R,R) diad) with the resonance lines for the diasteromeric syndiotactic diads ((R,S) and (S,R) diad). The ^{13}C NMR spectrum shows 8 main resonance lines at 171.0, 166.6, 62.1, 55.8, 36.5, 24.3, 15.1 and 11.1 ppm due to $NHCO$, COO, OCH_2CO, $NHCHCO$, $CHCH_3$, CH_2CH_3, $CHCH_3$ and CH_2CH_3, respectively.

The IR spectrum of poly(Glc-Ile) shows a strong absorption band at 3320 cm^{-1} which is assigned to the stretching band of the N-H group (not shown). The band at 1753 cm^{-1} is due to the C=O stretching mode of the ester group, and the band at 1677 cm^{-1} to the bending mode of the N-H band and the stretching mode of the C-N bond of the amide group. The amide II band appears at 1540 cm^{-1}. The IR spectrum of poly(Glc-Ile) prepared with PPL as a catalyst is similar to that of poly(Glc-Ile) obtained with $Sn(oct)_2$ as a catalyst.

The specific rotation of poly(Glc-Ile) prepared via PPL catalyzed ring-opening polymerization is significantly smaller than that of poly(Glc-Ile) prepared via $Sn(oct)_2$ catalyzed polymerization (Tab. 38). This is caused by the racemization of the amino acid residue during the PPL catalyzed polymerization.

Tab. 38. Specific rotations of poly(Glc-Ile)

Entry	Catalyst	wt%	Temp. in °C	Time in h	$\overline{M_n}$	α_D^{25} a) in degree
1 b)	PPL	3	110	72	2300	20
2 c)	PPL	3	110	72	2200	12
3	PPL	5	120	144	19900	21
4	PPL	5	110	144	14200	24
5	PPL	10	110	144	11500	21
6	$Sn(oct)_2$	0.36	140	9	25900	61

a) c = 0.20 g/dl, $CHCl_3$. b) 1.1 wt% water was added. c) 2.2 wt% water was added.

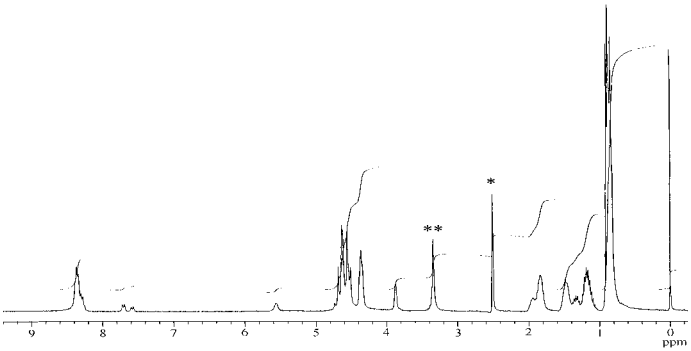

Fig. 64. ^{1}H-NMR of poly(Glc-Ile)(entry 3, in Tab. 38). * DMSO peaks, ** H_2O peaks.

The thermal behaviour of poly(Glc-Ile) was investigated by means of DSC. The sample was first heated to 200 °C, then cooled at a rate of 10 °C/min to -70 °C and finally heated at 10 °C/min from -70 to 200 °C. The DSC curve of poly(Glc-Ile) shows a glass transition ($T_{g\ (cooling)}$ = 44 °C, $T_{g\ (2nd\ heating)}$ = 50 °C) and a melting peak upon first heating (T_m=74 °C, ΔH= 41 J/g) (Fig. 65). This result corresponds to that obtained for poly(Glc-Ile) prepared with $Sn(oct)_2$ as a catalyst.

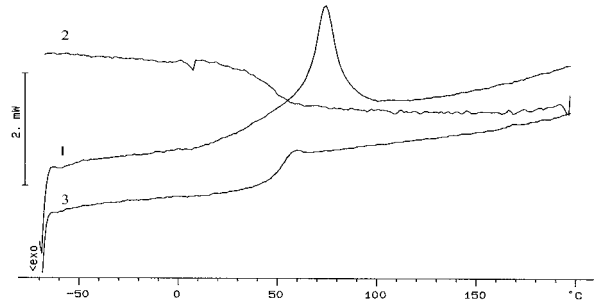

Curve 1: first heating;
Curve 2: cooling;
Curve 3: second heating.

Fig. 65. DSC thermograms of poly(Glc-Ile).

Effect of reaction time and concentration of PPL

The polymerization of Cyclo(Glc-Ile) in the melt at 110 °C with three different concentrations of PPL was studied with respect to the dependence of the monomer conversion and the molecular weight on reaction time. Samples were taken at different times, dissolved in chloroform, filtered to remove insoluble enzyme, then kept under reduced pressure to give the crude polymer, and analyzed by means of ^{1}H-NMR and GPC.

The apparent rate of polymerization increases with concentration of the enzyme PPL. Fig. 66 shows the results obtained for three PPL concentrations, for 5 wt% and 10 wt% a conversion of about 70% is reached after 5 d and 3 d, respectively, while for 1 wt% the conversion is less than 7% even after 6 d.

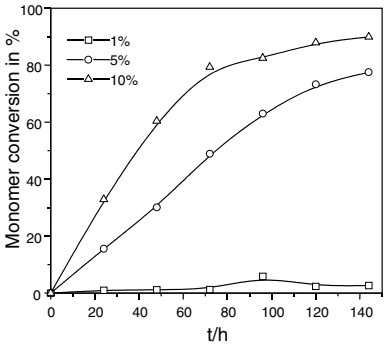

Fig. 66. Polymerization of Cyclo(Glc-Ile) in the bulk with PPL as a catalyst; dependence of monomer conversion on time. Polymerization temperature 110 °C.

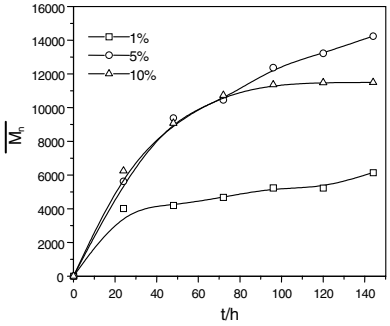

Fig. 67. Polymerization of Cyclo(Glc-Ile) in the bulk with PPL as a catalyst; dependence of the number average molecular weight $\overline{M_n}$ on time.

The dependence of the number average molecular weight $\overline{M_n}$ on time and PPL concentration reveals two important features:

(i) High concentration of PPL (Fig. 67 and 10 wt%) results in high $\overline{M_n}$ values; with lower concentration of PPL (1 wt %) poly(Glc-Ile) with lower molecular weight is obtained.

(ii) Increasing polymerization time (and conversion) leads to an increase in $\overline{M_n}$. For the polymerization experiments with 1 wt % the increase of $\overline{M_n}$ with time is not significant.

Effect of reaction temperature

Ring-opening bulk polymerizations of Cyclo(Glc-Ile) catalyzed with PPL were performed at 110, 120 and 130 °C for 144 h. Monomer conversion and molecular weight were determined by means of ^{1}H NMR and GPC at time intervals of 24 h. Fig. 68 shows that monomer conversion increases linearly with increasing reaction temperature from 110 to 120 °C. This means that the domain of PPL, which catalyzes the ring-opening polymerization of Cyclo(Glc-Ile), is heat stable. However, when the reaction temperature is increased from 120 °C to 130 °C, the conversion is lower at constant reaction time.

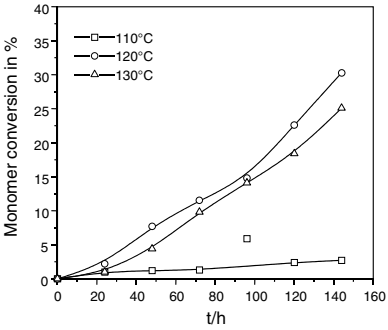

Fig. 68. Polymerization of Cyclo(Glc-Ile) in the bulk with PPL as a catalyst; dependence of monomer conversion on time. PPL/M = 1 wt %.

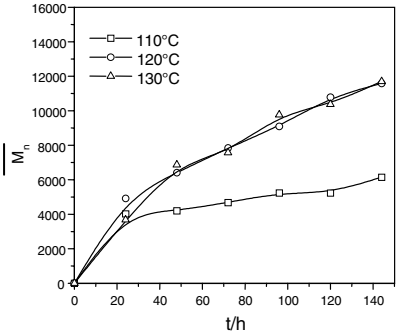

Fig. 69. Polymerization of Cyclo(Glc-Ile) in the bulk with PPL as a catalyst; dependence of molecular weight on time. PPL/M = 1 wt %.

Fig. 69 shows that the reaction temperature is an important parameter in regulating the molecular weight of poly(Glc-Ile). An increase in reaction temperature from 110 to 120 °C results in an increase of $\overline{M_n}$. However, the molecular weight of the polymer is unchanged when the polymerization is carried out at 120 and 130 °C.

In order to review the detailed effect of reaction temperature on the PPL catalyzed polymerization, reactions were performed at 110, 115, 120, 125 and 130 °C. Fig. 70 shows that the monomer conversion increases with increasing reaction temperature from 110 to 125 °C. The monomer conversion decreases as the reaction temperature is increased from 125 to 130 °C. Fig. 71 shows the general trends in $\overline{M_n}$: (i) the molecular weight increases substantially at all temperatures as the polymerization time is increased from 24 h to 72 h, (ii) increasing reaction temperature from 110 to 125 °C results in increased $\overline{M_n}$ values, (iii) along with monomer conversion, $\overline{M_n}$ decreases substantially when the reaction temperature

is increased from 125 to 130 °C. Thus, the highest molecular weights were observed by conducting the polymerization at about 125 °C. $\overline{M_n}$ > 19900 is achieved when carrying out polymerizations at about 120 °C with 5 wt% PPL. In other words, to achieve high molecular weights of poly(Glc-Ile) the concentration of PPL and the polymerization temperature must be carefully adjusted.

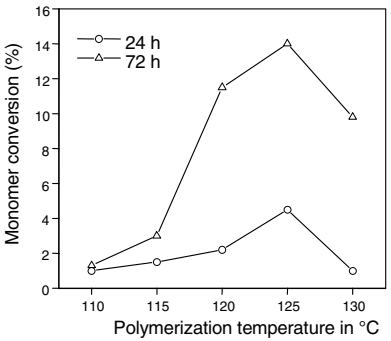

Fig. 70. Effect of polymerization temperature on monomer conversion for 1 wt% PPL catalyzed polymerization.

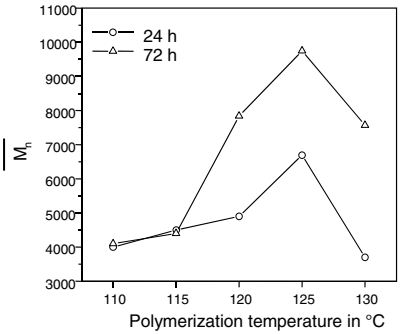

Fig. 71. Effect of polymerization temperature on poly(Glc-Ile) molecular weight for 1 wt% PPL catalyzed polymerization.

Effect of water content

In this study, the water content for PPL catalyzed Cyclo(Glc-Ile) polymerizations conducted at 110 °C for 24, 48 and 72 h was varied. The monomer conversion as a function of the water content is shown in Fig. 72. Increasing the water content results in an enhanced polymerization rate. For example, by increasing the water content from 1.1 to 2.2 wt%, monomer conversion increases from 19 to 62 % within 24 h. Interestingly, a small increase in water content from 0.14 to 1.1 wt% results in a rather large increase in monomer conversion, i.e., from 1.4 to 54% within 48 h. These observations are similar to those made for PPL catalyzed polymerization of 3(S)-isopropyl-morpholine-2,5-dione and can be explained in a similar fashion.

The water content was also found to be important in controlling the molecular weight. The effect of water content on $\overline{M_n}$ is shown in Fig. 73 for reactions conducted for 24, 48 and 72 h at 110 °C. $\overline{M_n}$ increases from 2300 to 4700 upon decreasing the water content from 1.1 to 0.14 wt%.

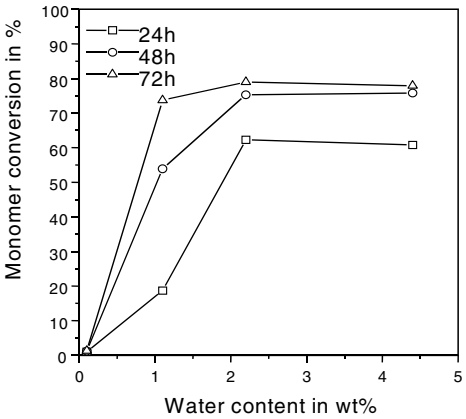

Fig.72. Variation in monomer conversion as a function of water content for polymerization conducted at 110 °C.

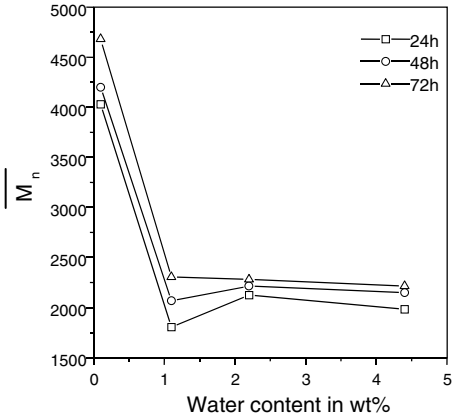

Fig. 73. Variation in poly(Glc-Ile) molecular weight as a function of water content for polymerization conducted at 110 °C.

2.3.5 PPL catalyzed copolymerization of 3(S)-isopropyl-morpholine-2,5-dione and DLLA

Matsumura et al. reported the lipase-catalyzed ring-opening polymerization of lactide[131]. The conversion of DLLA is over 80% after 7 days incubation of DLLA at 100 °C with 3 wt% lipase PS. However, the polymer yield based on monomer is less than 10%[131]. Both Cyclo(Glc-Val) and DLLA are six-membered cyclic monomers and can be homopolymerized in bulk in the presence of PPL as a catalyst. The copolymerization of Cyclo(Glc-Val) and DLLA was conducted under similar conditions in this study. Copolymers of Cyclo(Glc-Val) and DLLA were obtained by ring-opening polymerization of Cyclo(Glc-Val) and DLLA in the presence of PPL as a catalyst at 100 °C for 168 h (Scheme 14). The mole fraction of Cyclo(Glc-Val) in the feed and the results of homo- and co-polymerization are summarized in Tab. 39 and 40. Homopolymers (No. 1 and 7 in Tab. 39) were synthesized as control materials.

Tab. 39. Homo- and copolymerization of Cyclo(Glc-Val) and DLLA in the presence of 5wt% PPL as a catalyst at 100 °C for 168 h

No.	$F_{Cyclo(Glc-Val)}$ in %	Conv. of Cyclo(Glc-Val) in %[a)]	Conv. of DLLA in %[a)]	Polymer yield in %	$\overline{M_n}$ $\times 10^{-3}$ [b)]	$\overline{M_w}$ $\times 10^{-3}$ [b)]	$\overline{M_w}/\overline{M_n}$ [b)]
1	0	-	84	57	18.1	20.0	1.10
2	18	10	85	42	12.8	13.4	1.05
3	31	14	90	20	10.8	11.2	1.04
4	51	20	85	13	8.6	8.9	1.03
5	70	23	80	13	9.4	9.9	1.05
6	85	34	85	20	10.6	11.1	1.05
7	100	66	-	45	17.5	18.5	1.06

a) calculated from ^{1}H NMR. b) from GPC.

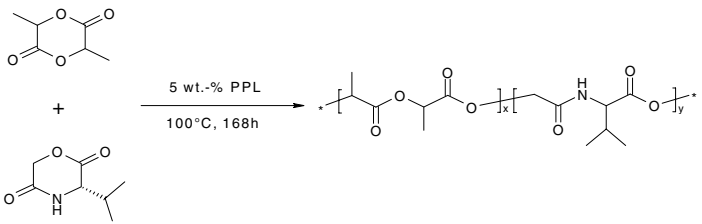

Scheme 14. PPL catalyzed copolymerization of Cyclo(Glc-Val) and DLLA.

Tab. 40. Composition of the copolymers and glass transition temperature

No.	$F_{Cyclo(Glc\text{-}Val)}$ in the feed in %	$f_{Cyclo(Glc\text{-}Val)}$ in copolymer [a] in %	T_g / °C [b]
1	0	0	40
2	18	7	41
3	31	9	42
4	51	29	45
5	70	46	48
6	85	70	56
7	100	100	74

a) calculated from ^{1}H NMR. b) from DSC upon second heating.

Tab. 39 shows that DLLA is polymerized at 100 °C for 168 h to yield PDLLA with an $\overline{M_n}$ of 18100. The conversion of DLLA is up to 84%. However, the yield of polymer is only 57%. From GPC analysis of the polymerization mixture, it is found that PPL-catalyzed polymerization of DLLA produces a high molecular weight polymer fraction with a low molecular weight oligomeric fraction (< 2500). The low molecular weight fraction was removed by precipitation resulting in a much lower polymer yield compared to the conversion. When the mole fraction of DLLA in the feed decreases from 100 to 15%, the conversion of DLLA in the copolymerization is about 85%. On the other hand, the conversion of Cyclo(Glc-Val) increases from 10 to 66% with increasing mole fraction of Cyclo(Glc-Val) in the feed from 18 to 100%. GPC analysis of the copolymerization mixture shows that PPL-catalyzed copolymerization of DLLA and Cyclo(Glc-Val) produces more oligomer (< 2500) than polymer (> 5000). The oligomer was removed by reprecipitation using acetone as a good solvent and water as a poor solvent. This results in a yield of the copolymer of less than 42%. The mole fraction of Cyclo(Glc-Val) in the copolymers increases with increasing mole fraction in the feed. Copolymers with various compositions were obtained (Tab. 39,40).

Fig. 74 shows the ^{1}H NMR spectrum (DMSO-d-6) of the purified PDLLA. The ^{1}H NMR spectrum of PDLLA shows two main resonances: two multiplets at 5.18 and 1.45 ppm due to proton of CH and protons of CH_3, respectively. Beside the main resonances, there are three small characteristic peaks: two quintets at 5.45 and 4.21 ppm due to CH proton of the terminal hydroxyl group and the terminal carboxylic acid unit, respectively, and two doublet peaks at the center of 1.29 ppm due to CH_3 protons of the two terminal groups. The data indicate that the enzymatic polymerization of DLLA produces PDLLA with a carboxylic acid group at one end and a hydroxyl group at the other end.

The ^{1}H NMR spectrum of copolymers shows five main resonances except the resonances of PDLLA: a doublet at 8.35 ppm due to the NH proton, a multiplet at 4.64 ppm due to protons of OC<u>H</u>$_2$CO, a multiplet at 4.33 ppm due to the proton of NHC<u>H</u>CO, and resonance lines at 2.12 and 0.91 ppm due to the proton of C<u>H</u>(CH$_3$)$_2$ and protons of CH(C<u>H</u>$_3$)$_2$ (Fig. 75). Beside the main resonances, there are three small characteristic peaks: a doublet at 7.65 ppm due to the NH proton of the terminal amide unit, a broad singlet at 5.54 ppm due to the proton of the end group <u>H</u>OCH$_2$, and a peak at 3.87 ppm due to the α-methylene protons of the terminal hydroxyl group. The characteristic peaks at 5.45 and 4.21 ppm, which are due to the CH proton of the terminal hydroxyl group and the terminal carboxylic acid unit resulting from DLLA also appeared in the ^{1}H NMR spectrum of the copolymers. The data indicate that the enzymatic copolymerization of Cyclo(Glc-Val) and DLLA produces poly[(Glc-Val)/DLLA] with a carboxylic acid group at one end and a hydroxyl group at the other end. In the ^{1}H NMR spectrum of the copolymer the resonances at 5.18 and 4.64 ppm are different from those of the homopolymers. The signals are sensitive to the microstructure of the copolymer and the configuration of valine in the copolymers.

The composition of the copolymers is estimated from ^{1}H-NMR spectra by the following formula:

Cyclo(Glc-Val) molar content(%) = $I_{Cyclo(Glc\text{-}Val)}/(I_{Cyclo(Glc\text{-}Val)}+I_{DLLA})$

where $I_{Cyclo(Glc\text{-}Val)}$ and I_{DLLA} are the intensities of the CH_3 peak at 0.95 ppm (due to valine residue) and CH_3 peak in the range from 1.20 to 1.40 ppm (due to DLLA residue), respectively.

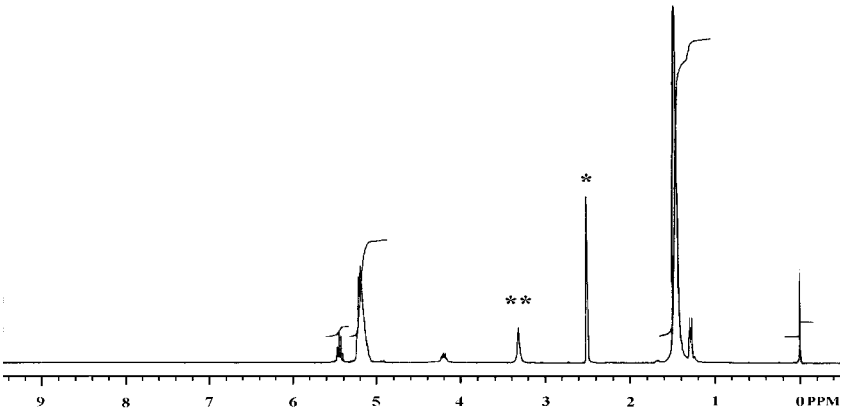

Fig. 74. H NMR spectrum (DMSO-d-6) of PDLLA. * =DMSO-d-6 peak, ** = H_2O peak.

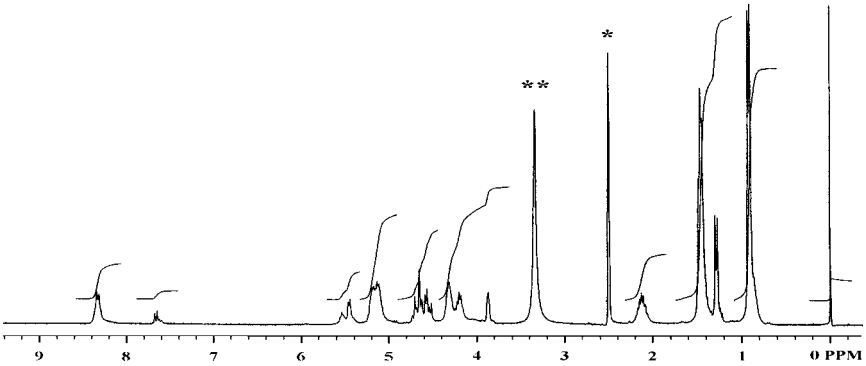

Fig. 75. ^{1}H NMR spectrum (DMSO-d-6) of copolymer. * =DMSO-d-6 peak, ** = H_2O peak.

The bands at 1757 and 1188 cm^{-1} in Fig. 76 curve 3 are assigned to C=O stretching and C-O asymmetric stretching frequencies of PDLLA, respectively. The IR of the copolymer shows the ester band at 1753 cm^{-1}, the amide I band at 1675 cm^{-1} and amide II band at 1537 cm^{-1}. The relative absorbance of band at 1675 cm^{-1} increases with increasing mole fraction of Cyclo(Glc-Val) in the copolymers.

The thermal behavior of purified poly(Glc-Val), PDLLA and copolymers was investigated by means of DSC. Glass transition temperatures of homopolymers and copolymers are presented in Tab. 40. The glass transition temperature decreases with increasing mole fraction of the DLLA residue in the copolymers. The copolymers reveal an increasing toughness with an increasing mole fraction of the DLLA residue.

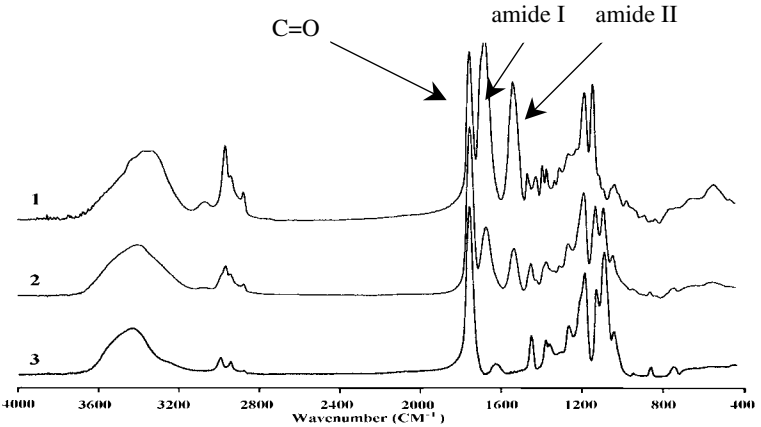

Fig. 76. IR spectra of poly(Glc-Val)(Curve 1), copolymer (Curve 2) and PDLLA(Curve 3).

3. EXPERIMENTAL PART

3.1 MATERIALS

S-Isoleucine, S-leucine, S-valine and glycine were purchased from Ajinomoto Co., Inc, Tokyo Japan. N^{ε}-(Benzyloxylcarbonyl)-(S)-lysine and β-benzyl-(S)-aspartate were obtained from Calbiochem-Novabiochem Corp. γ-Benzyl-(S)-glutamate, S-*p*-nitrobenzyl-(R)-cysteine and O-benzyl-(S)-tyrosine were prepared according to literature[132-134].

Butyl-glycolate, S-ethyl lactate and methane sulfonic acid were purchased from Fluka and stannous octoate (95%) from Sigma Chem. Corp. (Steinheim, Germany). Hydroxytelechelic PEO with a molecular weight of 1000 (PEO1000), 6000 (PEO6000), 8000 (PEO8000), 20000 (PEO20000) and monomethoxy-poly(ethylene oxide) with a molecular weight of 5000 (MPEO5000) were obtained from Fluka. All PEO-macroinitiators were dried i. vac. for 24 h before use. 4-N,N-Dimethylaminopyridine (DMAP) and *p*-toluene sulphonyl chloride were obtained from Aldrich.

D,L-Lactide and L-lactide were obtained from Boehringer Ingelheim, Germany.

Porcine pancreatic lipase (PPL) type II crude (activity 56 units/mg of protein), lipase type VII from *Candida rugosa* (CR) (activity 746units/mg solid) and lipase type XIII from *Pseudomonas species* (PS) (activity 25 units/mg of solid) were obtained from Sigma Chemical Co. Lipase from *Pseudomonas cepacia* (PC) (specified activity at pH 7.0 was 30000 u/g) was obtained from Fluka. Immobilized lipase from *C. Antarctica* (Novozym-435) was kindly donated by Novo Nordisk Bioindustrials, Inc. (Bagsvaerd, Denmark). All enzymes were employed without further purification.

All other reagents were obtained from Fluka and used as received.

3.2 MEASUREMENTS

^{1}H NMR and ^{13}C NMR spectra (DMSO-d-6 or $CDCl_3$) were recorded on a Bruker AC 300 Model spectrometer at 300 MHz and 75 MHz, respectively. The chemical shifts were referenced to internal tetramethylsilane (TMS).

IR spectroscopy on a Nicolet 60SXR Model was adopted using KBr pellets or diamond. $\overline{M_n}$ and $\overline{M_w}$ of polymers were determined by means of GPC. Analyses were carried out using a Bischoff model 2200 pump equipped with a Waters model 410 refractive index detector, micro UVIS20 detector (Carlo Erba) and Bischoff model 728 autosampler with 10^2, 10^3 and

10^4 Å Ultrastyragel columns in series. DMAc (HPLC grade, 1.220 g/L LiCl) was used as the eluent at a flow rate of 0.8 mL/min. The molecular weight was calculated on the basis of polystyrene standards without further correction.

The thermal behavior of the polymers was studied by means of differential scanning calorimetry with a Mettler DSC 40 system. Indium was used for calibration purposes. The specimens were heated in sealed aluminium pans and scanned from -70 °C to 200 °C, then cooled to -70 °C, and finally heated to 200 °C using heating and cooling rates of 10°C/min. All experiments were done under a flow of dry N_2.

Specific rotations ($[\alpha]_D^{25}$) were measured with a Perkin-Elmer-Polarimeter PE241 (l = 10cm, λ = 589.0 and 589.6 nm, $CHCl_3$ as solvent).

The static contact angle of the copolymers as a film on a glass plate was measured with the contact angle system G40 (Krüss GmbH) at room temperature.

Preparation of films

Films of the size 50 mm× 50 mm× 1.5mm were obtained from 1.3 g of the polymer by compression moulding at 60 or 110 °C and 40 kg/cm^2 for 10 min.

Mechanical properties

A Zwick BZ2.5/TN1S (Ulm, Germany) with a load cell of 0.03 N/mm^2 was used to study the mechanical properties of the samples. A gauge length of 6 cm and strain rate of 10 mm/min were used in this study. The measurements were performed at room temperature using specimen of 3.0 mm width, 6.0 mm length and 1.5 mm thickness.

Degradation tests

For degradation studies film specimens with 1.5 cm^2 surface area and approximately identical weights (60-90 mg) were obtained from plates prepared by compression moulding. The specimens were incubated in 5 mL of Na_2HPO_4/KH_2PO_4 buffer (pH 7.0) at 37 °C in a shaking air bath operating at a frequency of 60 rpm. At the end of each immersion period, the specimens were taken out, washed with distilled water three times, and dried at room temperature in a desiccator *in vacuo* over P_2O_5 for 14 days.

The water absorption was determined using the equation:

Water absorption = $(W_s - W_d) \times 100\% / W_d$

where W_d and W_s are the weight of the dried sample and the weight of the swollen sample at a given time.

The weight loss of each film was determined by comparing the dry weight of the degraded polymer with the initial weight:

Weight loss = $(W_0 - W_d) \times 100\% / W_0$

where W_0 is the initial weight and W_d is the weight of the sample dried for 14 days.

3.3 SYNTHESES

3.3.1 Syntheses of PEO-initiators

3.3.1.1 Synthesis of α-methoxy-ω-N,N-bis(hydroxyethyl)poly(ethylene oxide) (MPEO(OH)$_2$)

45 g of MPEO5000 (9 mmol) were dissolved in a mixture of methylene chloride and pyridine (80 ml, 1:1 v/v). 80 mg of DMAP were added to the resulting solution which was then cooled to 0 °C. *p*-Toluene sulphonyl chloride (9 g) dissolved in 40 mL of methylene chloride was added dropwise. The reaction was left overnight on an ice bath. Then 90 mL of conc. aqueous HCl, 200 g of ice and 100 mL of methylene chloride were added. The organic layer was separated and then washed with an aqueous solutions of HCl (9%), NaCl, $NaHCO_3$, and with water. The product was dried over $MgSO_4$. The resulting α-methoxy-ω-tosyl-poly(ethylene oxide) was added to an excess of dihydroxyethylamine (90 mL) and stirred for 4 h at 90 °C. The reaction mixture was cooled to room temperature by adding 100 mL of water. The water phase was extracted with methylene chloride and the organic phase was dried over $MgSO_4$. The resulting polymer was dissolved in methylene chloride and purified by precipitation in diethyl ether. MPEO(OH)$_2$ was analyzed by means of MALDI TOF MS and NMR.

3.3.1.2 Synthesis of α,ω-bis[N,N-bis(hydroxyethyl)]poly(ethylene oxide) ((HO)$_2$PEO(OH)$_2$)

48 g of PEO6000(8 mmol) were dissolved in a mixture of methylene chloride and pyridine (150 ml, 1:1v/v). 140 mg of DMAP were added to the resulting solution which was then cooled to 0 °C. *p*-Toluene sulphonyl chloride (18 g) dissolved in 40 mL of methylene chloride was added dropwise. The reaction was left overnight on a ice bath. Then 180 mL of conc. aqueous HCl, 300 g of ice and 200 mL of methylene chloride were added. The organic layer was separated and then washed with an aqueous solutions of HCl (9%), NaCl, $NaHCO_3$ and with water. The product was then dried over $MgSO_4$. The resulting α,ω-bistosyl-PEO6000 was added to an excess of dihydroxyethylamine (180 mL) and stirred for 4 h at 90 °C. The reaction mixture was cooled to room temperature by adding 200 mL of water. The water phase was extracted with methylene chloride and the organic phase was dried over $MgSO_4$. The resulting polymer was dissolved in methylene chloride and purified by

precipitation in diethyl ether. $(HO)_2PEO(OH)_2$ was analyzed by means of MALDI TOF MS and NMR.

3.3.2 Syntheses of morpholine-2,5-diones

3.3.2.1 Syntheses of N-(α-hydroxy acyl)-(S)-amino acids and N-(α-bromopropionyl)-amino acids

3.3.2.1.1 Synthesis of N-(α-hydroxyacetyl)-(S)-isoleucine

To a suspension of 131.2 g (1.0 mol) of S-isoleucine in 1000 mL of dry ethanol 2000 mL of a 0.5 M solution of sodium ethanolate in ethanol were added within 2 h. The resulting solution of the sodium salt of (S)-isoleucine was filtered in order to remove undissolved material and the solvent was evaporated under reduced pressure. To the solid residue 4 mol of butyl glycolate were added and stirred for 20 h at 80 °C. The reaction mixture was allowed to cool to room temperature and then 500 mL of water were added. The resulting solution was washed twice with 1000 mL diethyl ether, then acidified to pH 2.0 with conc. aqueous HCl. The solution was extracted twice with 500 mL of ethyl acetate. The organic layer was separated, dried with anhydrous Na_2SO_4 for 24 h and concentrated i. vac. to yield 177 g (93.7%) of a yellowish oil. The resulting oil was used without further purification in the next step.

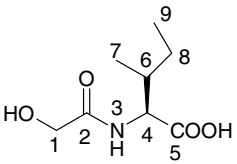

^{1}H NMR (300MHz, DMSO-d_6, ppm), 0.84-0.89(m, 6H, CH_3-7 and 9); 1.09-1.48(m, 2H, CH_2-8); 1.77-1.91(m, 1H, CH-6); 3.85 and 3.91 (AB-system, ^{AB}J = 16.0 Hz, 2H, CH_2-1); 4.22(d×d, ^{3}J = 8.7 Hz, ^{3}J = 5.4 Hz, 1H, CH-4); 7.49(d, ^{3}J = 8.8 Hz, 1H, NH-3).

^{13}C NMR (75.43MHz, DMSO-d_6, ppm), 11.3(CH_3-9); 15.3 (CH_3-7); 25.6(CH_2-8); 35.7(CH-6); 56.5(CH-4), 67.1(CH_2-1), 172.8(COO-5); 174.2(CONH-2).

3.3.2.1.2 Synthesis of N-(α-hydroxyacetyl)-(S)-leucine

N-(α-Hydroxyacetyl)-(S)-leucine was prepared by the reaction of S-leucine and butyl glycolate following the procedure described for the preparation of N-(α-hydroxyacetyl)-(S)-isoleucine. The resulting yellowish crystalline material (180 g, 95.3%) was purified by

recrystallization from THF/hexane to give 159.0 g (84.1%) of a white crystalline material, mp 126-127 °C.

^{1}H NMR (300MHz, DMSO-d_6, ppm), 0.85-0.90(m, 6H, CH_3-8 and 9); 1.47-1.76(m, 3H, CH_2-6 and CH-7); 3.84(s, 2H, CH_2-1); 4.27-4.34(m, 1H, CH-4); 7.71-7.74(d, ^{3}J = 8.4 Hz, 1H, NH-3).

^{13}C NMR (75.43MHz, DMSO-d_6, ppm), 21.3(CH_3-9 or 8); 22.8 (CH_3-9 or 8); 24.2(CH-7); 38.8(CH_2-6); 49.5 (CH-4); 61.1(CH_2-1); 171.6(C=O-5); 173.8(C=O-2).

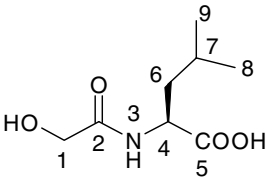

3.3.2.1.3 Synthesis of N-(α-hydroxyacetyl)-(S)-valine

N-(α-Hydroxyacetyl)-(S)-valine was prepared by the reaction of S-valine and butyl glycolate following the procedure described for the preparation of N-(α-hydroxyacetyl)-(S)-isoleucine. Yield 71%, mp 109 °C.

^{1}H NMR (DMSO-d_6, 300MHz, ppm): 0.87(d, ^{3}J=6.7Hz, 3H, CH_3-7 or 8); 0.89(d, ^{3}J=6.7Hz, 3H, CH_3-7 or 8); 2.05-2.16(m, 1H, CH-6); 3.85 and 3.91(AB-system, ^{AB}J=16.0Hz, 2H, CH_2-1); 4.23(d*d, ^{3}J=8.7Hz, ^{3}J=5.4Hz, 1H, CH-4); 7.50(d, ^{3}J=8.8Hz, 1H, NH-3).

^{13}C NMR(DMSO-d_6, 75.43MHz, ppm): 17.7(CH_3-7 or 8); 18.9(CH_3-7 or 8); 30.2(CH-6); 56.3(CH-4); 61.1(CH_2-1); 171.7(C=O-5), 172.7 (C=O-2).

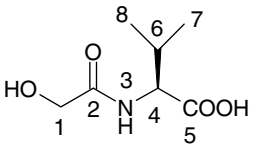

3.3.2.1.4 Synthesis of N-(2(S)-hydroxypropionyl)-(S)-isoleucine

N-(2(S)-Hydroxypropionyl)-(S)-isoleucine was prepared by the reaction of S-isoleucine and S-ethyl lactate following the procedure described for the preparation of N-(α-hydroxyacetyl)-(S)-isoleucine. Yield 93%.

^{1}H NMR (DMSO-d_6, 300MHz, ppm): 0.84-0.89(m, 6H, CH_3-9 and CH_3-10); 1.09-1.48(m, 2H, CH_2-8); 1.22(d, ^{3}J=6.8Hz, 3H, CH_3-6); 1.77-1.91(m, 1H, CH-7); 4.02-4.12(q, ^{3}J=6.8Hz, 1H, CH-1); 4.22(d*d, ^{3}J=8.7Hz, ^{3}J=5.4Hz, 1H, CH-4); 7.48(d, ^{3}J=8.8Hz, 1H, NH-3).

^{13}C NMR(DMSO-d_6, 75.43MHz, ppm): 11.3(CH_3-10); 15.4(CH_3-9); 21.2(CH_3-6); 24.6(CH_2-8); 36.8(CH-7); 55.6(CH-4); 67.1(CH-1); 172.8(C-2 or 5), 174.2(C-2 or 5).

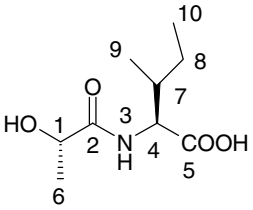

3.3.2.1.5 Synthesis of N-(2(R,S)-hydroxypropionyl)-(S)-isoleucine

N-(2(S)-Hydroxypropionyl)-(S)-isoleucine was prepared by the reaction of S-isoleucine and S-ethyl lactate following the procedure described for the preparation of N-(α-hydroxyacetyl)-(S)-isoleucine. Yield 90%.

^{1}H NMR (DMSO-d_6, 300MHz, ppm): 0.84-0.89(m, 6H, CH_3-9 and CH_3-10); 1.16-1.20(m, 2H, CH_2-8); 1.22(d, ^{3}J=6.5Hz, 3/2H, CH_3-6); 1.23(d, ^{3}J=6.5Hz, 3/2H, CH_3-6); 1.82-1.91(m, 1H, CH-7); 4.02-4.12(m, 1H, CH-1); 4.20-4.22(m, 1H, CH-4); 7.45(d, ^{3}J=9.0Hz, 1/2H, NH-3); 7.48(d, ^{3}J=9.0Hz, 1/2H, NH-3).

^{13}C NMR(DMSO-d_6, 75.43MHz, ppm): 12.1 (CH_3-10); 15.0(CH_3-9); 16.0(CH_3-9 or 10); 21.2(CH_3-6); 21.8(CH_3-6); 22.0(CH_3-6); 25.5(CH_2-8); 26.1(CH_2-8); 37.6(CH-7); 38.0(CH-7); 56.4(CH-4); 56.8(CH-4); 67.8(CH-1); 68.0(CH-1); 173.6(C-2 or 5), 175.1 (C-2 or 5).

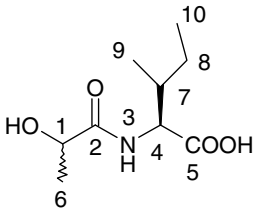

3.3.2.1.6 Synthesis of N-(2(R,S)-hydroxypropionyl)-(S)-valine

N-(2(R,S)-Hydroxypropionyl)-(S)-valine was prepared by the reaction of S-valine and R,S-ethyl lactate following the procedure described for the preparation of N-(α-hydroxyacetyl)-(S)-isoleucine. Yield 82%.

^{1}H NMR (DMSO-d_6, 300MHz, ppm): 0.85-0.89(m, 6H, CH_3-8 and CH_3-9); 1.21(d, ^{3}J=6.7Hz, 3/2H, CH_3-6); 1.25(d, ^{3}J=6.5Hz, 3/2H, CH_3-6); 2.06-2.16(m, 1H, CH-7); 4.00-4.10(m, 1H,

CH-1); 4.16-4.20(m, 1H, CH-4); 7.46(d, ^{3}J=9.1Hz, 1/2H, NH-3); 7.50(d, ^{3}J=9.1Hz, 1/2H, NH-3).

^{13}C NMR(DMSO-d_6, 75.43MHz, ppm): 17.6(CH_3-8 or 9); 17.7(CH_3-8 or 9); 18.9(CH_3-8 or 9); 21.1(CH_3-6); 21.4(CH_3-6); 30.3(CH-7); 30.4(CH-7); 56.3(CH-4); 56.4(CH-4); 67.1(CH-1); 67.3(CH-1); 172.7(C-2 or 5), 174.3 (C-2 or 5).

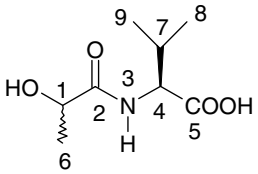

3.3.2.1.7 Synthesis of N-(2(S)-hydroxypropionyl)-glycine

To a suspension of 105 g (1.4 mol) of glycine in 1000 mL of dry ethanol 1400 mL of a 1.0 M solution of sodium ethanolate in ethanol were added within 2 h. The resulting solution of the sodium salt of glycine was filtered in order to remove undissolved material and the solvent was evaporated under reduced pressure. To the solid residue 4 mol of S-ethyl lactate were added and stirred for 18 h at 80 °C. The reaction mixture was allowed to cool to room temperature and then 500 mL of water were added. The resulting solution was acidified to pH 2.0 with conc. aqueous HCl, and concentrated i. vac. The obtained solid was extracted twice with 500 mL of ethanol. The organic layer was separated, dried with anhydrous Na_2SO_4 for 24 h and concentrated i. vac. to yield 186.2 g (90.5%) of a crystal, mp 103-104 °C, $[\alpha]^{25}_{D}$ 13.9 ° (1.28 g/dL methanol).

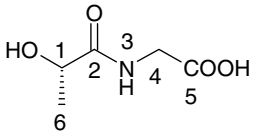

^{1}H NMR (DMSO-d_6, 300MHz, ppm): 1.24(d, ^{3}J=6.8Hz, 3H, CH_3-6); 3.77(d, ^{3}J=6.0Hz, 2H, CH_2-4); 4.01(q, ^{3}J=6.8Hz, 1H, CH-1); 7.91(t, ^{3}J=5.9Hz, 1H, NH-3).

^{13}C NMR(DMSO-d_6, 75.43MHz, ppm): 20.9(CH_3-6); 40.3(CH_2-4); 67.1(CH-1); 171.2(C=O-5); 174.9(C=O-2).

3.3.2.1.8 Synthesis of N-(2(R,S)-hydroxypropionyl)-glycine

N-(2(R,S)-Hydroxypropionyl)-glycine was prepared by the reaction of glycine and (R,S)-ethyl lactate following the procedure described for the preparation of N-(2(S)-hydroxypropionyl)-glycine. Yield 85%.

^{1}H NMR (DMSO-d_6, 300MHz, ppm): 1.24(d, ^{3}J=6.8Hz, 3/2H, CH_3-6); 1.23(d, ^{3}J=6.8Hz, 3/2H, CH_3-6); 3.75(d, ^{3}J=6.0Hz, 2H, CH_2-4); 4.01(m, 1H, CH-1); 7.86(t, ^{3}J=5.9Hz, 1H, NH-3).

^{13}C NMR(DMSO-d_6, 75.43MHz, ppm): 21.4(CH_3-6); 21.5(CH_3-6); 40.6(CH_2-4); 66.9(CH-1); 67.1(CH-1); 172.7(C=O-5); 175.2(C=O-2).

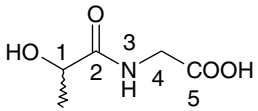

3.3.2.1.9 Synthesis of N^{α}-2(R,S)-[hydroxypropionyl]-N^{ε}-(benzyloxylcarbonyl)-(S)-lysine

N^{α}-2(R,S)-[Hydroxypropionyl]-N^{ε}-(benzyloxylcarbonyl)-(S)-lysine was prepared by the reaction of N^{ε}-(benzyloxylcarbonyl)-(S)-lysine and (R,S)-ethyl lactate following the procedure described for the preparation of N-(α-hydroxyacetyl)-(S)-isoleucine. Yield 97%.

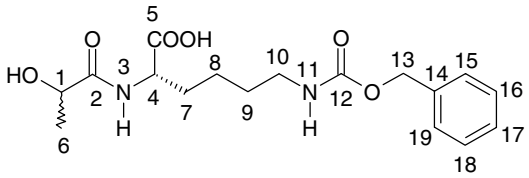

3.3.2.1.10 Synthesis of β–benzyl-N-[2(R,S)-bromopropionyl]-(S)-aspartate

To a cooled suspension (5-10 °C) of β-benzyl-(S)-aspartate (26.8 g, 0.12 mol) in 250 mL p-dioxane/water (1/1 V/V) 40 mL of a 3 M NaOH solution was added. The resulting solution was vigorously stirred and 50 mL of a p-dioxane solution containing 13.8 mL (0.13 mol) of 2(R,S)-bromopropionyl bromide was added in 5 mL portions, simultaneously with ten portions of 10 mL of a 14 M aqueous NaOH solution, while maintaining the reaction temperature at 0 °C by cooling with ice/salt mixture. After the addition was completed the reaction mixture was stirred for another 5 min, then the mixture was acidified to pH 2 with a concentrated HCl solution. The mixture was extracted with two 200 mL portions of diethyl ether. The combined organic layers were washed with a saturated aqueous NaCl solution, dried with $MgSO_4$ and concentrated i. vac. The crude product was recrystallized from toluene/hexane to give 23.2 g (54%) of β–benzy l-N-[2(R,S)-bromopropionyl]-(S)-aspartate. Mp. 121 °C, $[\alpha]_D^{25}$ = 46.1° (c= 0.20 g/dl chloroform).

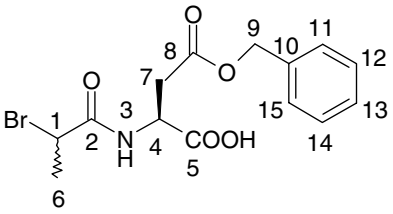

^{1}H NMR (300MHz, DMSO-d_6, ppm): 1.64(t, ^{3}J=7.1Hz, 3H, CH_3-6); 2.72-2.94(m, 2H, CH_2-7); 4.52-4.66(m, 2H, CH-1 and CH-4); 5.12(d, 2H, CH_2-9), 7.36(s, 5H, Ph-11-15); 8.70(d*d, ^{3}J=6Hz, NH-3).

^{13}C NMR(75.43MHz, DMSO-d_6, ppm): 21.5(CH_3-6); 21.6(CH_3-6); 35.5(CH_2-7); 35.7(CH_2-7); 43.2(CH-1); 43.3(CH-1); 48.7(CH-4); 48.8(CH-4); 65.7(CH_2-9); 65.6(CH_2-9); 127.7(Ph-13); 127.8 and 127.9(Ph-12 and 14); 128.3(Ph-11 and 15); 135.80 and 135.84(Ph-10); 168.6(C=O-5); 168.9(C=O-5); 169.8(C=O-8); 171.6(C=O-2).

3.3.2.1.11 Synthesis of γ–benzyl-N-[2(R,S)-bromopropionyl]-(S)-glutamate

γ – Benzyl-N-[2(R,S)-bromopropionyl]-(S)-glutamate was prepared by the reaction of γ-benzyl-(S)-glutamate and 2(R,S)-bromopropionyl bromide following the procedure described for the preparation of β–benzyl-N-[2(R,S)-bromopropionyl]-(S)-aspartate. The crude product was used in the synthesis of (3S, 6R,S)-3-[(benzyloxycarbonyl)-ethyl]-6-methyl-morpholine-2,5-dione without further purification. Yield 50.6%.

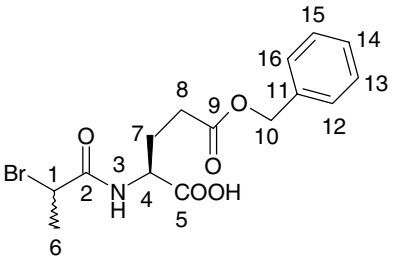

3.3.2.1.12 Synthesis of N-[2(R,S)-bromopropionyl]-S-(p-nitrobenzyl)-(R)-cysteine

N-[2(R,S)-Bromopropionyl]-S-(*p*-nitrobenzyl)-(R)-cysteine was prepared by the reaction of S-(*p*-nitrobenzyl)-(R)-cysteine and 2(R,S)-bromopropionyl bromide following the procedure described for the preparation of β–benzyl-N-[2(R,S)-bromopropionyl]-(S)-aspartate. Yield 92%.

^{1}H NMR (300MHz, DMSO-d_6, ppm): 1.71(t, ^{3}J=6.8Hz, 3H, CH_3-6); 2.70-2.94(m, 2H, CH_2-7); 3.95(two s., 2H, CH_2-8); 4.42-4.60(m, 1H, CH-4); 4.65-4.72(m, 1H, CH-1); 7.64(m, 2H, Ph-10 and 14); 8.20(m, 2H, Ph-11 and 13); 8.74(d*d, ^{3}J=7.7Hz, ^{3}J=8.1Hz, 1H, NH-3).

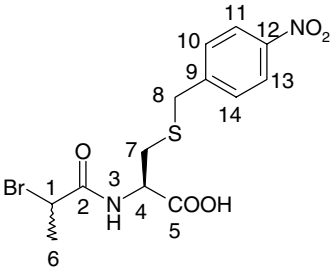

3.3.2.1.13 Synthesis of N-[2(R,S)-bromopropionyl]-O-(benzyl)-(S)-tyrosine

N-[2(R,S)-Bromopropionyl]-O-(benzyl)-(S)-tyrosine was prepared by the reaction of O-benzyl-(S)-tyrosine and 2(R,S)-bromopropionyl bromide following the procedure described for the preparation of β–ben z yl-N-[2(R,S)-bromopropionyl]-(S)-aspartate. Yield 73%.

^{1}H NMR (300MHz, DMSO-d_6, ppm): 1.50-1.71(three d., ^{3}J=6.7Hz, 3H, CH_3-6); 2.75-3.10(m, 2H, CH_2-7); 4.35-4.46(m, 1H, CH-4); 4.50-4.65(m, 1H, CH-1); 5.05(s, 2H, CH_2-14); 6.92(d, 2H, Ph-9 and 13); 7.15(t, ^{3}J=8.5Hz, 2H, Ph-10 and12); 7.30-7.45(m, 5H, Ph-16-20); 8.54(d*d, ^{3}J=8.1Hz, ^{3}J=8.4Hz, 1H, NH-3).

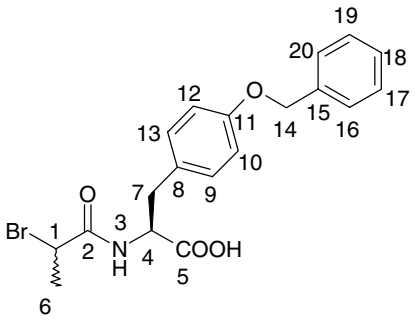

3.3.2.2 Syntheses of morpholine-2,5-diones

3.3.2.2.1 Synthesis of 3(S)-sec-butyl-morpholine-2,5-dione (Cyclo(Glc-Ile))

A mixture of 30.0 g (0.16 mol) of N-(α-hydroxyacetyl)-(S)-isoleucine, 3000 mL of dry methylene chloride, and 10.0 mL of methane sulfonic acid were placed in a 4 L round bottom flask equipped with a magnetic stirrer and an extractor to which a reflux condenser was

attached. The contents of the flask were heated to reflux until no water was formed any more. The resulting solution was cooled to room temperature and washed successively with 2×400 mL $NaHCO_3/H_2O$ and 3×400 mL H_2O. The organic layer was dried with anhydrous Na_2SO_4, the solvent subsequently evaporated, and the residual solid recrystallized from ethyl acetate and hexane. The yield was 7.0 g (25.8%), mp 107-108 °C.

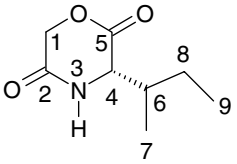

^{1}H NMR (300MHz, DMSO-d_6, ppm) 0.85-0.89(t, ^3J = 7.4 Hz, 3H, CH_3-9); 0.93-0.95 (d, ^3J = 7.0 Hz, 3H, CH_3-7); 1.17-1.50(m, 2H, CH_2-8); 1.85-1.95(m, 1H, CH-6); 4.02-4.04(q, ^3J = 2.7Hz, 1H, CH-4); 4.66-4.81(AB-system, ^{AB}J = 16.1 Hz, 2H, CH_2-1), 8.59(br. s, 1H, NH-3).
^{13}C NMR(75.43MHz, DMSO-d_6, ppm) 11.4(CH_3-9); 14.7(CH_3-7); 24.3(CH_2-8); 37.8(CH-6); 57.1(CH-4); 67.2(CH_2-1); 165.4(COO-5); 167.0(CONH-2).

3.3.2.2.2 Synthesis of 3(S)-isobutyl-morpholine-2,5-dione (Cyclo(Glc-Leu))

3(S)-Isobutyl-morpholine-2,5-dione was prepared by intra-molecular cyclization of N-(α-hydroxyacetyl)-(S)-leucine following the procedure described above for the preparation of 3(S)-*sec*-butyl-morpholine-2,5-dione. The yield was 3.7 g (26.3%), mp 129-130 °C.

^{1}H NMR (300MHz, $CDCl_3$, ppm) 0.96-0.98(d, ^3J = 6.0 Hz, 3H, CH_3-8 or 9); 1.00-1.02 (d, ^3J = 6.0 Hz, 3H, CH_3-8 or 9); 1.67-1.88(m, 3H, CH_2-6 and CH-7); 4.13-4.17(m, 1H, CH-4); 4.76(s, 2H, CH_2-1); 7.61(br. s, 1H, NH-3).
^{13}C NMR(75.43MHz, $CDCl_3$, ppm) 21.3(CH_3-9 or 8); 22.8 (CH_3-9 or 8); 24.2(CH-7); 41.5(CH_2-6); 51.7(CH-4); 67.4(CH_2-1); 166.4(COO-5); 167.3(CONH-2).

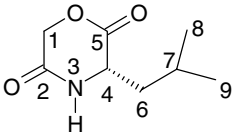

3.3.2.2.3 Synthesis of 3(S)-isopropyl-morpholine-2,5-dione (Cyclo(Glc-Val))

3(S)-Isopropyl-morpholine-2,5-dione was prepared by intra-molecular cyclization of N-(α-hydroxyacetyl)-(S)-valine following the procedure described for the preparation of 3(S)-*sec*-

butyl-morpholine-2,5-dione. Yield 29%, mp 96-97 °C, $[\alpha]_D^{25}$ = 35.9° (c= 0.876 g/dl chloroform).

^{1}H NMR (DMSO-d_6, 300MHz, ppm): 0.93(d, ^{3}J=6.8Hz, 3H, CH_3-7 or 8); 0.97(d, ^{3}J=7.0Hz, 3H, CH_3-7 or 8); 2.11-2.24(m, 1H, CH-6); 3.97(d*d, ^{3}J=4.6Hz, ^{3}J=2.5Hz, CH-4); 4.68 and 4.79(AB-system, ^{AB}J=16.0Hz, 2H, CH_2-1); 8.61(s, 1H, NH).

^{13}C NMR (DMSO-d_6, 75.43MHz, ppm): 17.3(CH_3-7 or 8); 18.1(CH_3-7 or 8); 31.3(CH-6); 58.0(CH-4); 67.2(CH_2-1); 165.5(C=O-5), 167.1(C=O-2).

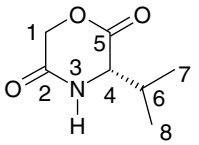

3.3.2.2.4 Synthesis of (3S, 6S)-3-sec-butyl-6-methyl-morpholine-2,5-dione (Cyclo(LLA-Ile))

(3S, 6S)-3-*sec*-Butyl-6-methyl-morpholine-2,5-dione was prepared by intramolecular cyclization of N-(2(S)-hydroxypropionyl)-(S)-isoleucine following the procedure described for the preparation of 3(S)-*sec*-butyl-morpholine-2,5-dione. Yield 33%, mp 110-111 °C.

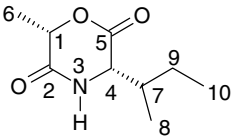

^{1}H NMR (300MHz, DMSO-d_6, ppm): 0.88(t, ^{3}J=7.4 Hz, 3H, CH_3-10); 0.98(d, ^{3}J=7.0 Hz, 3H, CH_3-8); 1.39(d, ^{3}J=6.8 Hz, 3H, CH_3-6); 1.30-1.47(m, 2H, CH_2-9); 1.86-1.99(m, 1H, CH-7); 4.26(d, ^{3}J=2.9Hz, 1H, CH-4); 5.01(q, ^{3}J=6.8Hz, 1H, CH-1); 8.40(br. s, 1H, NH-3).

^{13}C NMR(75.43MHz, DMSO-d_6, ppm): 11.9(CH_3-10); 14.5(CH_3-8); 15.9(CH_3-6); 24.1(CH_2-9); 36.0(CH-7); 57.1(CH-4); 73.5(CH_2-1); 168.2(C-5); 168.9(C-2).

3.3.2.2.5 Synthesis of (3S, 6R,S)-3-sec-butyl-6-methyl-morpholine-2,5-dione (Cyclo(DLLA-Ile))

(3S, 6R,S)-3-*sec*-Butyl-6-methyl-morpholine-2,5-dione was prepared by intra-molecular cyclization of N-(2-hydroxypropionyl)-(S)-isoleucine following the procedure described for the preparation of 3(S)-*sec*-butyl-morpholine-2,5-dione. Yield 33%, mp 98-100 °C, $[\alpha]_D^{25}$ = 19.4° (c= 0.538 g/dl chloroform).

^{1}H NMR (300MHz, DMSO-d_6, ppm): 0.88-0.99(m, 6H, CH_3-8 and 10); 1.17-1.23(m, 2H, CH_2-9); 1.37(d, ^{3}J=6.9 Hz, 0.6H, CH_3-6); 1.41(d, ^{3}J=6.9 Hz, 0.4H, CH_3-6); 1.86-1.90(m, 1H, CH-7); 3.92(d×d, ^{3}J=6.4Hz, ^{3}J=3.6Hz, 0.4H, CH-4); 4.26(d×d, ^{3}J=2.4Hz, 0.6H, CH-4); 5.01-5.09(m, 1H, CH-1); 8.38(s, 0.6H, NH-3); 8.60(s, 0.4H, NH-3).

^{13}C NMR(75.43MHz, DMSO-d_6, ppm): 11.0(CH_3-8 or 10); 12.0(CH_3-8 or 10); 14.5(CH_3-8 or 10); 14.9(CH_3-8 or 10); 24.1(CH_2-9); 24.6(CH_2-9); 36.0(CH-7); 37.6(CH-7); 58.1(CH-4); 58.9(CH-4); 73.6(CH_2-1); 73.8(CH_2-1); 167.2(C-5 or 2); 167.4(C-5 or 2); 168.2(C-5 or 2); 168.9(C-5 or 2).

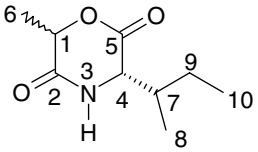

3.3.2.2.6 Synthesis of (3S, 6R,S)-3-isopropyl-6-methyl-morpholine-2,5-dione (Cyclo(DLLA-Val))

(3S, 6R,S)-3-Isopropyl-6methyl-morpholine-2,5-dione was prepared by intra-molecular cyclization of N-(2(R,S)-hydroxypropionyl)-(S)-valine following the procedure described for the preparation of 3(S)-*sec*-butyl-morpholine-2,5-dione. Yield 30%, mp 118-119 °C, $[\alpha]_D^{25}$ = -52.1° (c= 0.51 g/dl chloroform).

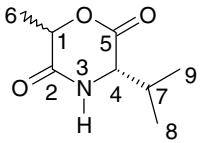

^{1}H NMR (DMSO-d_6, 300MHz, ppm): 0.92-1.03 (m, 6H, CH_3-8 and 9); 1.39 (d, ^{3}J=6.9Hz, 0.7H, CH_3-6); 1.41 (d, ^{3}J=6.9Hz, 0.3H, CH_3-6); 2.09-2.29 (m, 1H, CH-7); 3.87(d × d, ^{3}J = 6.3 Hz, ^{3}J = 3.5 Hz, 0.3H, CH-4); 4.21(d, ^{3}J = 2.2 Hz, 0.7H, CH-4); 5.00-5.10 (m, 1H, CH-1); 8.45 (s, 0.7H, NH-3); 8.65 (s, 0.3H, NH-3)

^{13}C NMR (DMSO-d_6, 75.43MHz, ppm): 15.9(CH_3-8 or 9); 16.5 (CH_3-8 or 9); 17.0 (CH_3-8 or 9); 17.8 (CH_3-8 or 9); 18.1 (CH_3-6); 18.4 (CH_3-6); 29.0 (CH-7); 31.5 (CH-7); 57.7 (CH-4); 59.3(CH-4); 73.5 (CH-1); 73.6(CH-1); 167.3 (C=O-5); 167.5 (C=O-5); 168.3(C=O-2); 169.9 (C=O-2).

3.3.2.2.7 Synthesis of 6(S)-methyl-morpholine-2,5-dione (Cyclo(LLA-Gly))

22 g of N-(2(S)-hydroxypropionyl)-glycine, 250 mL dry ethanol and a catalytic amount of a strong acidic ion exchange resin (Amberlyst 15) were place in a 500 mL round bottom flask equipped with a magnetic stirrer and a Soxhlet extractor to which a reflux condenser was attached. The Soxhlet extractor was filled with 70 g conditioned molecular sieve (4 Å). The contents of the flask were heated to reflux for 24 h. The reaction mixture was allowed to come to room temperature, the ion exchange resin was filtered off, the solvent removed, and the residual ester was used in the following synthesis without any purification.

A mixture of N-(2(S)-hydroxypropionyl)-glycine ethyl ester (16 g), 2500 mL of dry toluene and 10 g of Amberlyst 15 were placed in a 4 L round bottom flask equipped with a magnetic stirrer and a Soxhlet extractor to which a reflux condenser was attached. The Soxhlet extractor was filled with 70 g conditioned molecular sieve (4 Å). The contents of the flask were heated to reflux for 24 h. The reaction mixture was allowed to come to room temperature, the ion exchange resin was filtered off, the solvent removed, and the residual solid was purified by recrystallization in ethyl acetate. Yield 23%, mp 100 °C, $[\alpha]_D^{25}$ = -87.0° (c= 0.50 g/dl chloroform).

^{1}H NMR (DMSO-d_6, 300MHz, ppm): 1.40 (d, ^{3}J = 7.1 Hz, 3H, CH_3-6); 3.96, 4.22 (AB-System, ^{AB}J = 17.9 Hz, 2H, CH_2-4); 5.01 (q, ^{3}J = 6.9 Hz, 1H, CH-1); 8.39 (br. s, 1H, NH-3).

^{13}C NMR (DMSO-d_6, 75.43MHz, ppm): 16.0 (CH_3-6); 43.1 (CH_2-4); 74.0 (CH-1); 167.2 (C=O-5); 167.9 (C=O-2).

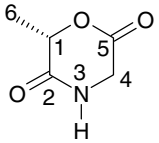

3.3.2.2.8 Synthesis of 6(R,S)-methyl-morpholine-2,5-dione (Cyclo(DLLA-Gly))

6(R,S)-Methyl-morpholine-2,5-dione was prepared by intra-molecular cyclization of N-(2(R,S)-hydroxypropionyl)-glycine following the procedure described for the preparation of 6(S)-metyl-morpholine-2,5-dione. Yield 20%, mp 100 °C, $[\alpha]_D^{25}$ = 0.0° (c= 0.50 g/dl chloroform).

^{1}H NMR (DMSO-d_6, 300MHz, ppm): 1.40 (d, ^{3}J = 6.9 Hz, 3H, CH_3-6); 3.93, 4.13 (AB-System, ^{AB}J = 17.7 Hz, 2H, CH_2-4); 5.00 (q, ^{3}J = 6.9 Hz, 1H, CH-1); 8.39 (br. s, 1H, NH-3).

^{13}C NMR (DMSO-d_6, 75.43MHz, ppm): 15.9 (CH_3-6); 43.1 (CH_2-4); 74.0 (CH-1); 167.1 (C=O-5); 167.9 (C=O-2).

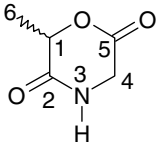

3.3.2.2.9 Synthesis of (3S,6R,S)-3-[(benzyloxycarbonylamino)-butyl]-6-methyl-morpholine-2,5-dione (Cyclo(DLLA-Lys(Z)))

(3S,6R,S)-3-[(Benzyloxycarbonylamino)-butyl]-6-methyl-morpholine-2,5-dione was prepared by intra-molecular cyclization of N^{α}-2(R,S)-[hydroxy-propionyl]-N^{ε}-(benzyl-oxylcarbonyl)-(S)-lysine following the procedure described for the preparation of 3(S)-*sec*-butyl-morpholine-2,5-dione. The yield was 25%, mp 95-120 °C, $[\alpha]_D^{25}$ = -61.0° (c= 0.20 g/dl chloroform).

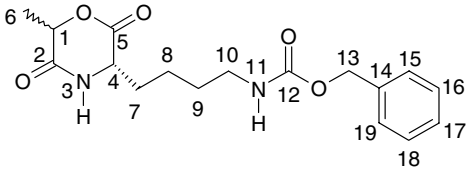

^{1}H NMR (DMSO-d_6, 300MHz, ppm): 1.25-1.45(m, 7H, CH_3-6, CH_2-8 and 9); 1.6-1.83(m, 2H, CH_2-7); 2.90-3.05(q, ^{3}J=6.1Hz, 2H, CH_2-10); 4.10-4.16(t, ^{3}J=6.7Hz, 0.4H, CH-4); 4.26-4.34(t, ^{3}J=5.0Hz, 0.6H, CH-4); 5.01(s, 2H, CH_2-13); 5.05(m, 1H, CH-1); 7.20-7.30(m, 1H, NH-11); 7.30-7.41(m, 5H, Ph-15-19); 8.46(s, 0.6H, NH-3); 8.58(s, 0.4H, NH-3).

^{13}C NMR (DMSO-d_6, 75.43MHz, ppm): 15.5(CH_3-6); 16.8(CH_3-6); 21.4(CH_2-8); 21.7(CH_2-8); 28.7(CH_2-7); 29.1(CH_2-7); 29.2(CH_2-7); 31.7(CH_2-9); 52.4(CH-4); 53.2(CH-10); 65.0(CH_2-13); 73.8(CH-1); 73.9(CH-1); 127.6(Ph-17); 128.3(Ph-15,16,18,19); 137.2(Ph-14); 156.0(C=O-12); 167.4(C=O-5); 168.1(C=O-5); 168.7(C=O-2); 169.3(C=O-2).

3.3.2.2.10 Synthesis of (3S,6R,S)-3-[(benzyloxycarbonyl)methyl]-6-methyl-morpholine-2,5-dione (Cyclo(DLLA-Asp(OBzl)))

3.6 mL (0.025 mol) of triethylamine was added to a solution of 9.0 g (0.025 mol) of β-benzyl-N-[2(R,S)-bromopropionyl]-(S)-aspartate in 75 mL of DMF. The reaction mixture was heated

at 100 °C for 3 h. After removal of the solvent i.vac., the residue was partitioned between ethyl acetate and water. The organic layer was separated and subsequently extracted with water and a saturated aqueous NaCl solution, dried over $MgSO_4$ and concentrated i. vac. to yield a brown oil. Purification by crystallization from toluene two times afforded 4.7 g of (3S,6R,S)-3-[(benzyloxycarbonyl)methyl]-6-methyl-morpholine-2,5-dione. Mp 80-100 °C, $[\alpha]^{25}_D$ = -49 ° (0.2 g/dL in chloroform).

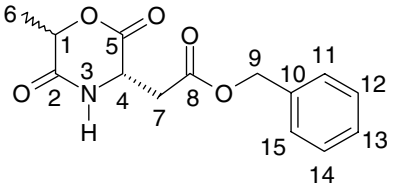

^{1}H NMR (DMSO-d_6, 300MHz, ppm): 1.40(d, ^{3}J=6.7Hz, 2.2H, CH_3-6); 1.48(d, ^{3}J=7.1Hz, 0.8H, CH_3-6); 2.91(d, ^{3}J=5.0Hz, 2H, CH_2-7); 4.58-4.64(t, ^{3}J=4.4Hz, 0.26H, CH-4); 4.66-4.72(t, ^{3}J=5.4Hz, 0.74H, CH-4); 4.90-4.99(q, ^{3}J=7.0Hz, 0.26H, CH-1); 5.14(s, 2H, CH_2-9); 5.14-5.25(q, ^{3}J=6.7Hz, 0.74H, CH-1); 7.38(m, 5H, Ph-11-15); 8.53(br. s, 0.26H, NH-3); 8.60(br. s, 0.74H, NH-3).

^{13}C NMR (DMSO-d_6, 75.43MHz, ppm): 15.5(CH_3-6); 17.8(CH_3-6); 34.5(CH_2-7); 36.6(CH_2-7); 49.5(CH-4); 65.8(CH_2-9); 66.1(CH_2-9); 74.1(CH-1); 74.8(CH-1); 127.8(Ph-13); 127.9,128.0(Ph-12 and 14); 128.1 and 128.3(Ph-11 and 15); 135.6 and 135.7(Ph-10); 166.8(C=O-5); 167.2(C=O-5); 167.9(C=O-8); 168.7(C=O-8); 169.3(C=O-2); 169.7(C=O-2).

3.3.2.2.11 Synthesis of (3S,6R,S)-3-[(benzyloxycarbonyl)-ethyl]-6-methyl-morpholine-2,5-dione (Cyclo(DLLA-Glu(OBzl)))

(3S,6R,S)-3-[(Benzyloxycarbonylethyl]-6-methyl-morpholine-2,5-dione was prepared by intra-molecular cyclization of γ-benzyl-N-2(R,S)-bromopropionyl-(S)-glutamate following the procedure described for the preparation of (3S,6R,S)-3-[(benzyloxycarbonyl)-methyl]-6-methyl-morpholine-2,5-dione. The purification of this compound was carried out by column chromatography on silica gel using ethyl acetate as the eluent, followed by recrystallization from ethyl acetate/hexane. The yield was 15%, mp 97 °C.

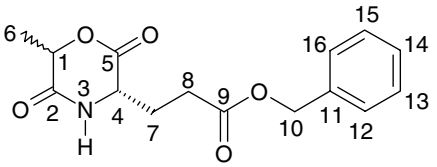

^{1}H NMR (DMSO-d_6, 300MHz, ppm): 1.39(d, ^{3}J=7.0Hz, 2.6H, CH_3-6); 1.40(d, ^{3}J=7.0Hz, 0.4H, CH_3-6); 1.90-2.20(m, 2H, CH_2-7); 2.52-2.61(m, 2H, CH_2-8); 4.20-4.25((t, ^{3}J=5.4Hz, 0.1H, CH-4); 4.34-4.42(t, ^{3}J=5.7Hz, 0.9H, CH-4); 5.04-5.09(q, ^{3}J=6.8Hz, 1H, CH-1); 5.11(s, 2H, CH_2-10); 7.38(m, 5H, Ph-12-16); 8.56(br. s, 0.9H, NH-3); 8.63(br. s, 0.1H, NH-3).

^{13}C NMR (DMSO-d_6, 75.43MHz, ppm): 15.3(CH_3-6); 16.7(CH_3-6); 24.9(CH_2-7); 27.2(CH_2-7); 29.1(CH_2-8); 51.8(CH-4); 52.5(CH-4); 65.5(CH_2-10); 73.8(CH-1); 74.0(CH-1); 127.9(Ph-14); 128.0(Ph-13 and 15); 128.4(Ph-12 and 16); 136.1(Ph-11); 167.4(C=O-5); 167.8(C=O-5); 168.9(C=O-9); 169.2(C=O-9); 171.8(C=O-2); 172.0(C=O-2).

3.3.2.2.12 Synthesis of (3R,6R,S)-3-[(p-nitro-benzyl)-thiomethyl]-6-methyl-morpholine-2,5-dione (Cyclo(DLLA-Cys(pNBzl)))

(3R,6R,S)-3-[(*p*-Nitro-benzyl)-thiomethyl]-6-methyl-morpholine-2,5-dione was prepared by intra-molecular cyclization of N-[2(R,S)-bromopropionyl]-S-(*p*-nitrobenzyl)-(R)-cysteine following the procedure described for the preparation of (3S,6R,S)-3-[(benzyloxycarbonyl)-methyl]-6-methyl-morpholine-2,5-dione. The reaction was carried out at room temperature for 17 h, then at 50 °C for 1 h. The yield was 9%, mp 139-145 °C.

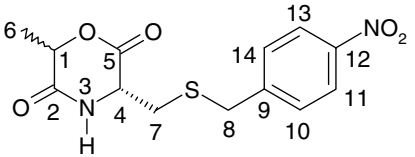

^{1}H NMR (DMSO-d_6, 300MHz, ppm): 1.46(d*d, ^{3}J=6.8Hz, 3H, CH_3-6); 2.88(d, ^{3}J=4.5Hz, 1.4H, CH_2-7); 3.00(d, ^{3}J=5.5Hz, 0.6H, CH_2-7); 3.96(s, 2H, CH-8); 4.56(m, 0.3H, CH-4); 4.67(m, 0.7H, CH-4); 5.10-5.18(m, 1H, CH-1); 7.65(d, ^{3}J=8.4Hz, 2H, Ph-10 and 14); 8.21(d, ^{3}J=8.4Hz, 2H, Ph-11 and 13); 8.54(br. s, 0.7H, NH-3); 8.67(br. s, 0.3H, NH-3).

^{13}C NMR (DMSO-d_6, 75.43MHz, ppm): 16.4(CH_3-6); 17.3(CH_3-6); 32.0(CH_2-7); 34.1(CH_2-7); 34.9(CH_2-8); 35.2(CH_2-8); 53.5(CH-4); 53.7(CH-4); 74.3(CH-1); 74.4(CH-1); 123.6(Ph-11 and 13); 130.1 and 130.0(Ph-10 and 14); 146.4(Ph-9); 146.8(Ph-12); 166.8(C=O-5); 167.2(C=O-5); 167.9(C=O-2); 168.1(C=O-2).

3.3.2.2.13 Synthesis of (3S,6R,S)-3-(p-benzyloxy-benzyl)-6-methyl-morpholine- 2,5-dione (Cyclo(DLLA-Tyr(OBzl)))

(3S,6R,S)-3-(*p*-Benzyloxy-benzyl)-6-methyl-morpholine-2,5-dione was prepared by intramolecular cyclization of N-[2(R,S)-bromopropionyl]-O-(benzyl)-(S)-tyrosine following the procedure described for the preparation of (3S,6R,S)-3-[(benzyloxycarbonyl)-methyl]-6-methyl-morpholine-2,5-dione. The yield was 20%, mp 141 °C.

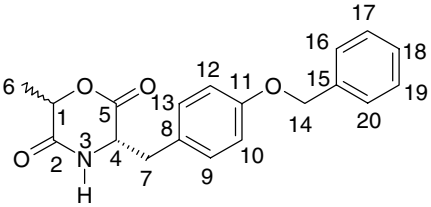

^{1}H NMR (DMSO-d_6, 300MHz, ppm): 1.00(d, ^{3}J=6.9Hz, 3H, CH_3-6); 2.98-3.04(m, 2H, CH_2-7); 4.60(t, ^{3}J=4.5Hz, 1H, CH-4); 4.87-4.96(q, ^{3}J=6.8, 1H, CH-1); 5.08(s, 2H, CH_2-14); 6.9-7.2(d*d, ^{3}J=8.8Hz, 4H, Ph-9, 10, 12 and 13); 7.3-7.5(m, 5H, Ph-16-20); 8.21(d, ^{3}J=8.4Hz, 2H, Ph-11 and 13); 8.54(br. s, 0.7H, NH-3); 8.67(br. s, 0.3H, NH-3).

3.4 POLYMERIZATION

3.4.1 Sn(oct)$_2$ catalyzed polymerization

3.4.1.1 Synthesis of homopolymer and block copolymers

The polymerization (PGI/EO1 in Tab. 2) was performed in a tube equipped with a stirring bar and heated at 120 °C for 24 h. Subsequently the tube was cooled to room temperature i. vac. and filled with dry nitrogen. In a nitrogen atmosphere, PEO6000 (0.1425 g, 2.38×10^{-5} mol) and 0.9476 g (5.51×10^{-3} mol) of Cyclo(Glc-Ile) were placed into the tube, and a freshly prepared 0.25 M solution of stannous octoate in dry toluene was added in an equimolar amount with respect to PEO (for the preparation of the homopolymer no PEO was added, the initiator then being alcoholic impurities of the catalyst). The solvent was removed by evaporation i. vac. for 24 h. The tube was refilled with dry nitrogen and then placed in an oil bath at 140 °C. After 9 h the tube was removed from the oil bath and allowed to cool to room temperature. The product was dissolved in 10 mL of methylene chloride and precipitated in 200 mL of diethyl ether. The resulting block copolymer was dried i.vac. at room temperature

for 24 h. The block copolymer was purified by immersing in ethanol and water to remove the unreacted PEO.

DMSO was used as a solvent in the treatment of homopolymers and block copolymers of Cyclo(Glc-Leu) and Cyclo(LLA-Gly), because they are not soluble in methylene chloride,

3.4.1.2 Synthesis of copolymers with functional group

The polymerization was performed in a tube equipped with a stirring bar and heated at 120 °C for 24 h. Subsequently the tube was cooled to room temperature i. vac. and filled with dry nitrogen. In a nitrogen atmosphere, appropriate amounts of morpholine-2,5-dione with functional group, DLLA, or CL were placed into the tube, and a freshly prepared 0.25 M solution of stannous octoate in dry toluene was added in a molar ratio M/I=125. The solvent was removed by evaporation i. vac. for 24 h. The tube was refilled with dry nitrogen and then placed in an oil bath at 140 °C. After 48 h the tube was removed from the oil bath and allowed to cool to room temperature. The product was dissolved in 10 mL of methylene chloride and precipitated in 200 mL of cooled ethanol or hexane. The resulting copolymer was dried i.vac. at room temperature for 24 h.

Deprotection of poly[DLLA-Asp(OBzl)]

The copolymer of poly[DLLA-Asp(OBzl)] (9.0 g) was dissolved in 250 mL of ethyl acetate whereafter 100 mL of methanol and 0.5 g of 10% Pd/C were added. The suspensions was vigorously stirred in a hydrogen atmosphere at room temperature for 48 h. The catalyst was removed by filtration over Celite 545. The filtrate was added dropwise to a twenty-fold excess of ethanol or hexane. The precipitated polymer was collected and dried i.vac. for 24 h.

3.4.1.3 Synthesis of block copolymers with functional group

The polymerization was performed in a tube equipped with a stirring bar and heated at 120 °C for 24 h. Subsequently the tube was cooled to room temperature i. vac. and filled with dry nitrogen. In a nitrogen atmosphere, appropriate amounts of morpholine-2,5-dione with functional group, DLLA, and PEO8000 were placed into the tube, and a freshly prepared 0.25 M solution of stannous octoate in dry toluene was added in a molar ratio M/I=125. The solvent was removed by evaporation i. vac. for 24 h. The tube was refilled with dry nitrogen and then placed in an oil bath at 140 °C. After 24 h the tube was removed from the oil bath and allowed to cool to room temperature. The product was dissolved in 20 mL of methylene chloride and precipitated in 400 mL of cooled diethyl ether. The resulting copolymer was dried i.vac. at room temperature for 24 h.

Deprotection of poly[DLLA-Asp(OBzl)]-b-PEO

The deprotecttion of poly[DLLA-Asp(OBzl)]-*b*-PEO was carried out following the procedure described for the deprotection of poly[DLLA-Asp(OBzl)].

3.4.1.4 Synthesis of block copolymers from morpholine-2,5-diones, PEO8000 and DLLA or LLA

In a nitrogen atmosphere, appropriate amounts of morpholine-2,5-dione, DLLA or LLA, and PEO8000 were placed into the tube, and a freshly prepared 0.25 M solution of stannous octoate in dry toluene was added in an equimolar amount with respect to PEO. The solvent was removed by evaporation i. vac. for 24 h. The tube was refilled with dry nitrogen and then placed in an oil bath at 140 °C. After 9 h the tube was removed from the oil bath and allowed to cool to room temperature. The product was dissolved in 30 mL of methylene chloride and precipitated in 600 mL of cooled diethyl ether. The resulting copolymer was dried i.vac. at room temperature for 24 h. DMSO was used as a solvent in the treatment of block copolymers containing leucine or glycine residue.

3.4.2 Synthesis of block copolymers in the presence of CaH_2 as a co-initiator

Under nitrogen, PEO6000 was introduced into the tube. The number average molecular weight of PEG6000, as determined by MALDI-TOF MS, was used for the calculation of the reagent quantity. The tube was heated to 50 °C and degassed and refilled with dry nitrogen. A predetermined amount of Cyclo(Glc-Val) was added, and the mixture degassed under stirring for 6 h. CaH_2 was added in a 1/1 mole ratio with respect to the hydroxyl end groups of PEO. The tube was refilled with dry nitrogen and then placed in an oil bath at 140 °C. After 24 h or 96 h the tube was removed from the oil bath and allowed to cool to room temperature. The product was dissolved in 10 mL of methylene chloride and precipitated in 100 mL of diethyl ether. The resulting block copolymer was collected and dried i.vac. at room temperature for 24 h.

3.4.3 Enzyme catalyzed polymerization

A typical polymerization of 3(S)-isopropyl-morpholine-2,5-dione was carried out as follows. A mixture of Lipase PPL (50 mg) and 3(S)-isopropyl-morpholine-2,5-dione (0.500 g) was reacted in an N_2 atmosphere in a dried (i.vac. for 24 h) and sealed test tube placed in an oil bath at 100 °C for 3 d. After the reaction, the reaction mixture was dissolved in chloroform

(10 mL), and the insoluble enzyme was removed by filtration. Chloroform was then evaporated under reduced pressure to give the crude polymer which was purified by reprecipitation (chloroform as a good solvent; ether as a poor solvent) to remove any oligomeric fractions to result in the polydepsipeptide.

4. REFERENCES

1) R. L. Kronenthal, *Polymers in Medicine and Surgery*; Plenum: NY, 119 (1975).
2) D. K. Gilding, *Biocompatibility of clinical implant materials*, CRC: Boca Raton, Chapter IX (1981).
3) J. Kopecek, K. Ulbrich, *Prog. Polym. Sci.* **9**, 1(1983).
4) B. D. Ratner, *Comprehensive Polym. Sci.* **7**, 201(1989).
5) A. U. Daniels, M. K. O. Chang, K. P. Andriano, J. Heller, *J. Appl. Biomater.* **1**, 57(1990).
6) M. Vert, S. M. Li, G. Splenhauer, P. Guerin, *J. Mater. Sci. Med.* **3**, 432(1992).
7) M. Vert, *Angew. Makromol. Chem.* **166/167**, 155(1989).
8) J. Knüffermann, Dissertation, RWTH Aachen (1999).
9) R.A. Miller, J.M. Brady, D.E. Cutright, *J. Biomed. Mater. Res.* **11**, 711(1977).
10) C.C. Chu, Biomaterials, Wiley: New York, 781(1982).
11) B. Eling, S. Gogloewski, A. Pennings, *J. Polymer* **23**, 1587(1982).
12) R.J.M. Zwiers, S. Gogloewski, A. Pennings, *J. Polymer* **24**, 167(1983).
13) D. K. Gilding, A. M. Reed, *Polymer* **20**, 1459 (1979).
14) J.M. Anderson, K.L. Spilizewski, A. Hiltner, *Biocompatibility of Tissue Analogs*; CRC; Boca Raton, 67 (1985).
15) M. Spira, J. Fissette, C.W. Hall, S.B. Hardy, F.J. Gerow, *J. Biomed. Mater. Res.* **3**, 213 (1969).
16) S. Aiba, N. Minoura, Y. Fujiwara, S. Yamada, T. Nakagawa, *Biomaterials* **6**, 290(1985).
17) L.A. McCormick-Thomson, R. Duncan, *J. Bioact. Biocompat. Polym.* **4**, 242(1989).
18) F.H.C. Stewart, *Aust. J. Chem.* **22**, 1291(1969).
19) B. Ridge, H.N. Rydon, C.R. Snell, *J. Chem. Soc., Perkin Trans.***1**, 2041(1972).
20) D. Nissen, C. Gilon, M. Goodman, *Makromol. Chem. Suppl.* **1**, 23(1975).
21) L.J. Mathias, W.D. Fuller, D. Nissen, M. Goodman, *Macromolecules* **11**, 534(1978).
22) R.T. Ingwall, C. Gilon, W.J. Becktel, M. Goodman, *Macromolecules* **11**, 540(1978).
23) M. Goodman, *J. Polym. Sci., Polym. Symp.* **62**, 173(1978).
24) R. Katakai, M. Goodman, *Macromolecules* **15**, 25(1982).
25) R. Katakai, *J. Chem. Soc. Perkin Trans.* **1**, 2249(1987).
26) M.Yoshida, M. Asano, M. Kumakura, R. Katakai, T. Mashimo, H. Yuasu, K. Imai, H. Yamanaka, *J. Biomed. Mater. Res.* **24**, 1173(1990).

27) M. Yoshida, M. Asano, M. Kumakura, R. Katakai, T. Mashimo, H. Yuasa, K. Imai, H. Yamanaka, *Colloid Polym. Sci*. **268**, 726(1990).

28) M. Yoshida, M. Asano, M. Kumakura, R. Katakai, T. Mashimo, H. Yuasa, H. Yamanaka, *Eur. Polym. J.* **27**, 325(1991).

29) J. Helder, F.E. Kohn, S. Sato, J.W. van den Berg, J. Feijen, *Makromol. Chem., Rapid Commun*., **6**,9 (1985).

30) V. Jörres, Dissertation, RWTH Aachen (1997).

31) G. John, S. Tsuda, M. Morita, *J. Polym. Sci. Part A: Polym. Chem*. **35**, 1901 (1997).

32) T. Ouchi, T. Nozaki, Y. Okamoto, M. Shiratani, Y. Okya, *Makromol. Chem. Phys*., **197,** 1823 (1996).

33) S.W. Shakaby, D.F. Koelmel, *Eur. Pat. Appl.* 86613(1983).

34) N. Yonezawa, F. Toda, M. Hasegawa, *Makromol. Chem., Rapid Comm*. **6**, 611(1985).

35) J. Helder, S.J. Lee, S.W. Kim, J. Feijen, *Makromol. Chem., Rapid Comm*. **7**, 193(1986).

36) C. Samyn, M. van Beylen, *Makromol. Chem., Makromol. Symp*. **19**, 225(1988).

37) F.N. Fung, R.C. Glowaky, *Eur. Pat. Appl. EP.* 322154(1989).

38) P.J.A. In´t Veld, W.-P. Ye. R. Klap, P.J. Dijkstra, J. Feijen, *Makromol. Chem.* **193**, 1927(1992).

39) P.J.A. In´t Veld, P.J. Dijkstra, J. Feijen, *Makromol. Chem*. **193**, 2713(1992).

40) P.J.A. In´t Veld, Z.R. Shen, G.A.J. Takens, P.J. Dijkstra, J. Feijen, *J. Polym. Sci*. **32**, 1063(1994).

41) J.S. Hrkach, J. Ou, N. Lotan, R. Langer, *ACS Symposium Series* 627, American Chemical Society: Washington DC, 93 (1996).

42) T. Ouchi, M. Shiratani, M. Jinno, M. Hirao, Y. Ohya, *Makromol. Chem., Rapid Commun.* **14**, 825 (1993).

43) D. Wang, X.D. Feng, *Macromolecules* **31**, 3824 (1998).

44) G.D. Zhang, D. Wang, X.D. Feng, *Macromolecules* **31**, 6390(1998).

45) P.J.A. in't Veld, P.J. Dijkstra, J.H. van Lochem, J. Feijen, *Macromol. Chem.* **191**, 1813(1990).

46) V. Jörres, H. Keul, H. Höcker, *Macromol. Chem. Phys*. **199**, 835(1998).

47) F.N. Fung, EP 322154 (1995).

48) F.S. Du, W.P. Ye, Z.W. G. J.Y. Yang, *J. Appl. Polym. Sci*. **63**, 643(1997).

49) D.A. Barrera, E. Zylstra, P.T. Lansbury, R. Langer, *Macromolecules* **28**, 425(1995).

50) F. Tasaka, H. Miyazaki, Y. Ohya, T. Ouchi, *Macromolecules* **32**, 6386(1999).

51) T. Ouchi, H. Seike, T. Nozaki, Y. Ohya, *J. Polym. Sci., Polym. Chem.* **36**, 1283(1998).

52) T. Ouchi, A. Hamada, Y. Ohya, *Macromol. Chem. Phys*. **200**, 436(1999).

53) G. John, M. Morita, *Macromol Rapid Commun.* **20**, 265(1999).

54) G.A. Millis, Kirk-Othmer, *Encyclopedia of Chemical Technology,* 3rd ed., John Wiley & Sons: New York, Vol. 5 (1979).

55) A. Zaks, A.M. Klibanov, *Proc. Natl. Acad. Sci.* USA **82**, 3192 (1985).

56) M.H. Keyes, D. Albert, *Encyclopedia of Polymer Science and Engineering*, 2nd ed., John Wiley & Sons: New York, Vol. 6 (1988).

57) S. Bloomer, P. Adlercreutz, B. Mattiasson, *J. Am. Oil Chem. Soc.* **69**, 966(1992).

58) K. Faber, M.C.R. Franssen, *Trends Biotech*. **11**, 461 (1993).

59) A.M. Klibanov, *Chemtech.* **16**, 353(1986).

60) H. Ritter, *Trends Polym. Sci*. **1**, 171(1993).

61) S. Kobayashi, S. Shoda, H. Uyama, *Adv. Polym. Sci.* **121**, 1(1995).

62) K. Nilsson, *Trends Biotechnol*. **6**, 256(1988).

63) K. Ajisaka, H. Nishida, H. Fujimoto, *Biotechnol. Lett.* **9**, 243(1987).

64) K. Ajisaka, H. Nishida, H. Fujimoto, *Biotechnol. Lett.* **9**, 387(1987).

65) J.E.G. Barnett, W.T.S. Jarvis, K.A. Munday, *Biochem. J.* **105**, 669(1967).

66) S. Kobayashi, K. Kashiwa, T. Kawasaki, S. Shoda, *J. Am. Chem. Soc.* **113**, 3079(1991).

67) H.L. Hai, L.G. Butter, B. Axelord, *Biochem. Biophys. Res. Commun*. **60**, 635(1974).

68) S. Shoda, E. Okamoto, T. Kiyosada, S. Kobayashi, *Macromol. Rapid Commun*. **15**, 751 (1994).

69) S. Kobayashi, J. Shimada, K. Kashiwa, S. Shoda, *Macromolecules* **25**, 3237 (1992).

70) J.S. Fruton, W.R. Hearn, V.M. Ingram, D.S. Wiggans, M. Wintz, *J. Biol. Chem*. **204**, 891(1953).

71) C.P. Heinrich, J.S. Fruton, *Biochemistry* **7**, 3556(1968).

72) M. Brenner, H.R. Müller, R.W. Pfister, *Helv. Chim. Acta* **33**, 568(1950).

73) M. Brenner, R.W. Pfister, *Helv. Chim. Acta* **34**, 2085(1951).

74) L.A.E. Sluyterman, J. Wijdenes, *Biochim. Biophys. Acta* **289**, 194(1972).

75) G. Anderson, P.L. Luisi, *Helv. Chim. Acta*, **62**, 488(1979).

76) K. Aso, T. Uemura, Y. Shiokawa, *Agric. Biol. Chem*. **52**, 2443(1988).

77) C.H. Wong, S.T. Chen, W.J. Hennen, J.A. Bibbs, Y.F. Wang, J.L. Liu, M.W. Pantoliano, M. Whitlow, P.N. Bryan, *J. Am. Chem. Soc*. **112**, 945(1990).

78) Z. Zhong, J.L.C. Liu, L.M. Dinterman, M.A.J. Finkelman, W.T. Mueller, M.L. Rollence, M. Whitlow, C.H. Wong, *J. Am. Chem. Soc*. **113**, 683(1991).

79) J.S. Wallace, C.J. Morrow, *J. Polym. Sci. Polym. Chem. Ed*. **27**, 2553(1989).

80) J.S. Wallace, C.J. Morrow, *J. Polym. Sci. Polym. Chem. Ed*. **27**, 3271(1989).

81) A. Ajima, T. Yoshimoto, K. Takahashi, Y. Tamaura, Y. Saito, Y. Inada, *Biotechnol. Lett*. **7**, 303(1985).

82) C.J. Morrow, J.S. Wallace, *Biocatalysis,* Van Nostrand Reinhold, New York (1990).

83) H.G.Park, H.N. Chang, J.S. Dordick, *Biotechnol. Letters*, **17**, 1085(1995).

84) D. Knani, A.L. Gutman, D.H. Kohn, *J. Polym. Sci. Polym. Chem. Ed*. **31**, 1221(1993).

85) R.T. MacDonald, S.K. Pulapura, Y.Y. Svirkin, R.A.Gross, D.L. Kaplan, J.A. Akkara, G. Swift, S. Wolk, *Macromolecules* **28**, 73(1995).

86) S. Kobayashi, K. Takeya, S. Suda, H. Uyama, *Macromol. Chem. Phys*. **199,** 1729(1998).

87) A. Gordova, T. Iversen, K. Hult, *Macromolecules* **31**, 1040(1998).

88) S. Namekawa, H. Uyama, S. Kobayashi, *Polym. J.* **28**, 730(1996).

89) H. Uyama, K. Takeya, S. Kobayashi, *Proc. Acad. Jpn.* **69B**, 203(1993).

90) H. Uyama, S. Suda, S. Kobayashi, *Acta Polym.* **49**, 700(1998).

91) K.S. Bisht, F. Deng, R.A. Gross, D.L. Kaplan, G. Swift, *J. Am. Chem. Soc.* **120**, 1363 (1998).

92) T. Ouchi, H. Yuyama, O. Vogl, *J. Macromol. Sci., Chem.* A**24**(9), 1011 (1987).

93) S.M. Li, I. Rashkov, J. L. Espartero, N. Manolova, M. Vert, *Macromolecules*, **29**, 57 (1996).

94) Z. H. Gan, B. Z. Jiang, J. Zhang, *J. Appl. Polym. Sci*., **59**(6), 961 (1996).

95) P. Cerrai, G. D. Guerra, L. Lelli, M. Tricoli, J. *Mat. Sci.: Mat. in Med.* **5**, 33(1994).

96) B. Bogdanov, A. Vidts, A. van den Bulcke, R. Verbeeck, E. Schacht, *Polymer*, **39**(8-9), 1631(1998).

97) Y.J. Du, P. J. Lemstra, A. J. Nijenhuis, H. A. M. van Aert, C. Batiaansen, *Macromolecules*, **28**, 2124 (1995).

98) D. Cohn, H. Younes, *J. Biomed. Mater. Res.* **22**, 993 (1988).

99) X. Chen, S. P. McCarthy, R. A. Gross, *Macromolecules*, **30**, 4295 (1997).

100) D. K. Han, J. A. Hubbell, *Macromolecules,* **29,** 5233 (1996).

101) W. M. Stevels, M.J.K. Ankone, P.J. Dijkstra, J.Feijen, *Macromol. Chem. Phys*., **196,** 3687 (1995).

102) H. R. Kircheldorf, J. Meier-Haack, *Makromol. Chem*. **194**, 715(1993).

103) B. Wunderlich, *Macromolecular Physics, Crystal Nucleation, Growth, Annealing*, Vol. 2, Academic Press, New York, 1976, p.218.

104) H. Wang, J.H. Dong, K.Y. Qiu, *J. Polym. Sci., Part A: Polym. Chem*. **36**, 695 (1998).

105) J. Mohammadi-Rovshandeh, S.M.F. Farnia, M.N. Sarbolouki, *J. Appl. Polym. Sci.* **68**, 1949(1998).

106) P.J. Flory, *J. Chem. Phys.* **17**, 233(1949).

107) D. W. Grijpma, E. Kroeze, A. J. Nijenhuis, A. J. Pennings, *Polymers,* **34**, 1496(1993).

108) A.S. Sawhney, C.P. Pathak, J. A. Hubbell, *Macromolecules,* **26**, 581(1993).

109) S. Li, J. Biomed. Mater. Res. (Appl. Biomater.), 48, 342 (1999).

110) Z. Jedlinski, P. Kurcok, W. Walach, H. Janeczek, I. Radecka, *Makromol. Chem.* **194**, 1681 (1993).

111) I. Rashkov, N. Manolova, S.M. Li, J.L. Espartero, M. Vert, *Macromolecules*, **29**, 50 (1996).

112) M.C. Tanzi, P. Verderio, M.G. Lampugnani, M. Resnati, E. Dejana, E. Sturani, *J. Mater. Sci.; Mater. Med.* **5**, 397 (1994).

113) F.E.Jr. Bailey, J.V. Kpleske, Poly(ethylene oxide), Academic Press: New York, 1976, Chapter IV.

114) H. R. Kricheldorf, A. Serra, *Polymer Bulletin*, **14**, 497 (1985).

115) H. R. Kricheldorf, I. Kreiser-Saunders, *Makromol. Chem*., **191**, 1057 (1990).

116) A.L. Margol. J.-Y. Crenne, A.M. Klibanov, *Tetrahedron Lett*. **28,** 1607(1987).

117) D.R. Patil, D.G. Rethwisch, J.S. Dordick, *Biotechnol. Bioeng*. **37**, 639(1991).

118) H. Uyama, S. Kobayashi, *Chem. Lett*. 1687(1994).

119) E.M. Brazwell, D.Y. Filos, C.J. Morrow, *J. Polym. Sci., Part A: Polym. Chem*. **33,** 89 (1995).

120) O. Noll, H. Ritter, *Macromol. Rapid Commun*. **17**, 553(1996).

121) H. Uyama, S. Kobayashi, *Chem. Lett*. 1149(1993).

122) D. Knai, A.L. Gutman, D.H. Kohn, , *J. Polym. Sci., Part A: Polym. Chem*. **31,** 1221 (1993).

123) H. Uyama, K. Takeya, S. Kobayashi, *Bull. Chem. Soc. Jpn.* **68,** 56(1993).

124) H. Uyama, K. Takeya, N. Hoshi, S. Kobayashi , *Macromolecules* **28**, 7046(1995).

125) H. Uyama, S. Namekawa, S. Kobayashi, *Polym. J*. **29,** 299(1997).

126) A. Cordova, T. Iversen, K. Hult, M. Martinelle, *Polymer,* **39**(25), 6519 (1998).

127) K. S. Bisht, Y. Y. Svirkin, L.A. Henderson, R. A. Gross, D. L. Kaplan, G. Swift, *Marcomolecules*, **30**, 7735 (1997).

128) K. S. Bisht, L. A. Henderson, R. A. Gross, D. L. Kaplan, G. Swift, *Macromolecules* **30**, 2705 (1997).

129) Y. Y. Svirkin, J. Xu, R. A. Gross, D. L. Kaplan, G. Swift, *Macromolecules* **29**, 4591 (1996).

130) A. Zaks, A.M. Klibanov, *J. Bio. Chem.* **263**, 3194 (1988).

131) S. Matsumura, K. Mabuchi, K. Toshima, *Macromol. Rapid Commun*. **18**, 477 (1997).

132) D. Wang, X. Feng, *Macromolecules*. **30**, 5688(1997) .

133) C. Berse, R. Boucher, L. Piche, *J. Org. Chem*. **22**, 805(1957).

134) J. S. Morley, *J. Chem. Soc*. (C), 2410(1967).

Lebenslauf

Persönliche Daten

Familienname:	FENG
Vorname:	Yakai
Geschlecht:	männlich
Geburtsdatum:	20.12.1966
Geburtsort:	Hebei (V.R. China)
Staatsangehörigkeit:	chinesisch
Familienstand:	verheiratet

Schulbildung

Sept. 1979 - Juli 1982	Grundschule in Xinji, Provinz Hebei
Sept. 1982 - Juli 1985	Mittelschule in Xinji, Provinz Hebei

Studium

Sept. 1985 - Juli 1989	Studium an der Nankai Universität Studienfach : Chemie
Juli 1989	Abschluß : " Bachelor of Science "
Sept. 1989 - Juni 1992	Aspirant an der Nankai Universität Studienfach : Makromolekulare Chemie
Juni 1992	Abschluß: " Master of Science "

Promotion

Sept. 1997 - Aug. 2000 Beginn der Promotion am Deutschen Wollforschungsinstitut an der RWTH Aachen e.V./Lehrstuhl für Textilchemie und Makromolekulare Chemie unter der Leitung von Herrn Univ.-Prof. Dr. rer. nat. H. Höcker; Dissertationsthema: "Synthese und Charakterisierung von bioabbaubaren Polymeren auf der Basis von Polydepsipetiden"

Berufstätigkeit

Juni 1992 - Juni 1994	Assistent an der Tianjin Universität
Juni 1994 - Aug. 1997	Dozent an der Tianjin Universität

Yakai Feng

Aachen den 18.11.2000